USING X-RAY FLUORESCENCE SPECTROMETRY TO ASSESS VARIANCE IN OBSIDIAN SOURCE DISTRIBUTION IN SOUTHERN IDAHO

by

Marielle Loryn Pedro Black

A thesis
submitted in partial fulfillment
of the requirements for the degree of
Master of Arts in Anthropology
Boise State University

May 2014

BOISE STATE UNIVERSITY GRADUATE COLLEGE

DEFENSE COMMITTEE AND FINAL READING APPROVALS

of the thesis submitted by

Marielle Loryn Pedro Black

Thesis Title: Using X-Ray Fluorescence Spectrometry to Assess Variance in Obsidian Source Distribution in Southern Idaho

Date of Final Oral Examination: 04 April 2014

The following individuals read and discussed the thesis submitted by student Marielle Loryn Pedro Black, and they evaluated her presentation and response to questions during the final oral examination. They found that the student passed the final oral examination.

Mark G. Plew, Ph.D.	Chair, Supervisory Committee
Christopher L. Hill, Ph.D.	Member, Supervisory Committee
David A. Nolin, Ph.D.	Member, Supervisory Committee

The final reading approval of the thesis was granted by Mark G. Plew, Ph.D., Chair of the Supervisory Committee. The thesis was approved for the Graduate College by John R. Pelton, Ph.D., Dean of the Graduate College.

DEDICATION

This thesis is dedicated to my wonderful husband, Brandon Black, without whom this task may have been insurmountable.

ACKNOWLEDGEMENTS

Without the help and guidance of others, this thesis would not have been possible. I would like to thank my advisor, Dr. Mark Plew, whose guidance has been instrumental in creating a manageable project. Dr. Christopher Hill has helped me clarify the missing steps in addressing obsidian sourcing studies. Additionally, Dr. David Nolin has been immeasurably important in tackling the relatively extensive statistical analysis.

Obsidian source data for Idaho was graciously shared by Craig Skinner, Program Director, Northwest Research Obsidian Studies Laboratory. Further, access to the archaeological collections at Boise State University and the Idaho Museum of Natural History allowed the study of existing collections. The cooperation and assistance of the Idaho Museum of Natural History, and Idaho State University staff, specifically Buck Benson, Amber Tews, Amy Commendador, and Herbert Maschner, were instrumental in my conducting this thesis research.

Funding was provided by the Boise State University Student Research Initiative to run the XRF analysis.

AUTOBIOGRAPHICAL SKETCH OF AUTHOR

Marielle Black is a GIS Manager with technical expertise in archaeology. She is currently pursuing an M.A. in Anthropology from Boise State University and holds two graduate certificates in GIS. Marielle has been conducting cultural resource studies in the Northwest since 2007. Her experience includes projects completed for the BLM and Tribal entities in Oregon, Washington, Nevada, and Idaho and conducting GIS analysis, excavation, and data recovery on land and under water.

ABSTRACT

This study explores the use of portable X-ray fluorescence (pXRF) and X-ray fluorescence (XRF) spectrometry to assist in associating artifacts with geological sources of obsidian from Southern Idaho. XRF spectrometry measures trace element abundance within obsidian artifacts, which is then compared, using a variety of statistical techniques, with known obsidian source geochemical profiles. Results from previous obsidian provenance studies have been used in archaeology as a proxy in measuring prehistoric hunter-gatherer mobility. Artifacts from 11 site assemblages were measured using pXRF to augment data for previously analyzed sites and to collect artifact geochemical data from previously unanalyzed sites. Using pXRF geochemical reference profiles from only one lab, artifact-to-source assignment resulted in 75% of analyzed artifacts attributed to an obsidian source. The addition of XRF geochemical reference profiles from a second lab and standardized values of all geochemical reference profiles and artifacts allows for a more complete assignment of artifacts to sources. With the original and additional geochemical reference profiles, artifact-to-source assignment increased to 87%. This study demonstrates the need for regional databases of standardized geochemical reference profiles as well as a thorough understanding of the underlying XRF technology to inform conclusions regarding prehistoric mobility. An additional, and possibly even more important, conclusion of this study is to question the validity and assumptions of previous XRF analysis studies based on past methodologies.

TABLE OF CONTENTS

LIST OF TABLES

LIST OF FIGURES

LIST OF PICTURES

LIST OF ABBREVIATIONS

AFW	American Falls/ Walcott
BB	Browns Bench
BBA	Browns Bench Area
BG	Bear Gulch
BSB	Big Southern Butte
BSU	Boise State University
BVA	Butte Valley A
CB	Cedar Butte
CC	Conant Creek
CF	Chesterfield
CM/1	Cannonball Mountain/ Cannonball Mountain 1
DHR	Deadhorse Ridge
Fe	Iron
Ga	Gallium
IMNH	Idaho Museum of Natural History
ISU	Idaho State University

JC	Jordan Creek
KC	Kelly Canyon
keV	kiloelectronvolt
kV	kilovolt
µA	Microampere
MD	Malad
MHS	Murphy Hot Springs
Mn	Manganese
NWROSL	Northwest Research Obsidian Studies Laboratory
*l*pXRF	Laboratory Portable X-Ray Fluorescence
*l*XRF	Laboratory X-Ray Fluorescence
Nb	Niobium
OC	Obsidian Cliff
OY	Owyhee
PS	Pack Saddle
pXRF	Portable X-Ray Fluorescence
Rb	Rubidium
RP	Reas Pass
RY	Reynolds

SBG	Striker Basin Gulch
SC	Sinker Canyon
Sr	Strontium
TB	Timber Butte
Th	Thorium
TP1	Teton Pass 1
UNK	Unknown
UNK-C	Unknown- Conflicting Sources
WB	Wedge Butte
XRF	X-Ray Fluorescence
Y	Yttrium
Zn	Zinc
Zr	Zirconium

CHAPTER ONE: INTRODUCTION

X-Ray fluorescence spectrometry is used to determine the geochemical characteristics of obsidian artifacts measured in parts per million. Certain elements or sets of elements appear to be unique to the geologic history of particular regional obsidian sources. Using a set of multivariate statistical techniques, this study compares XRF analysis results from two labs: the Idaho Museum of Natural History (IMNH) and the Northwest Research Obsidian Studies Laboratory (NWROSL). In addition, it determines the set of elements most important in assigning obsidian sources to artifacts in Southern Idaho. A comprehensive regional obsidian source reference database would provide the means for provenance assignment of previously unsourced artifacts by assessing the regionally relevant set of elements.

One main area of interest in prehistoric archaeology is prehistoric mobility and settlement patterns, specifically the manner in which humans move across the landscape in relation to the location of subsistence resources (edible and nonedible) and their settlement patterns (Binford 1980; Kelly 1983, 1992). Since there is no direct way to measure the mobility of prehistoric peoples, proxies in the form of resource distribution studies have been used to examine mobility and its relationship to past settlement patterns (Beck and Jones 1988, 1990a, 1990b, 1997; Beck, Taylor, Jones, Fadem, Cook, and Millward, 2002; Jones and Beck 1999; Jones, Beck, Jones, and Hughes 2003; Kelly 1988, 1992, 2001; Smith 2005a, 2005b). While Binford (1979) and Goodyear (1979), among others, helped establish lithic source distribution studies, numerous researchers have continued to argue for large lithic procurement ranges for prehistoric hunter-gatherers (Hughes 1986; Kelly and Todd 1988; Shackley 1990, 1996).

In reality, obsidian sourcing studies are a “measure of the physical displacement of materials, not direct evidence for trade, exchange, direct procurement, or mobility” (Hughes 1998). Obsidian distribution studies allow for the interpretation of distances and directions in which lithic resources were naturally or culturally conveyed from their primary or secondary source locations (Shackley 2005). The movement of resources, especially lithics, from their primary or secondary locations to archaeological residential/logistical sites is one line of evidence that can *suggest* the use of resources as well as the movement and settlement of people in relation to these resources in the past, but not the specific mechanisms of such accomplishments (Binford 1973, 1977, 1979; Jones et al. 2003; Kuhn 1995; Parry and Kelly 1987; Shott 1989). This interpretation of prehistoric mobility inferred from the spatial location of obsidian in relation to an archaeological site, assumes a direct relationship between obsidian conveyance and human mobility that may not have existed.

Although the presence of obsidian artifacts in archaeological sites has been used as evidence of prehistoric mobility, in reality such presence could be due to direct procurement, exchange, or a combination or the two (Hughes 2012). While the distinction between direct procurement and exchange can be impossible to distinguish, it is useful to recognize modes of conveyance that could be represented in any or every archaeological assemblage. To arrive at potential explanations for these questions, it is useful to consider the petrogenesis of obsidian and have a basic understanding of what conditions lead to the geochemical variation with a source. There are two sources of variation: 1) variability within the geologic source and 2) variation originating in the instruments used to measure the geochemical profiles of obsidian.

Regional Setting

The study area includes obsidian sources and archaeological sites within Idaho. The 11 archaeological sites are located in Southern Idaho and adjacent upland areas, while obsidian sources are located in the uplands and mountains that surround the arc of the Snake River Plain (Figure 1.1). The Snake River Plain extends across approximately 23,550 square miles in Southern Idaho (Freeman, Forrester, and Lupher 1945:71). The western Snake River Plain is bounded on the north and south by extensive mountain ranges, whereas the central plain is bounded by mountains to the north and rolling hills to the south. The eastern Snake River Plain rises in elevation and blends into the surrounding mountain foothills while curving northeast toward the Yellowstone Plateau. The Snake River Plain has a geologic history of explosive silicic (high silica content) volcanic events and floods, which create diversity in obsidian source geochemistry as well as extensive secondary obsidian source locations (Armstrong 1975; Clemens 1993; Malde 1991; Perkins, Nash, Brown, and Fleck 1995). Ninety percent of the Snake River Plain is covered with Quaternary basalts with many areas of minimal soil coverage (Thornbury 1965:459). The “Quaternary feature of the Snake River Plain express the latest stages of tectonic and depositional events that began in late Tertiary times” (Malde 1965:255).

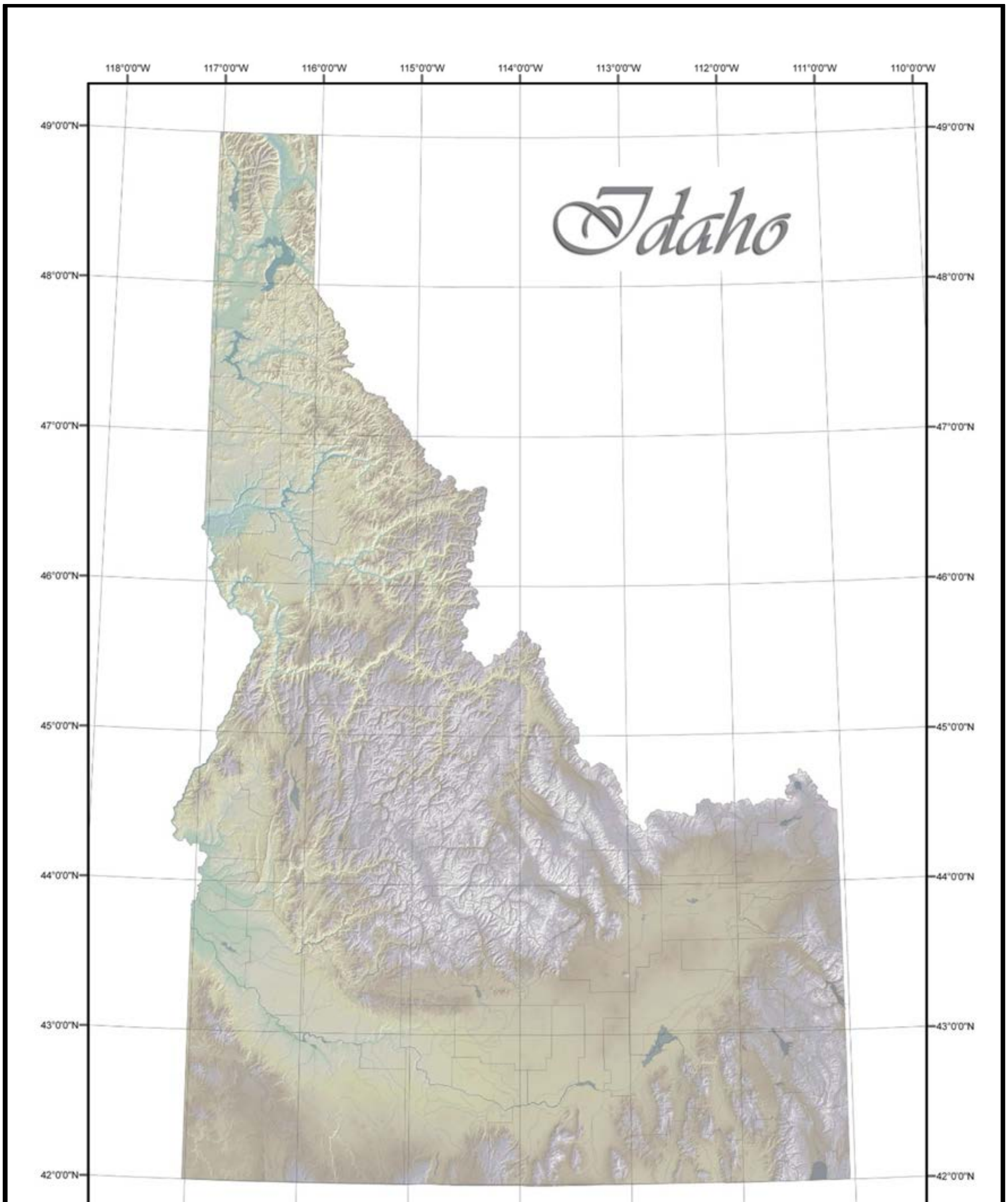

Figure 1.1. Relief Map of Idaho (Idaho State University 2014)

Idaho Obsidian Source Formation

Most obsidian has the same chemical composition as rhyolite or granite (high silica content, especially). Rhyolite results from the mixing of magma and water at a relatively shallow depth below the earth's surface and has smaller crystals than granite, which results from a mixture of magma and water at a relatively deep depth. Obsidian is an extrusive rock that can form when silicic magma cools so rapidly that crystals do not have time to form or as in the case of obsidian flows can be hundreds of feet thick and therefore not cool as quickly, but be so viscous that crystals cannot form (Shackley 2005). Eruptions of obsidian can occur more than once in the same area, resulting in numerous overlaying flows of slightly different geochemical profiles (King 1982).

Obsidian can be found in numerous settings in central and Southern Idaho (Figure 1.2). These settings include Challis volcanic rocks, Idavada volcanics, the Owyhee Plateau, the Snake River Plain, and the Basin and Range Province. The Challis volcanic rocks cover approximately 1,900 square miles in North-Central Idaho and are interbedded with rhyolitic volcanic flows. The Idavada volcanics consist of rhyolitic volcanic rocks located along U.S. Highway 93 and the Idaho-Nevada border. The Owyhee Plateau, located in Southwest Idaho, is characterized by intrusive rhyolites and the Bruneau-Jarbidge eruptive center with rhyolitic flows, located on the eastern margin of the plateau. The Snake River Plain is divided into west and east and was formed by the movement of the continent from northeast to southwest over a volcanic hotspot that creates settling in the crust as the hotspot passes (Brott, Blackwell, and Mitchell 1978; Pierce and Morgan 1992). The Bruneau-Jarbidge eruptive center is believed to be the inception of the Yellowstone "Hotspot" in Idaho, which has created successive calderas from southwest to northeast along the Snake River Plain (Bonnichsen 1982; Pierce and Morgan 1992). Due to this Yellowstone “Hotspot,” the volcanic activity of the eastern Snake River Plain is younger than that of the western Snake River Plain (Pierce and Morgan 1992). The western Snake River Plain trends northwest to southeast, parallel to the orientation of the Basin and Range Province formation of which it is a member. The western Snake River Plain consists of rhyolite and basalt. The eastern Snake River Plain consists of rhyolite from extinct silicic volcanoes along the hotspot’s path (Pierce and Morgan 1992). The northern margin of the Basin and Range Province extends into the eastern half of Idaho and is divided into north and south by the Snake River Plain. The Basin and Range Province is riddled with open fissures constituting the so-called the Great Rift, which has created a thin layer of basalt over the rhyolite present throughout the Snake River Plain (Pierce and Morgan 1992). This suggests that rhyolite flows that may contain obsidian are likely patchy throughout the Snake River Plain. The differing ages and modes of formation of the Challis volcanic rocks, Idavada volcanics, Owyhee Plateau, Snake River Plain, and Basin and Range Province hint at the diversity of the geochemical profiles of any geologic obsidian sources found within similar and very different geologic formations. This diversity of individual elements in the geochemical profiles of known obsidian sources affirms the variability within Idaho. The potentially patchy nature of the rhyolite and possible obsidian outcroppings suggest that our knowledge of the different obsidian sources within Idaho is incomplete.

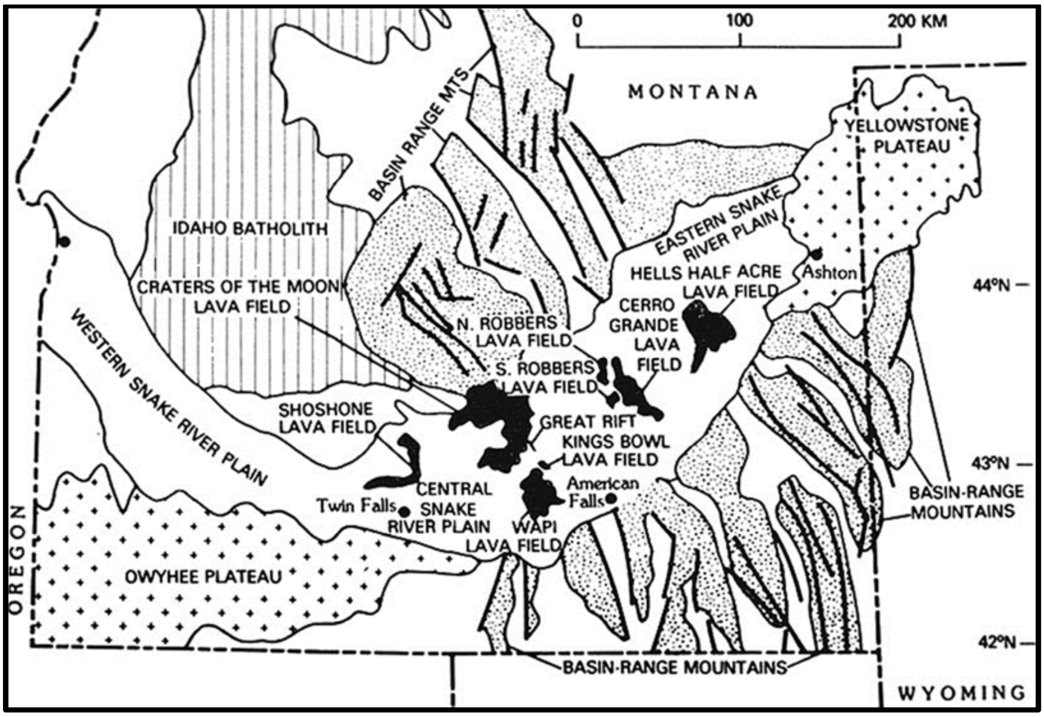

Figure 1.2. Idaho Volcanics (After Kuntz, Champion, Spiker, Lefebvre, and McBroome 1982)

Idaho Obsidian Deposition

Obsidian in Idaho can be deposited in a number of ways through volcanic activity, the result of pyroclastic rocks, and volcanic cones. Pyroclastic rocks consisting of pumice, cinders, crystals, and glass shards (i.e., obsidian) are deposited after violent gas explosions from volcanic vents in decreasing size as the distance increases (Perkins et al. 1995; Shackley 2005). Volcanic cones consist of cinder cones, shield volcanoes (lava domes), and composite cones (stratovolcanoes), all of which are common in Southern Idaho. Cinder cones are loosely consolidated pyroclastic materials located along the Snake River Plain and susceptible to erosion and therefore movement of obsidian material. Lava domes are not as susceptible to erosion because they consist mostly of basalt ranging in size from 100 meters in diameter to 1,000 square kilometers (Shackley 2005). Stratovolcanoes consist of alternating layers of lava and pyroclastic materials, like alternating layers of a cake, some of which are more easily eroded than others. The collapse or explosion of these volcanoes can result in calderas, which are common in southern and East-Central Idaho (Smith and Braile 1994).

Additionally, deposition of loose clastic fragments of obsidian (nodules) of varying sizes occurs through non-volcanic activity as well. Water erodes and moves obsidian clasts. For example, catastrophic events such as the Bonneville Flood 14,500-15,000 years ago moved large amounts of sediment and rock through Red Rock Pass in Southeastern Idaho westward all the way through the Snake River Plain (Malde 1965; O’Connor 1993). Over the duration of the flood, any loose obsidian clasts could have moved downstream hundreds of miles and potentially been deposited up side drainages along the route of the flood. These types of events allow for the possibility of movement downstream, upstream, downhill, and even uphill. These processes can compromise the implied integrity of primary obsidian resource location, resulting in a secondary and equally archaeologically important obsidian resource location. In addition, there can be an expansion of the original size of the source by a factor of 10 or more (Shackley 2005).

CHAPTER TWO: LITERATURE REVIEW

This chapter includes a brief history of X-ray fluorescence, the basic principles used in applying XRF to archaeological provenance studies, and an introduction to previous Idaho provenance studies.

X-Ray Fluorescence Spectrometry of Archaeological Obsidian

The ability to characterize archaeological obsidian is part of the sourcing process. Weigand, Harbottle, and Sayre (1977) proposed the Provenance Postulate, later refined by Neff (2001:107-108): “Sourcing is possible as long as there exists some qualitative or quantitative chemical or mineralogical difference between natural sources that exceeds the qualitative or quantitative variation within each source.” The assumption is that if 1) individual obsidian sources are homogeneous, and 2) the differences between sources are significant, then obsidian sources can be differentiated (Glascock 2002). Obsidian source characterization on a regional level has become increasingly important because samples that were originally considered to originate from a single source have been assigned to multiple sources (Hughes 1998; Shackley 1998a). In the past, entire areas have been grouped as a single source as a result of field sampling strategies and not based on geochemistry or geologic mapping (Hughes 1998).

A Brief History of X-Ray Fluorescence

While X-ray technology was commercially available in the 1950s, it wasn’t until Cann and Renfrew (1964) characterized Mediterranean obsidian that it was first applied to archaeology. For the purpose of geochemical sourcing the first applications of XRF to archaeology in the New World occurred at Berkeley in 1968, 1969, and 1971 (Jack and Heizer 1968; Jack and Carmichael 1969; Shackley 2011; Stevenson, Stross, and Heizer 1971). Brown (1982) and Ebinger (1984) used XRF to discriminate potential obsidian sources by using multivariate statistical methods and were greatly hampered by the lack of comprehensive obsidian source data (Hughes 1997; Nelson 1984).

Studies conducted with portable X-ray fluorescence (pXRF) spectrometry have grown exponentially in the past decade. Between 2007 and 2013, at least 70 publications related to the application of pXRF to obsidian studies, many of which discuss a comparison between XRF and pXRF (Speakman and Shackley 2013).

X-Ray Fluorescence Spectrometry and Obsidian

Obsidian has many attributes relevant to sourcing of artifacts. Obsidian sources are typically geographically restricted to areas of volcanism, except where transported as alluvial clasts. Obsidian artifacts are found in many more locations than are geologic sources. Archaeologically, larger amounts of debitage (and larger sizes of debitage) are typically found closer to prehistoric quarries, and there is a high rate of replacement of tools. The assumption is that a particular source or flow is relatively chemically homogeneous whereas different sources or flows are chemically heterogeneous in a way that can be measured by XRF (Glascock, Braswell, and Cobean 1998; Nelson 1984). In the past, the analyses performed by physicists and chemists have focused on the precision of XRF measurements rather than the archaeological context and application whereas archaeologists have often trusted the accuracy and precision of XRF results without a technical understanding of the process and sources of error (Shackley 2005).

X-ray fluorescence spectrometry measures trace elements in parts per million by either a destructive (ground and pressed pellet sample) or non-destructive (whole rock sample) method of obsidian geochemical profile detection (Shackley 2011). An obsidian sample is irradiated and will re-emit radiation, or fluoresce, which is detected by the instrument in varying intensities depending on the element detected (Jenkins 1974; Goffer 1980; Shackley 2005).

Characterization of obsidian is possible due to trace elements concentrated in the liquid silicic magma, which are often variable between sources and also potentially variable between different eruptions of the same magma source (see Hughes and Smith 1993; Shackley 1992, 1998b, 1998c). For example, obsidian deposited on one side of a caldera can be geochemically heterogeneous from those found miles away (Shackley 2005). Therefore, when these conditions are met, trace elements can be used to indicate an obsidian source and possible sub-sources.

Portable XRF

Over the past decade numerous studies have compared the results of a laboratory XRF analyzer (*l*XRF) and those of a laboratory based pXRF (*l*pXRF) (e.g., Craig, Speakman, Popelka-Filcoff, Glascock, Robertson, Shackley, and Aldenderfer 2007; Nazaroff and Shackley 2009; Pessanha, Guilherme, and Carvalho 2009; Shackley 2005; Williams-Thorpe 2008). Craig et al. (2007) analyzed the same obsidian artifacts with both types of instruments and concluded that there was statistically significant agreement between the source assignment results although there were significant differences between some individual elements. Pessanha et al. (2009:497) concluded that the *l*pXRF had a relatively high background (atmospheric effects) when compared to an *l*XRF, to the point where "some of the trace elements were almost not detected."

Idaho Obsidian Source Studies

Before 1969, the majority of Idaho obsidian sources were unknown or not geochemically characterized, but within a span of three years there were 11 known and recorded obsidian quarry areas (Holmer 1997). Geochemical analysis was performed on these quarry areas in 1979 by Charles Nelson at the University of Massachusetts; no publications resulted from this analysis (Gallagher 1979; Holmer 1997). In 1979, Sappington began a comprehensive study of Idaho obsidian and came to four conclusions (Sappington, 1981a, 1981b): 1) obsidian sourcing was applicable in Idaho; 2) prehistoric peoples had used Idaho obsidian sources; 3) obsidian from multiple Idaho obsidian sources were present in site assemblages; and 4) locating, describing, and geochemically characterizing Idaho obsidian quarries had been achieved. Sappington may have been overly optimistic as Idaho obsidian source geochemical studies continued throughout the 1980s (Green 1982, 1983, 1984; Reed 1985). Bailey's (1992) analysis of obsidian artifacts from the 1988-1989 excavations of Wilson Butte Cave nearly doubled the number of known geochemically distinct Idaho obsidian sources.

Obsidian source geochemical characterization studies in Idaho have continued throughout the intervening 20 years (e.g., Holmer 1997; Skinner, Davis, and Origer 1995; Plager 2001; Willson 2005). Holmer (1997) surveyed the obsidian sources in the 24 eastern counties of Idaho to coincide with the Idaho Museum of Natural History's curated archaeological collections from those same counties. Hughes and Pavesic (2009) examined an existing collection from the DeMoss site in 1985, conducting XRF analysis to augment existing information about the site. There have also been numerous masters' theses regarding Idaho obsidian sources in the last 15 years (Corn 2006; Plager 2001; Thompson 2004; Willson 2005). Plager (2001) from Idaho State University focused on the distribution patterns of obsidian in Southern Idaho and concluded that relatively little exchange occurred across the Snake River. Thompson (2004) from Idaho State University focused on the Malad source on the Snake River Plain and the conveyance of obsidian through direct procurement or exchange/trade to places as far away as Arkansas and Texas. Additionally, Willson (2005) from the University of Idaho addressed issues of mobility, concluding that the incomplete knowledge and point provenance nature of current obsidian source studies in Idaho constrains potential interpretations based on obsidian source characterizations.

In the last decade, only one master's thesis has directly characterized an obsidian source before drawing conclusions about prehistoric mobility. Corn (2006) recorded the extent of the Timber Butte source and established the extent of the geochemical profile of the primary depositional context of the source as part of a systematic survey of the source material and any sites encountered.

CHAPTER THREE: METHODOLOGY

This chapter examines some methodological concerns of applying XRF to the analysis of obsidian and then evaluates the characteristics of obsidian sources.

XRF and Obsidian Sourcing Methods

One issue with lithic sourcing is the difficulty in differentiating between lithic sources geochemically (XRF Analysis), especially when there is variation within a single source (Jones et al. 2003; Shackley 1998a, 2005). A potential source of error exists when comparing data from different labs and different XRF units. This potential source of error can be mitigated to some extent by using sourcing data for artifacts determined by the same laboratory, which increases the likelihood of meaningful comparisons between sites. Creating an accurate or meaningful analysis necessitates recognizing that currently, as well as in the past, there is incomplete knowledge (characterization) of the obsidian sources that were available to prehistoric peoples of any region.

XRF and Obsidian: Methodological Concerns

Potential benefits of XRF are that it is 1) non-destructive, 2) fast, 3) easy to use, 4) cost-effective, 5) and requires minimal preparation (Shackley 2005). Because XRF is non-destructive, it has been used often in geochemical analysis of artifacts. Potential limitations in XRF analysis include artifact size and morphology, variable accuracy due to analysis techniques, and inability of some elements to be detected by XRF (Burley, Sheppard, and Simonin 2011; Davis, Jackson, Shackley, Teague, and Hampel 2011;

Eerkens, Ferguson, Glascock, Skinner, and Waechter 2007; Forster and Grave 2012; Frahm 2013a; Goodale, Bailey, Jones, Prescott, Scholz, Stagliano, and Lewis 2012; Liritzis and Zacharias 2011; Lundblad, Mills, and Hon 2008; Nazaroff, Prufer, and Drake 2010; Phillips and Speakman 2009; Shackley 2005, 2011).

Methodological concerns regarding obsidian artifact samples relate to their size and morphology. Artifact size is restricted for XRF and pXRF in order to provide enough material for analysis and to cover the detection window in pXRF. XRF does not allow for non-destructive analysis of smaller tools (less than 10 mm) that could be indicative of a greater distance between the source and site that is not apparent from the analysis of larger tools (Davis et al. 2011; Eerkens et al. 2007; Frahm 2013a; Goodale et al. 2012; Lundblad et al. 2008; Shackley 2011). Morphologically, an artifact should have a smooth flat surface in order to maintain the best point of contact with x-rays (Burley et al. 2011; Forster and Grave 2012; Frahm 2013a; Goodale et al. 2012; Liritzis and Zacharias 2011; Nazaroff et al. 2010; Phillips and Speakman 2009). These methodological concerns can be addressed by polishing an artifact to create a flat surface, grinding it into a fused powder pellet, and/or relying mainly on the elements least affected by surface morphology: Rb, Sr, Y, Zr, and Nb (Forster and Grave 2012; Frahm 2013a).

Potential issues with pXRF highlighted by Eerkens et al. (2007), Goodale et al. (2012), and Shackley (2005, 2011) include morphological, chemical/elemental, and technical protocols. As a mass analysis technique, variation within an individual artifact is not measured (e.g., banding and multicolor obsidian). The accuracy can be variable, due to the absence of widely accepted and appropriate analytical protocols and standardized techniques. Best suited for metal alloys, pXRF has been used to analyze artwork, ceramics, and lithics. The variable physical properties of lithic materials could affect the analysis (morphology). Additionally, only some elements can be detected due to pXRF power constraints. Fortunately, the elements detected by pXRF are the most relevant to volcanic rocks, although some of the most discriminating elements (e.g., Ba) may not be detected due to power constraints.

There are other differences between the two measurement techniques. Atmospheric effects (absorption of low energy x-rays) may become a concern for *l*pXRF, whereas *l*XRF runs samples in a vacuum. For both instruments, there is a trade-off between increased analysis time (greater precision) and the time and effort requirements of doing so (Giauque, Asaro, Stross, and Hester 1993; Shackley 2002). To create opportunities for comparison between lab and instrument results, it is necessary to calibrate all *l*pXRF and *l*XRF instruments using international standards (Shackley 2011).

A related pXRF methodological debate is reflected in the exchange between Ellery Frahm, and Robert Speakman and M. Steven Shackley (Frahm 2013a, 2013b; Speakman and Shackley 2013). The parties disagree as to the result expected from pXRF analysis. Frahm (2013a, 2013b) evaluates artifact source assignment on a more or less case-by-case basis. In contrast, Speakman and Shackley (2013) focus on the underlying methodology, the geochemistry of the obsidian source, and the comparability of datasets by calibration with an international standard. The goal of pXRF should consider and address both these points of view. Frahm (2013a, 2013b) and Speakman and Shackley (2013) agree that validity and reliability in pXRF analysis are essential in sourcing studies but disagree on how to best attain this. Frahm maintains that obtaining validity and reliability is best achieved by correlating measurements (e.g., ppm). Speakman and

Shackley assert that if one experiment cannot be compared with others, and therefore evaluated, it may be internally consistent (internally reliable) but is unreliable across labs and instruments because it cannot be reproduced. Accuracy is not straightforward in pXRF analysis because it implies that the result of the measurement and the truth of the source are in agreement. With changing technology, geochemical profiles need to be revisited and updated, even if producing at best only a precise (consistent) measurement, which may or may not be accurate. It is important that an obsidian source be exhaustively geochemically characterized if the intention is to source obsidian artifacts and results that are replicable by different labs and instruments.

Frahm’s approach may not be a best practice for Idaho because a large proportion of the landscape has been formed by spatially continuous and varying volcanic events. To enable comparison between studies, it may be useful to create a statistically based analysis protocol to assign an obsidian source to an artifact rather than to trust an analyst’s judgment and potential observer error. It may be useful to also create a publicly available online database of obsidian source geochemical profiles and information regarding how such geologic sample data was collected.

Idaho Obsidian Source Profiles and Locations

Obsidian source profiles are a distinct set of elements (absolute measurements and ratios) that define and characterize a particular spatially restricted obsidian locality. Obsidian source data from Idaho Museum of Natural History (IMNH) indicates numerous sources in Eastern Idaho and a relative scarcity of sources in Western Idaho. Conversely, obsidian source data from Northwest Research Obsidian Studies Laboratory (NWROSL) indicates numerous sources in Western Idaho and a relative scarcity of sources in Eastern Idaho. Source data from both labs could be complimentary if pooled for future studies. Idaho obsidian data from the IMNH includes 19 unique source profiles and 33 unique source locations (Holmer 1997). This IMNH discrepancy between source data and location information exists because the data is unpublished and unavailable for analysis. Idaho obsidian source data from the NWROSL included 18 unique source profiles and the corresponding locations. Obsidian source profiles and locations from the two XRF labs do not have a one-to-one correspondence. There appear to be gaps in both labs' source profiles, as well as a problem of scale, likely due to a local or regional approach to data collection. Of the 37 total source profiles (19 from IMNH and 18 from NWROSL), ten have the same name and general location while 27 source profiles have different names and locations (Figure 3.1). NWROSL has source profiles from all the states in the northwest, while IMNH only has source profiles from Southern Idaho.

While IMNH may have many more distinct source profiles from the eastern half of Idaho at a smaller scale than NWROSL, NWROSL has source and sub-source profiles on a larger scale. NWROSL also has more distinct source profiles from the western half of Idaho but appears to aggregate potential subsources in Eastern Idaho (Figure 3.1 & 3.3, Table 3.1, Appendix Table A).

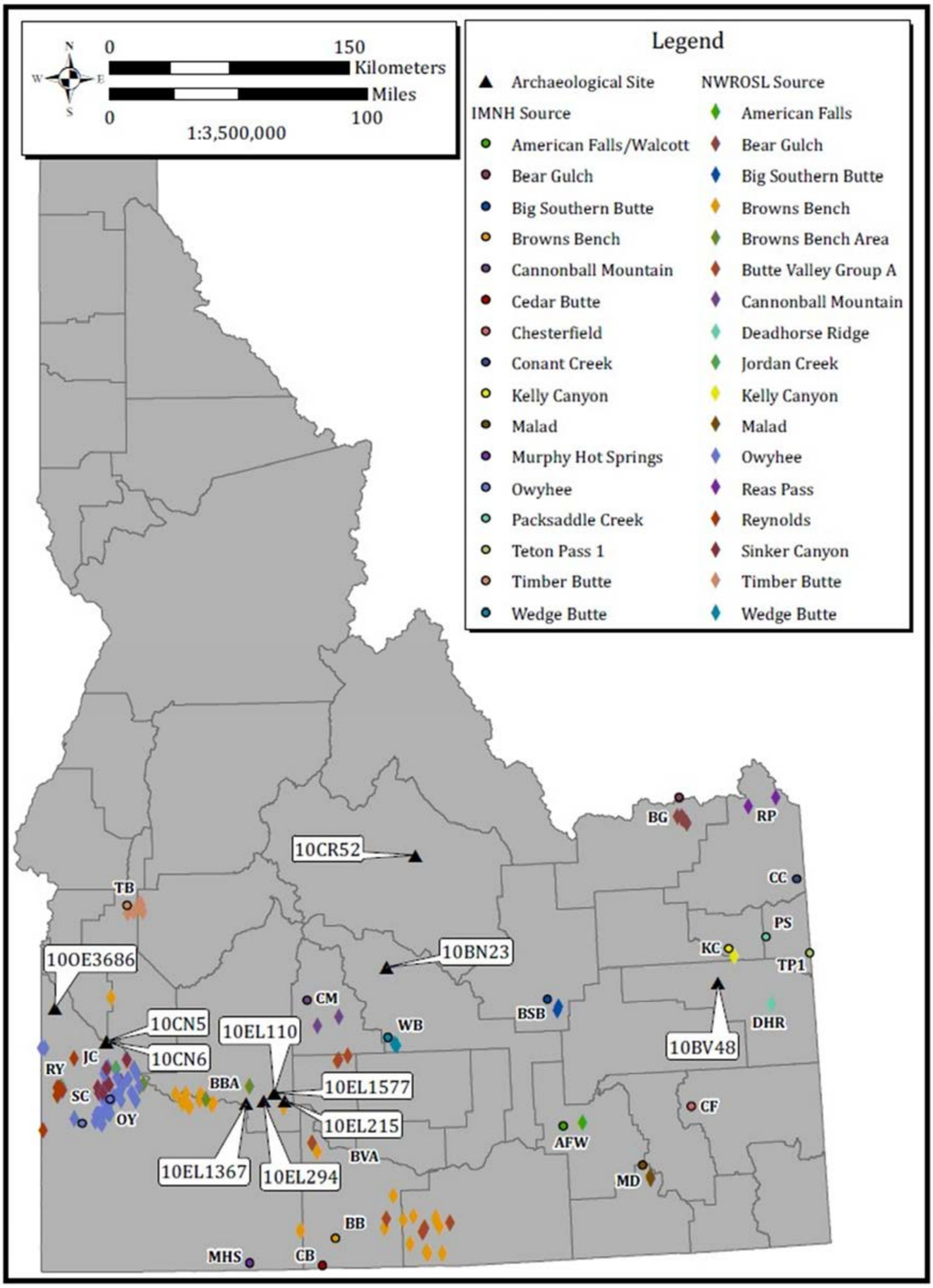

Figure 3.1. Idaho Obsidian Sources and Sites in this Study

Table 3.1 Idaho Obsidian Source Profiles by XRF Lab

Source	County	IMNH	NWROSL
American Falls (Walcott)	Power	X	X
Bear Gulch	Clark	X	X
Big Southern Butte	Butte	X	X
Browns Bench	Cassia Twin Falls Owyhee	X	X
Browns Bench Area	Elmore Twin Falls Owyhee	--	X
Butte Valley A	Cassia Gooding Twin Falls Owyhee	X	X
Cannonball Mountain (Cannonball Mountain 1)	Camas	X	X
Cannonball Mountain 2	Camas	X	--
Cedar Butte	Twin Falls	X	--
Chesterfield	Caribou	X	--
Conant Creek	Fremont	X	--
Deadhorse Ridge	Bonneville	--	X
Jordan Creek	Owyhee	--	X
Kelly Canyon	Madison	X	X
Malad	Bannock Oneida	X	X
Murphy Hot Springs	Owyhee	X	--
Obsidian Cliff	In Wyoming State	X	--
Owyhee	Owyhee	X	X
Pack Saddle	Teton	X	--
Reas Pass	Fremont	X	X
Reynolds	Owyhee	X	X
Sinker Canyon	Owyhee	--	X
Striker Basin Gulch	Owyhee	--	X
Teton Pass 1	Teton	X	--
Timber Butte	Boise Gem	X	X
Wedge Butte	Blaine	X	X

Comparison of IMNH and NWROSL Obsidian Source Characteristics

Only 10 elements characterize the obsidian source profiles at IMNH, while the profiles at NWROSL are characterized by 13 elements. Skinner (personal communication 2014) has indicated that the analytical precision for rubidium (Rb), strontium (Sr), yttrium (Y), zirconium (Zr), and niobium (Nb) at NWROSL is particularly good and that barium (Ba) can be especially helpful in discriminating between obsidian subsources and sources. For example, Malad, Idaho, and Cow Canyon, Arizona, require a precise barium measurement to discern between the two sources (Shackley 2011). Due to power constraints, the Bruker *l*pXRF used at IMNH is unable to detect a measurable amount of barium (Ba). Because of this constraint, Ba cannot be used in inter-lab comparisons. This difference in measurable elements may provide an explanation for the incorrect assignment of sources (Hughes 1984; Shackley 2011).

Mapping of Lithic Sources Relative to Sites

Latitudinal and longitudinal coordinates of the geologic samples from NWROSL were plotted against locations digitized from the map of obsidian sources in Holmer (1997). Latitude and longitude were plotted to two decimal points, which introduces a potential for error of approximately one mile in establishing the location of the geologic source. The digitization of the source map in Holmer (1997) can potentially introduce as many as six miles of error in plotted locations. Additionally, archaeological sites were plotted according to their Township, Range, and Section location, thus introducing the potential for one mile of error in site location. Considering these potential sources of error, while there are many co-occurrences of sources between labs, there are also instances of no overlap. The co-occurrences of sources between labs correspond to the sources with the same or similar names (Table 3.1, Figure 3.2).

Data Collection Methods

Analysis of 174 obsidian artifacts from 11 Idaho archaeological sites was performed with a pXRF Bruker Tracer 3-V spectrometer at IMNH in Pocatello, Idaho (Picture 1). The IMNH Bruker is equipped with a rhodium (Rh) tube, a 170 eV resolution silicon PIN diode detector, operating at 40kV and 12µA with an external power source (at 1000 counts per second) for 200 live seconds in an area of 7 mm^2 (Bruker 2014).

Four of these sites were previously analyzed by NWROSL with a Spectrace 5000 spectrometer (Picture 2). This includes artifacts from 10CN5 (n=7) and 10CN6 (n=7), as well as artifacts from 10EL110 (n=3) and artifacts from 10EL215 (n=4) (Figure 3.2). Three of the 11 sites are from collections housed at the Idaho Museum of Natural History (IMNH): 10BN23, 10BV48, and 10CR52; and eight sites from Boise State University (BSU): 10CN5, 10CN6, 10EL110, 10EL215, 10EL294, 10EL1367, 10E L1577, and 10OE3686.

Non-destructive *l*pXRF analysis has two main constraints: 1) the size of the artifact needs to be at least 10 mm wide or cover the detector window to result in a consistent element profile, and 2) artifacts need to be at least 3 mm thick (Forster, Grave, Vickery, and Kealhofer 2011; Nazaroff and Shackley 2009; Shackley 1998a). A stratified sample of artifacts was selected from each site using the following order of decreasing priority: any samples previously run by NWROSL; temporally or culturally diagnostic projectile points representative of each point type for each site; and samples from horizontally and vertically dispersed excavation units for relatively complete coverage of the site and relative temporal control. Specimens from the three IMNH sites include flakes and cores as well as diagnostic projectile points. Specimens from sites 10CN5, 10CN6, 10EL110, and 10EL215 (which were previously analyzed at NWROSL) included diagnostic projectile points in addition to flakes and cores.

The whole rock obsidian artifacts were analyzed over a one-week period at IMNH using a Bruker Tracer 3-V portable XRF spectrometer and accompanying S1PXRF software. The instrument was calibrated at the beginning of each day with an electronic file of element (considered useful in obsidian source identification) values of obsidian sources from around the world as determined by the University of Missouri Research Reactor Archaeometry Laboratory. The following elements were calibrated: manganese (Mn), iron (Fe), zinc (Zn), gallium (Ga), thorium (Th), rubidium (Rb), strontium (Sr), yttrium (Y), zirconium (Zr), and niobium (Nb) (Speakman 2012). The Bruker was mounted in a plastic stand to fix the position and standardize the distance between the detector and the artifact. Artifacts were analyzed for 200 live seconds three separate times with a slight rotation/shift over the instrument detector to address morphological variation and obtain an average reading. Artifacts were positioned with the unlabeled side (if there was a label) toward the detector and positioned with the flattest or concave portion over the detector to minimize the diffusion of x-rays and maximize contact with the artifact (following Nazaroff et al., 2010). The Bruker measured 10 elements: manganese (Mn), iron (Fe), zinc (Zn), gallium (Ga), thorium (Th), rubidium (Rb), strontium (Sr), yttrium (Y), zirconium (Zr), and niobium (Nb). Of these elements, Fe, Rb, Sr, Y, Zr, and Nb are considered most reliable for non-destructive XRF as well as geochemical markers for obsidian sourcing (e.g., Nelson 1984).

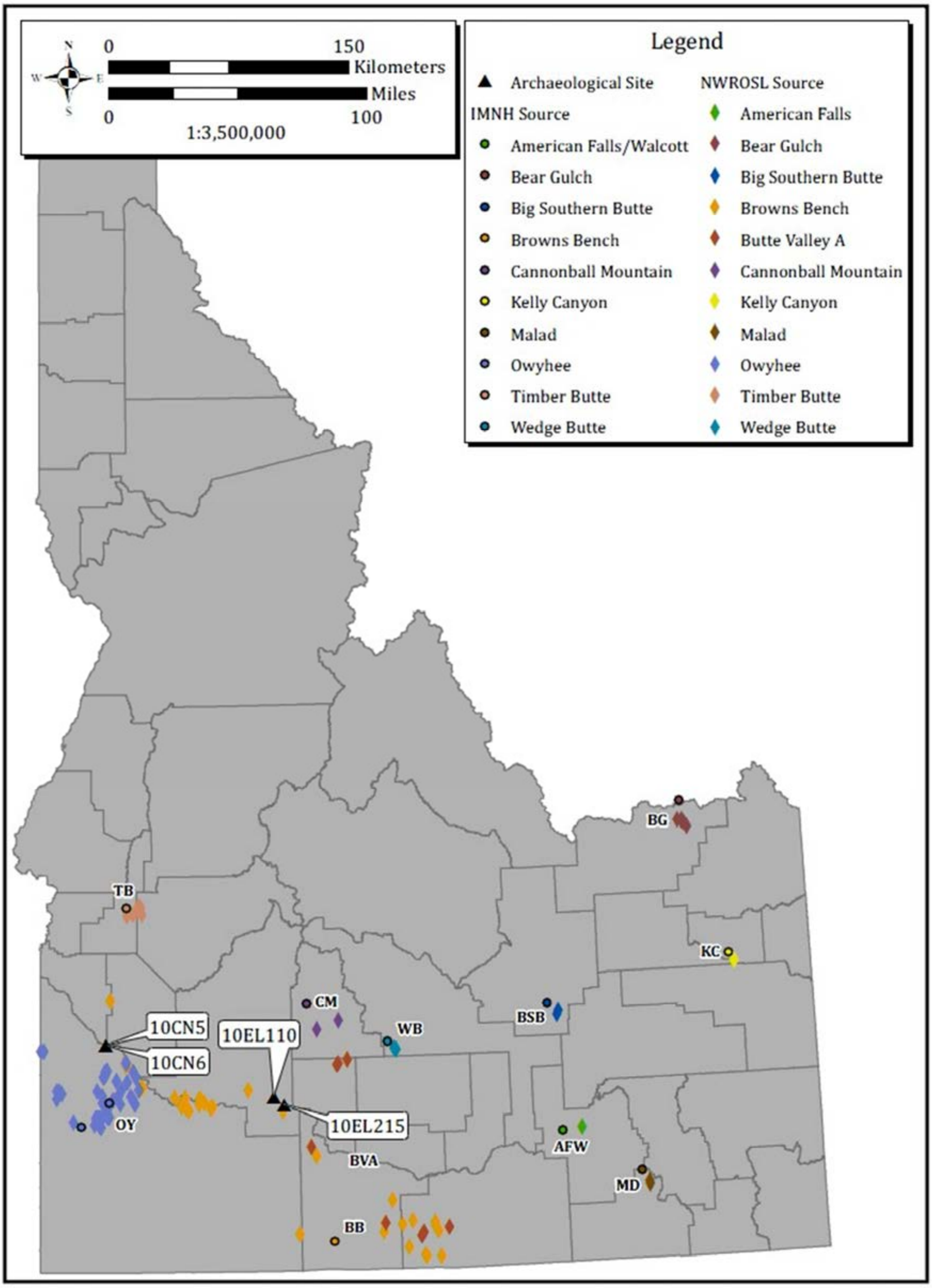

Figure 3.2. Similarly Named Obsidian Sources and Selected Sites

The initial artifact-to-source assignment was done non-statistically by comparing ratios of absolute mean values of elements, considering one standard deviation for each artifact and each source (Table 3.2). One standard deviation was used because the use of more than one standard deviation of artifact or source resulted in an individual being assigned to multiple obsidian sources.

Table 3.2 XRF Sourcing of Archaeological Site Samples

Site	**County**	**Known**	**Unknown**	**Total**	**Assigned to Source**
10BN23	Blaine	25	7	32	78%
10BV48	Bonneville	21	3	24	88%
10CN5	Canyon	4	4	8	50%
10CN6	Canyon	8	5	13	62%
10CR52	Custer	16	6	22	73%
10EL110	Elmore	13	1	14	93%
10EL215	Elmore	20	5	25	80%
10EL294	Elmore	4	1	5	80%
10EL1367	Elmore	3	2	5	60%
10EL1577	Elmore	12	0	12	100%
10OE3686	Owyhee	4	10	14	29%
Total		**130**	**44**	**174**	

A total of 130 artifacts were assigned to a particular source using this approach, while 44 artifacts could not be assigned to any specific source. It appears that the farther west the location of the site, and possibly the source, the less likely the artifacts are to be assigned to a particular geologic source using IMNH source reference profiles (Figure 3.1). A potential reason for this is apparent in the map of Idaho obsidian sources provided by Holmer (1997) (Figure 3.3). While obsidian sources are distributed along the margins of the entire Snake River Plain, a preponderance of recorded sources occur in Eastern Idaho. Obsidian sources present in sites in Western Idaho may not have been adequately sourced by IMNH, or there may be fewer known obsidian sources. Another reason for the disparate number of sources between Eastern and Western Idaho could be related to the age of the obsidian source. Sources in Western Idaho are older than those in Eastern Idaho and are more likely to be eroded or covered in silt and therefore less defined or recognizable as sources.

Previous artifact analysis at Northwest Research Obsidian Studies Laboratory (NWROSL) was performed between 1995 and 2013 using a Spectrace 5000 X-ray fluorescence spectrometer, which detects 13 elements relevant to obsidian identification (Picture 2). The Spectrace 5000 is equipped with a Si (Li) detector having a resolution of 155 eV FWHM for 5.9 keV X-rays (at 1000 counts per second) in an area of 30 mm^2. It has a Bremsstrahlung type X-ray tube, a rhodium (Rh) target, and a 5 mil beryllium (Be) window with a 50kV 1 mA high-voltage power supply and a voltage range of 4 to 50 kV (e.g. Skinner et al. 1995, Skinner and Thatcher 2013). The Spectrace 5000 measures 13 elements: manganese (Mn), iron (Fe), zinc (Zn), gallium (Ga), thorium (Th), rubidium (Rb), strontium (Sr), yttrium (Y), zirconium (Zr), niobium (Nb), barium (Ba), lead (Pb), and titanium (Ti).

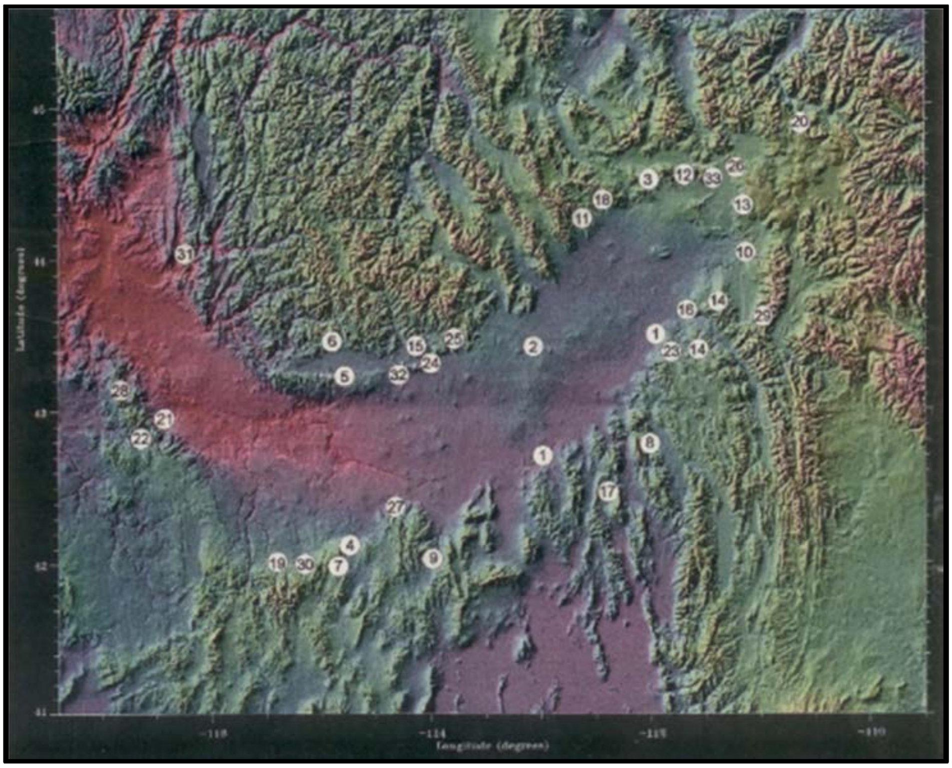

Figure 3.3. Volcanic Glass Quarry Locations (Holmer 1997)

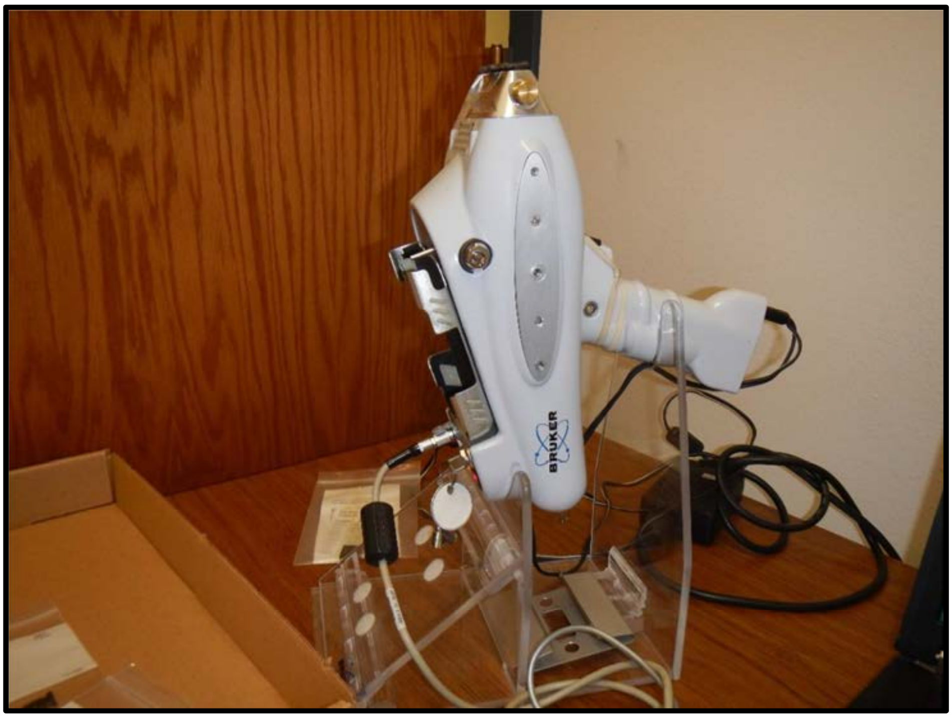

Picture 1. Bruker Tracer 3-V Portable XRF Spectrometer

Picture 2. **Spectrace 5000 X-ray Fluorescence Spectrometer**

CHAPTER FOUR: DATA ANALYSIS

The intent of this chapter is to report the applicability of combining obsidian source geochemical profiles from different labs in an effort to assign sources to obsidian artifacts in instances in which labs do not have completely characterized source profiles of the region.

XRF Analysis Steps

First, the analysis of a library standard was used to determine the reliability or drift inherent in the pXRF instrument used in the analysis. This was accomplished by performing a one-sample t-test on the means and coefficients of variation obtained over the course of the analysis (in this case a week) (Glascock et al. 1998). After the Bruker pXRF instrument was determined to be internally reliable, the next step was to perform a paired sample t-test on the means and coefficients of variation for artifact geochemical profiles of samples run at both the IMNH and NWROSL labs. This was done in an effort to determine to what extent the artifact profiles might be comparable. As a last check of inter-lab comparability, a one-tailed Pearson’s correlation coefficient was used to compare the measurements of elements at each lab.

Analysis of IMNH Library Standard

The Bruker pXRF and S1PXRF software is calibrated whenever in operation by an obsidian calibration file from the University of Missouri Research Reactor Archaeometry Laboratory (Buck Benson, IMNH, personal communication 2014). In addition to the calibration file, the IMNH uses a library standard (Tile 0) to test the reliability of the Bruker pXRF over time. The obsidian source used as the standard is a sample collected from Bear Gulch, located near the Idaho-Montana border in Clark County, Idaho. The Bear Gulch reference tile was analyzed 18 times (Tile 1-18) over the week at the IMNH. Measurement intervals were established as occurring at least once each morning, midday, and end of the day or during any break in analysis runs (Appendix Table B.). A one-sample t-test was used to compare the element means of the reference tile (Tile 0) to the tile analyzed 18 times over the course of the week. The means of the 10 elements (Mn, Fe, Zn, Ga, Th, Rb, Sr, Y, Zr, and Nb) measured by the Bruker were not significantly different ($p<.05$) from those of the reference tile (Tile 0). This implies that the Bruker's measurement of the elements was internally consistent (reliable) over the course of the week (Table 4.1).

Table 4.1 Bruker Reliability Measured by Element Means

Element	Tile 0	Tile Means	Significance
Manganese	308.0556	299.2891	.438
Iron (Fe)	11229.1100	11207.9948	.692
Zinc (Zn)	63.2105	61.8739	.155
Gallium (Ga)	17.2086	17.1040	.249
Thorium (Th)	19.7930	19.4774	.298
Rubidium (Rb)	165.2724	165.6109	.701
Strontium (Sr)	49.6528	49.2374	.445
Yttrium (Y)	42.4712	42.5879	.802
Zirconium (Zr)	300.3661	302.2822	.133
Niobium (Nb)	52.1023	52.0218	.823
Barium (Ba)	N/A	N/A	N/A
Lead (Pb)	N/A	N/A	N/A
Titanium (Ti)	N/A	N/A	N/A

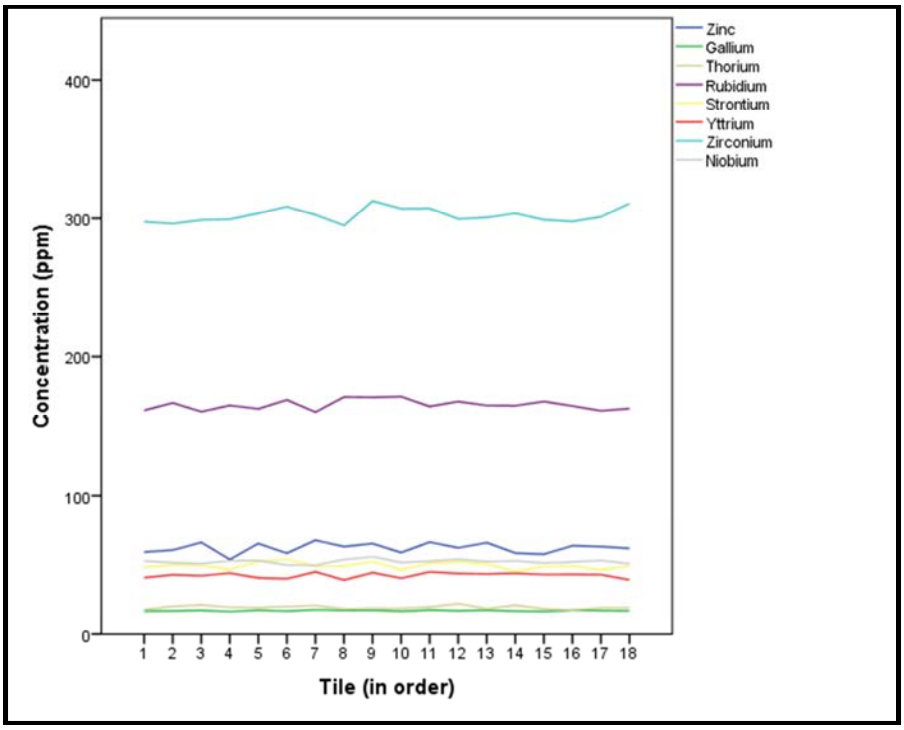

Figure 4.1. **Element Concentration (ppm) of 18 Runs of the Reference Tile.**

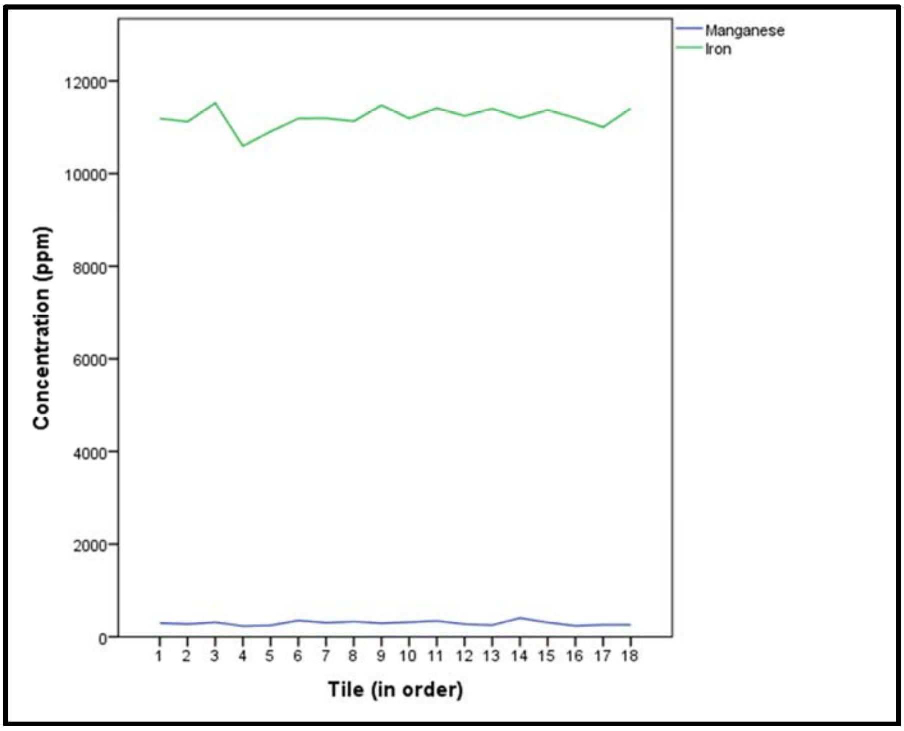

Figure 4.2. **Element Concentration (ppm) of 18 Runs of the Reference Tile.**

Figures 4.1 and 4.2 support the assessment drawn from the comparison of means of the tile runs that instrumental drift is a not an issue due to the relative “flatness,” or stability, of the readings over time, suggesting that there was little analytical error introduced into the artifact readings from the instrument. This within-lab reliability test suggests that any variation in measurements of elements from the artifacts run over the course of the week was due to geochemical variation in the artifact and not due to the instrument.

Analysis of Obsidian Profiles

Common source profiles indicate the relative frequency of a set of elements. A comparison of means and coefficients of variation was performed on the common source profiles and the obsidian artifacts run at both labs. The mean assesses the between-lab reliability while the coefficient of variation indicates within-lab reliability and precision. Additionally, Pearson’s correlation coefficient was performed element by element to measure the standardized strength of any relationship that might exist between the elements as measured at each lab.

Artifact Profile Means, Coefficients of Variation, and Correlation

Comparison of the means for artifacts analyzed at both labs shows that iron (Fe), rubidium (Rb), and yttrium (Y) are consistently measured differently at each lab. The means for the other elements are not significantly different between labs, suggesting that such means are comparable. The coefficient of variation is significantly different for all elements except manganese (Mn) and iron (Fe), suggesting that NWROSL has greater measurement variation (lower within-lab reliability) for seven elements (Zn, Ga, Th, Sr, Y, Zr, and Nb) and lower measurement variation for one element (Rb) (Table 4.2). The results of the paired sample t-tests of means and coefficients of variation on the same artifacts suggest that there is measurement error between the instruments.

Table 4.2 Obsidian Artifact Profile Comparison Between Labs

Element	**Test**	**IMNH**	**NWROSL**
Manganese	Mean	258	235
(Mn)	CV	.19	.19
Iron	Mean	10140*	9779*
(Fe)	CV	.09	.12
Zinc	Mean	59	63
(Zn)	CV	.09*	.19*
Gallium	Mean	17	18
(Ga)	CV	.02*	.30*
Thorium	Mean	22	21
(Th)	CV	.05*	.21*
Rubidium	Mean	198*	224*
(Rb)	CV	.04*	.02*
Strontium	Mean	35	35
(Sr)	CV	.08*	.29*
Yttrium	Mean	43*	46*
(Y)	CV	.05*	.08*
Zirconium	Mean	253	253
(Zr)	CV	.03*	.05*
Niobium	Mean	29	29
(Nb)	CV	.06*	.10*
*means or coefficients of variation are significantly different between labs, paired-sample t-tests, *p* < .05.			

A one-tailed Pearson’s correlation coefficient of artifacts analyzed at both labs provides a significant (*p* < .01) positive relationship between the means of all the elements except thorium (Th) and gallium (Ga). Thorium (Th) has a weakly positive correlation (*p* < .05) for the paired artifact measurement, whereas gallium (Ga) is not significantly correlated between labs for the paired artifact measurements (Table 4.3).

Gallium (Ga) continues to be non-significant in further analysis (e.g., discriminant function analysis). This suggests that as the concentration (ppm) increases or decreases at one lab, a similar increase or decrease in the absolute measurement value should occur at the other lab. In the case of thorium (Th), there is also a correlated increase or decrease between labs, but the strength of the correlation is notably weaker ($r = 0.402$). Positively correlated elements between labs for a given artifact should reflect the same relative abundance across all elements in a profile, even though the absolute values of individual elements may be significantly different. Significant correlations exist for most of the elements between the two labs despite having a relatively small sample size because the correlations were so strong (between .929 and .999). A larger sample size would permit determining if the weaker correlation (Ga) would have a significant relationship.

Table 4.3 Pearson's Correlation Coefficient of Artifact Elements

Element	Coefficient
Manganese (Mn)	.852**
Iron (Fe)	.915**
Zinc (Zn)	.941**
Gallium (Ga)	.321
Thorium (Th)	.402*
Rubidium (Rb)	.945**
Strontium (Sr)	.929**
Yttrium (Y)	.993**
Zirconium (Zr)	.999**
Niobium (Nb)	.996**

*significant correlation between elements at both labs, $p < .05$.

**significant correlation between elements at both labs, $p < .01$.

Source Profile Means, Coefficients of Variation, and Correlation

The obsidian source profile comparison of means between labs also shows that the elements gallium (Ga), rubidium (Rb), strontium (Sr), and yttrium (Y) are consistently detected differently between the labs. The means for the other elements are not significantly different between labs, suggesting the means for those elements are comparable. The coefficients of variation are significantly different for iron (Fe) and gallium (Ga), suggesting that NWROSL has greater measurement variation (lower within-lab reliability) than IMNH for these elements (Table 4.4). The results of the paired sample t-tests of means and coefficients of variation on the same artifacts suggest that there is measurement error between the instruments as well as natural variation within the source.

A one-tailed Pearson’s correlation coefficient of sources common to both labs but independently created indicates a significant ($p < .01$) positive relationship between the means of all of the elements detected at both labs (Table 4.5). This suggests that as the concentration (ppm) increases or decreases in measurements at one lab, the other lab should see a correlated increase or decrease in measurements. Positively correlated elements between labs for a given source should reflect the same relative abundance across all elements in a profile, even though the absolute values of individual elements may be significantly different. Significant correlations exist for the elements between the two labs despite having a relatively small sample size because the correlations were so strong (between .774 and .996).

Table 4.4 Obsidian Source Profile Comparison Between Labs

Element	Test	IMNH	NWROSL
Manganese (Mn)	Mean	328	317
	CV	.17	.17
Iron (Fe)	Mean	13162	15333
	CV	.06*	.12*
Zinc (Zn)	Mean	92	105
	CV	.15	.14
Gallium (Ga)	Mean	20*	24*
	CV	.05*	.18*
Thorium (Th)	Mean	27	27
	CV	.07	.14
Rubidium (Rb)	Mean	222*	249*
	CV	.04	.05
Strontium (Sr)	Mean	36*	33*
	CV	.09	.10
Yttrium (Y)	Mean	78*	87*
	CV	.05	.08
Zirconium (Zr)	Mean	314	326
	CV	.08	.04
Niobium (Nb)	Mean	78	80
	CV	.10	.07

*means or coefficients of variation are significantly different between labs, paired-sample t-tests, *p* < .05.

Table 4.5 Pearson's Correlation Coefficient of Source Elements

Element	Coefficient
Manganese (Mn)	.904**
Iron (Fe)	.774**
Zinc (Zn)	.882**
Gallium (Ga)	.918**
Thorium (Th)	.830**
Rubidium (Rb)	.996**
Strontium (Sr)	.994**
Yttrium (Y)	.990**
Zirconium (Zr)	.995**
Niobium (Nb)	.993**

*significant correlation between elements at both labs, *p* < .05.

**significant correlation between elements at both labs, *p* < .01.

Summary of Comparisons Between IMNH and NWROSL Source Profiles

The tests within this chapter provide information about the viability of using pXRF and the IMNH lab's ability to be combined into a wider dataset. The Bruker's measurement of trace elements was internally reliable over the course of the analysis. The results of the means and coefficients of variation tests indicates the between-lab and within-lab analysis is to be cautiously optimistic in moving forward with further analysis. The Pearson's correlation coefficient indicates that, although the means and coefficients of variation differences suggest caution, the significantly positive correlations on an element-by-element basis reflect a potentially quantifiable consistent and systematic difference between the labs. Thus a future application of a correction may be appropriate for a direct one-to-one comparison between labs in a master database of regional obsidian source geochemical profiles. Given that most variation is between-source (not between-lab), and that sourcing methods are more sensitive to the relative abundance of elements across a profile rather than to differences in absolute amounts of single elements, minor measurement variations between these labs should not preclude a pooling of profiles from the two labs in statistical procedures that assign geologic sources to artifacts.

CHAPTER FIVE: ADDITIONAL DATA ANALYSIS

The previous chapter indicated the potential for pooling obsidian source geochemical profiles in order to fill any gaps in sources that may exist between the two labs. This chapter explores statistical approaches of source assignment to artifacts.

Additional XRF Analysis Steps

Data manipulation for further analysis includes removing records and replacing missing values with the group mean where appropriate (Table 5.1). In one case, Obsidian Cliff in Wyoming was not considered in further analysis due to this study being limited to Idaho sources and archaeological sites. Means could not be imputed for any missing values of IMNH source profiles due to lack of availability of individual records. Analysis that included IMNH source profiles was conducted using the known average and standard deviation for those sources. IMNH source profiles for Butte Valley A and Timber Butte were removed from further analysis due to the missing mean thorium (Th) values because thorium appears to be useful in discriminating between sources. For the 769 individual source profiles from NWROSL, only one case was from Striker Basin Gulch. Therefore, along with missing values for four elements (Mn, Fe, Ba, Ti), it was dropped from further analysis.

The comparison of elements between labs using the Pearson’s correlation coefficient (Table 4.5) suggests that a comparison of standardized measurements of the data is possible. Glascock et al. (1998), Craig et al. (2007), Millhauser, Rodrigues-

Alegria, and Glascock (2011) have found that “best practice” for obsidian source comparison and assignment is to carry out a Log-10 transformation of both artifact and source data. A Log-10 transformation has two purposes: 1) it normalizes the data, and 2) it standardizes the values to help insure that each element contributes relatively equal weight in determining source attributions (Glascock et al. 1998). Therefore, all additional statistical tests were conducted on Log-10 transformed values. Values of zero existed for barium (Ba) for a number of the NWROSL samples, which resulted in a missing Log-10 value in SPSS; since the Log-10 of zero is undefined, the cases would be dropped from further analysis. To include these cases and barium (Ba), which can be important in the analysis, it became necessary to create a value that would not obscure the barium (Ba) values of other samples; hence, a value of 0.01 was substituted for these zeroes before the Log-10 transformation (Table 5.2).

Table 5.1 Number of Cases for Which Means Were Imputed for NWROSL Missing Values by Source and Element

Source	**Mn**	**Fe**	**Zn**	**Ga**	**Th**	**Sr**	**Ba**	**Pb**	**Ti**
Browns Bench	8	8	8	8	10			8	8
Big Southern Butte						5			
Butte Valley A					5				
Owyhee	3	3	9				3		3
Reynolds	1	1				3			1
Timber Butte			1						

The sample size of individual source profiles provided by the NWROSL was reduced from 769 to 705 after initial data exploration to remove the outliers. These outliers are explored more fully in the discussion section of this thesis, but it is relevant to know that 64 samples were not statistically indicative of the obsidian sources to which they were attributed and were therefore removed.

Table 5.2 NWROSL Values of Zero Changed to 0.01 Prior to Log-10 Transformation

Source	Barium
Big Southern Butte	4
Cannonball Mountain	17
Reynolds	23
Wedge Butte	14

Analysis of Obsidian Profiles

Multivariate statistical analysis, such as discriminant function analysis and principal component analysis, can isolate the elements most indicative of obsidian resources in a region and provide a means to assign artifacts to particular obsidian sources (Glascock et al. 1998). Hierarchical cluster analysis can combine cases from the bottom up, assigning sources and artifacts into clusters of similar cases.

Discriminant Function Analysis (DFA) of Obsidian Sources

DFA creates a predictive model of group membership based on the combination of a set of variables (in this case, elements) that discriminate the best between known groups (SPSS 20.0). The variables have been entered with a step-wise method using a Mahalanobis distance technique that measures how much a case's values differ from the average of all cases (Glascock et al. 1998; Hughes 1984). The Mahalanobis distance is used to identify and measure the similarity between an unknown and known sample. It is different than Euclidean distance, because it takes into account the correlations within the data set (SPSS 20.0). A potential limitation of using DFA is that it assumes that all artifacts and/or sources belong to a known group (Glascock et al. 1998). Due to this limitation, DFA is only used to check source-to-source assignment in this thesis. The benefit of using all or most of the elements for DFA is that the relationship between all or most of the elements can be analyzed, whereas with a bi-plot or ternary plot only two or three elements can be used.

Table 5.3 Discriminant Function Analysis Eigenvalues

Function	Eigenvalue	% of Variance	Cumulative %	Canonical Correlation	Element(s)
1	224.264	69.2	69.2	.998	Zr
2	47.195	14.6	83.7	.990	Zr, Y
3	30.739	9.5	93.2	.984	Zr, Y, Sr
4	9.977	3.1	96.3	.953	Zr, Y, Sr, Th
5	7.550	2.3	98.6	.940	Zr, Y, Sr, Th, Rb
6	1.756	.5	99.1	.798	Zr, Y, Sr, Th, Rb, Pb
7	1.316	.4	99.5	.754	Zr, Y, Sr, Th, Rb, Pb, Mn
8	.809	.2	99.8	.669	Zr, Y, Sr, Th, Rb, Pb, Mn, Nb
9	.370	.1	99.9	.520	Zr, Y, Sr, Th, Rb, Pb, Mn, Nb, Zn
10	.167	.1	100.0	.378	Zr, Y, Sr, Th, Rb, Pb, Mn, Nb, Zn, Ba
11	.101	.0	100.0	.303	Zr, Y, Sr, Th, Rb, Pb, Mn, Nb, Zn, Ba, Ti
12	.030	.0	100.0	.170	Zr, Y, Sr, Th, Rb, Pb, Mn, Nb, Zn, Ba, Ti, Fe
The first 12 canonical discriminant functions were used in the analysis.					

DFA identified a set of elements that best discriminated 16 geographic sources for 705 NWROSL samples of known origin in Idaho. The variables were entered using a step-wise method that entered variables forward and backward, with addition or removal depending on the Mahalanobis distance. The results of DFA of individual Log-10 transformed NWROSL source profiles observations, including all 13 elements (12 elements retained), show that only five elements (Zr, Y, Sr, Th, Rb) common between labs are necessary to account for 98.6% of the variation observed (Table 5.3). The 13th element gallium (Ga) was dropped entirely, suggesting that it is not an important element in discriminating obsidian sources (Craig et al. 2007).

Bi-plots of the top two functions of the 12 and five elements DFAs are displayed in Figures 5.1 and 5.2, respectively.

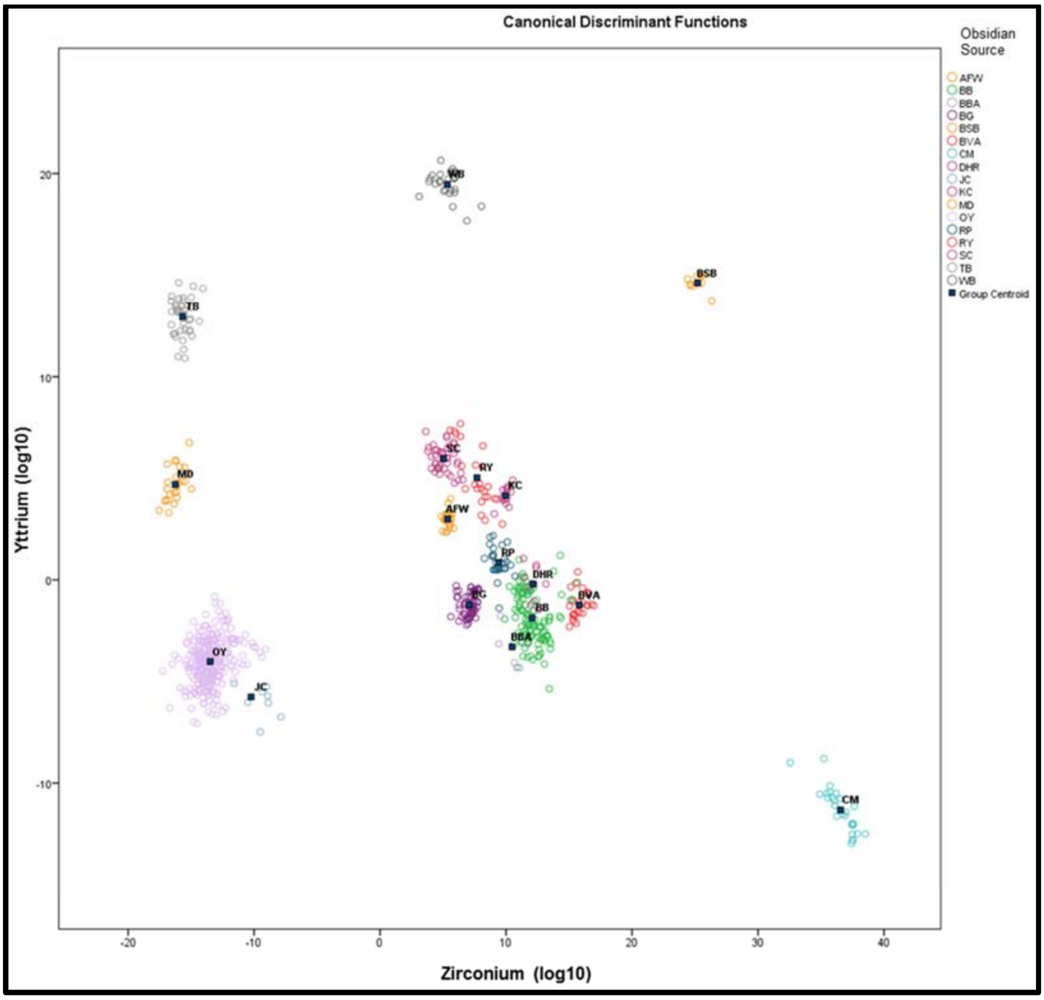

Figure 5.1. 12-Element DFA, First Two Functions

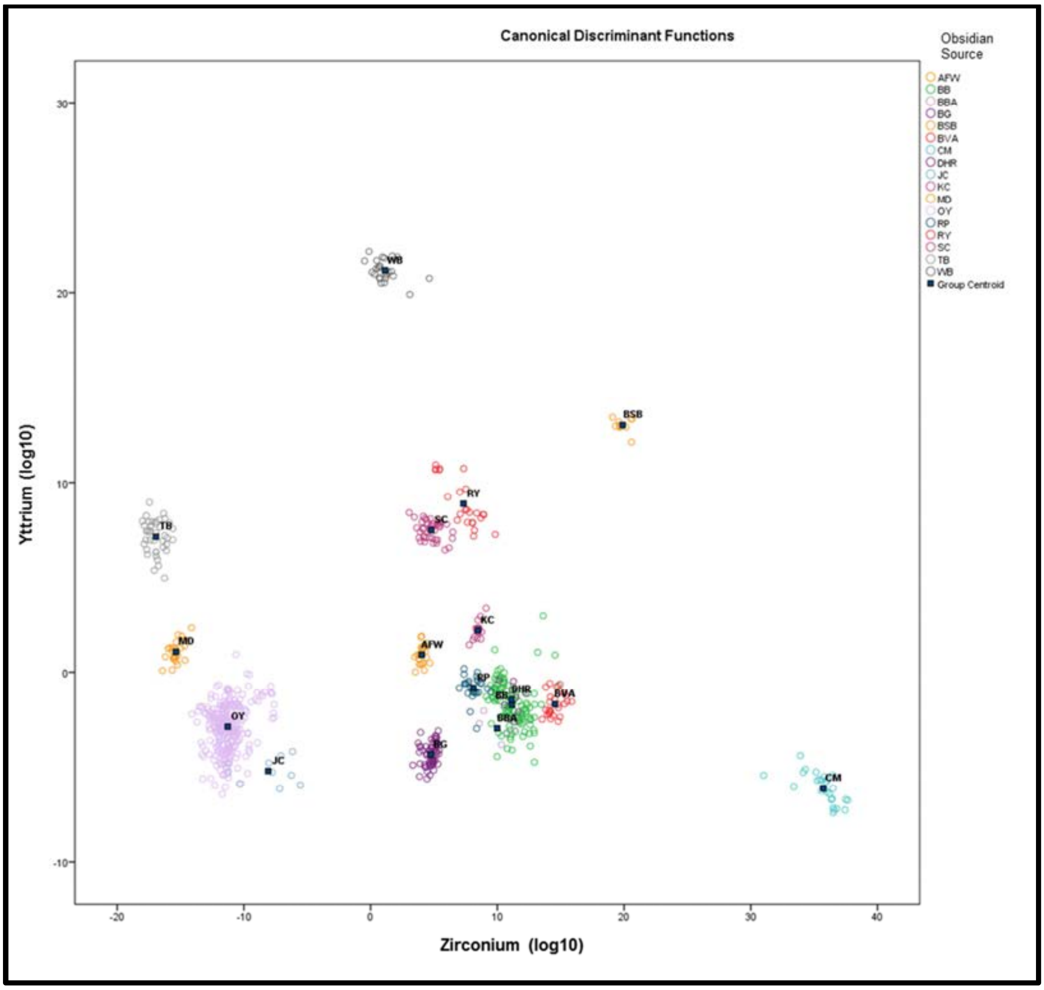

Figure 5.2. 5-Element DFA, First Two Functions

Generating a crosstabs of the predicted source group membership compared to the actual source membership shows the number of cases correctly and incorrectly assigned to a source group. Including all 12 elements correctly assigned 99.6% of all cases, whereas five elements were correctly assigned 99.4% (Table 5.4 and 5.5). Using only five elements does not significantly reduce source discrimination of Idaho sources. Furthermore, it allows the comparison of the Bruker pXRF analyzer to a Spectrace 5000 XRF analyzer because the 5 elements can be detected by both instruments.

Table 5.4 12-Element Crosstabs of Assigned Cases (Sources with 100% Correct Assignments Not Listed)

	Putative Source		
Assigned Source	**DHR**	**OY**	**Total**
DHR	9	0	
JC	0	2	
OY	0	247	
RP	1	0	
Total Incorrect	1	2	3/705

Table 5.5 5-Element Crosstabs of Assigned Cases (Sources with 100% Correct Assignments Not Listed)

	Putative Source		
Assigned Source	**DHR**	**OY**	**Total**
DHR	9	0	
JC	0	3	
OY	0	246	
RP	1	0	
Total Incorrect	1	3	4/705

Bi-Plot Analysis

Bi-plot analysis uses the two most discriminatory elements to indicate the relationship between obsidian sources in a graphical format. Bi-plots are ideal for comparing relatively small groups of sources. As the number of sources increases, the ability of a bi-plot to indicate differentiation between sources diminishes. Bi-plots are one of the most common statistical exploratory methods in obsidian studies (e.g., Craig et al. 2007; Frahm 2013a; Glascock et al. 1998; Millhauser et al. 2011; Shackley 2005). For this analysis, the Log-10 transformations of the three most discriminating elements (Zr, Y, and Sr) for all Idaho obsidian sources included in this study are used to indicate the relationship between sources at both labs.

The bi-plot of two Log-10 transformed elements (zirconium [Zr] and yttrium [Y]), which explains 84.0% of the variation (determined by the DFA), was conducted on source profiles, resulting in grouping of profiles by source (rather than by lab). In the case of paired sources, there is a consistent underestimation of IMNH means compared to NWROSL means for these elements (Figure 5.3, Appendix Table C.1-C.4). Except for one source (KC), measurement error between labs is far smaller than the natural variation occurring between sources, suggesting that source profiles from both labs may be pooled despite systematic measurement error (Nazaroff et al., 2010; Sheppard , Trichereau, and Milicich 2010).

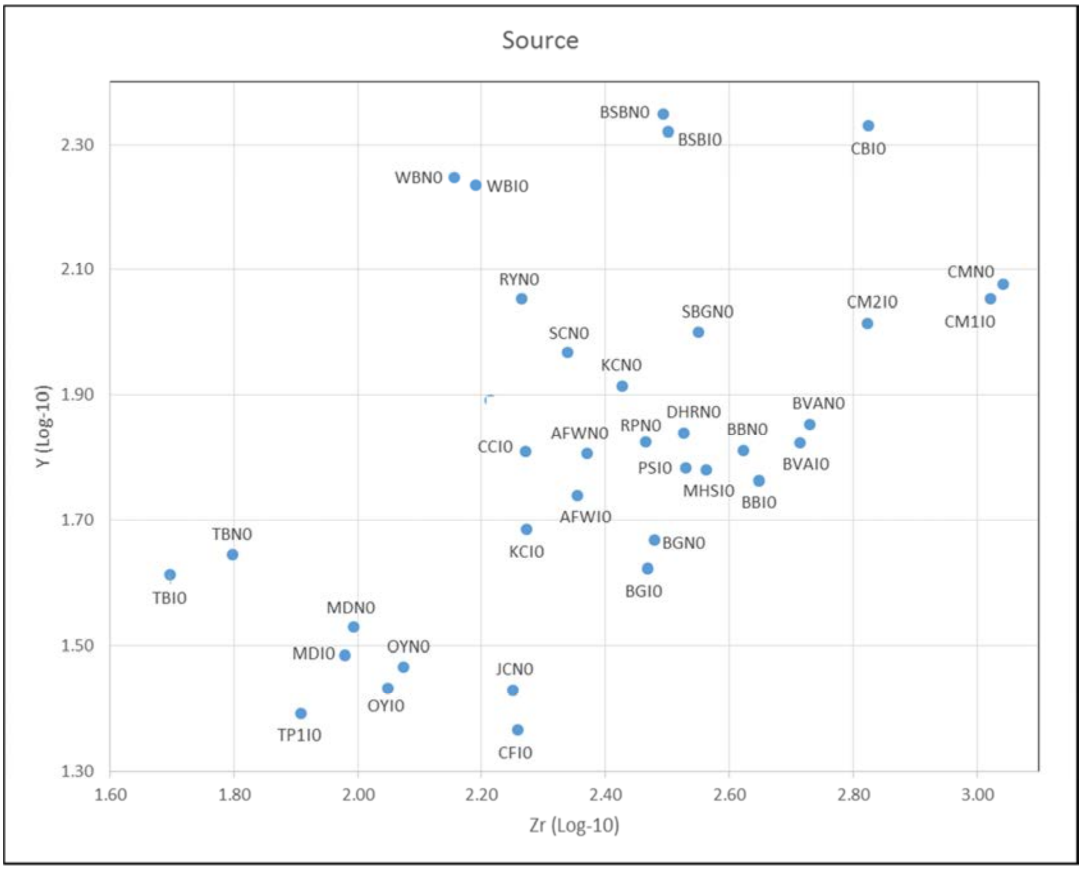

Figure 5.3. Bi-plot of Zirconium and Yttrium (Log-10 Transformation)

The bi-plot of two Log-10 transformed elements (zirconium [Zr] and strontium [Sr]), two of the three elements important in discriminating obsidian sources (determined by the DFA), was conducted on source profiles, resulting in grouping of profiles by source (rather than by lab). In the case of paired sources, there is a consistent underestimation of IMNH means compared to NWROSL means for these elements (Figure 5.4, Appendix Table C.1-C.4). Except for two sources (CM and KC), measurement error between labs is far smaller than the natural variation occurring between sources, suggesting that source profiles from both labs may be pooled despite systematic measurement error (Nazaroff et al., 2010; Sheppard et al., 2010).

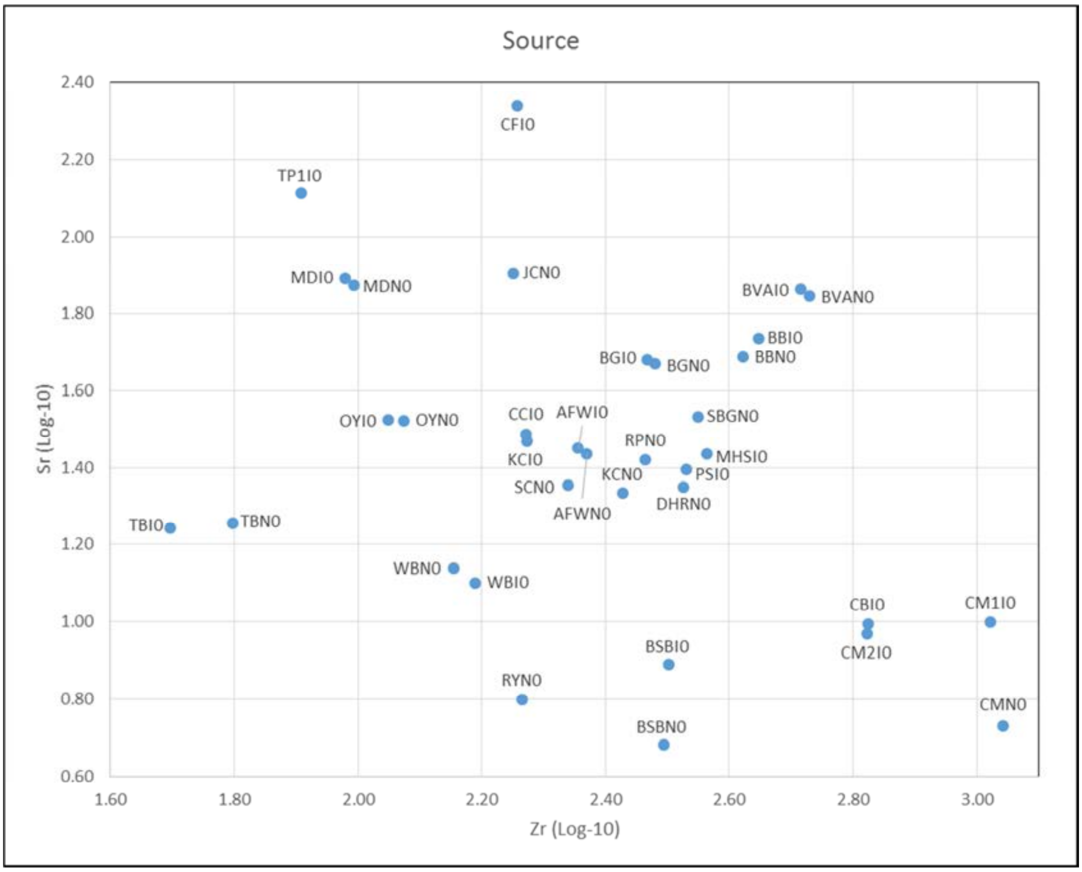

Figure 5.4. Bi-plot of Zirconium and Strontium (Log-10 Transformation)

The bi-plot of two Log-10 transformed elements (yttrium [Y] and strontium [Sr]), two of the three elements important in discriminating obsidian sources (determined by the DFA), was conducted on source profiles, resulting in grouping of profiles by source (rather than by lab). In the case of paired sources, there is a consistent underestimation of IMNH means compared to NWROSL means for these elements (Figure 5.5, Appendix Table C.1-C.4). Except for two sources (CM and KC), measurement error between labs is far smaller than the natural variation occurring between sources, suggesting that source profiles from both labs may be pooled despite systematic measurement error (Nazaroff et al., 2010; Sheppard et al., 2010).

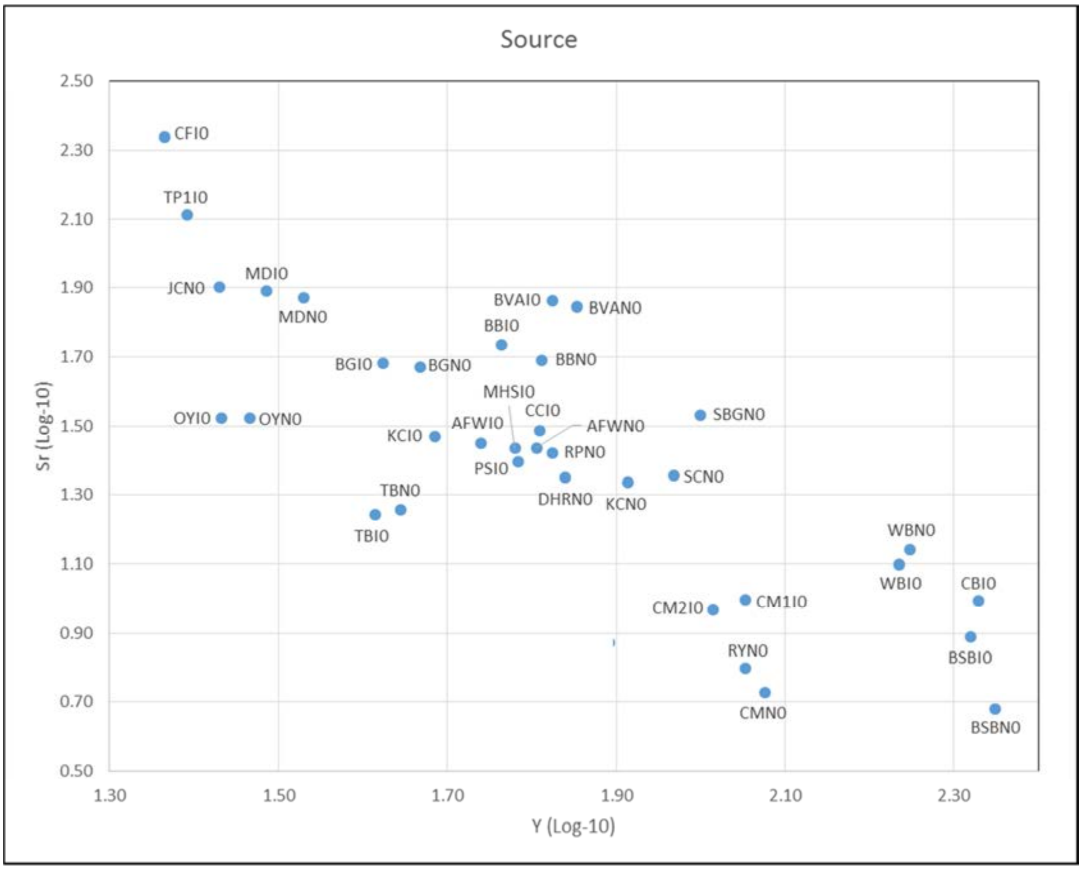

Figure 5.5. **Bi-plot of Yttrium and Strontium (Log-10 Transformation)**

Measurement error between labs is less than the natural variation within a geographic source, as demonstrated by the three bi-plots. However, measurement error between labs does not necessarily rule out further analysis, since source assignment methods are more sensitive to relative proportions of elements across source profiles, not absolute amounts of individual elements.

Principal Component Analysis (PCA)

PCA in GAUSS Runtime determines the principal components that explain the variation, much as DFA does (Aptech Systems, Inc. 2006). PCA accounts for as much variation as possible while reducing the dimensionality of the set of variables by maximizing the correlations of quantified variables for the number of dimensions (components) specified (Glascock et al. 1998; SPSS 20.0). The first principal component accounts for the most variability in the data (the largest variance) while each succeeding component explains the remaining variation uncorrelated with the preceding components (Figure 5.6, Table 5.6). Like DFA, a potential limitation to using PCA is that it also assumes that all artifacts and/or sources belong to a known group (Glascock et al. 1998).

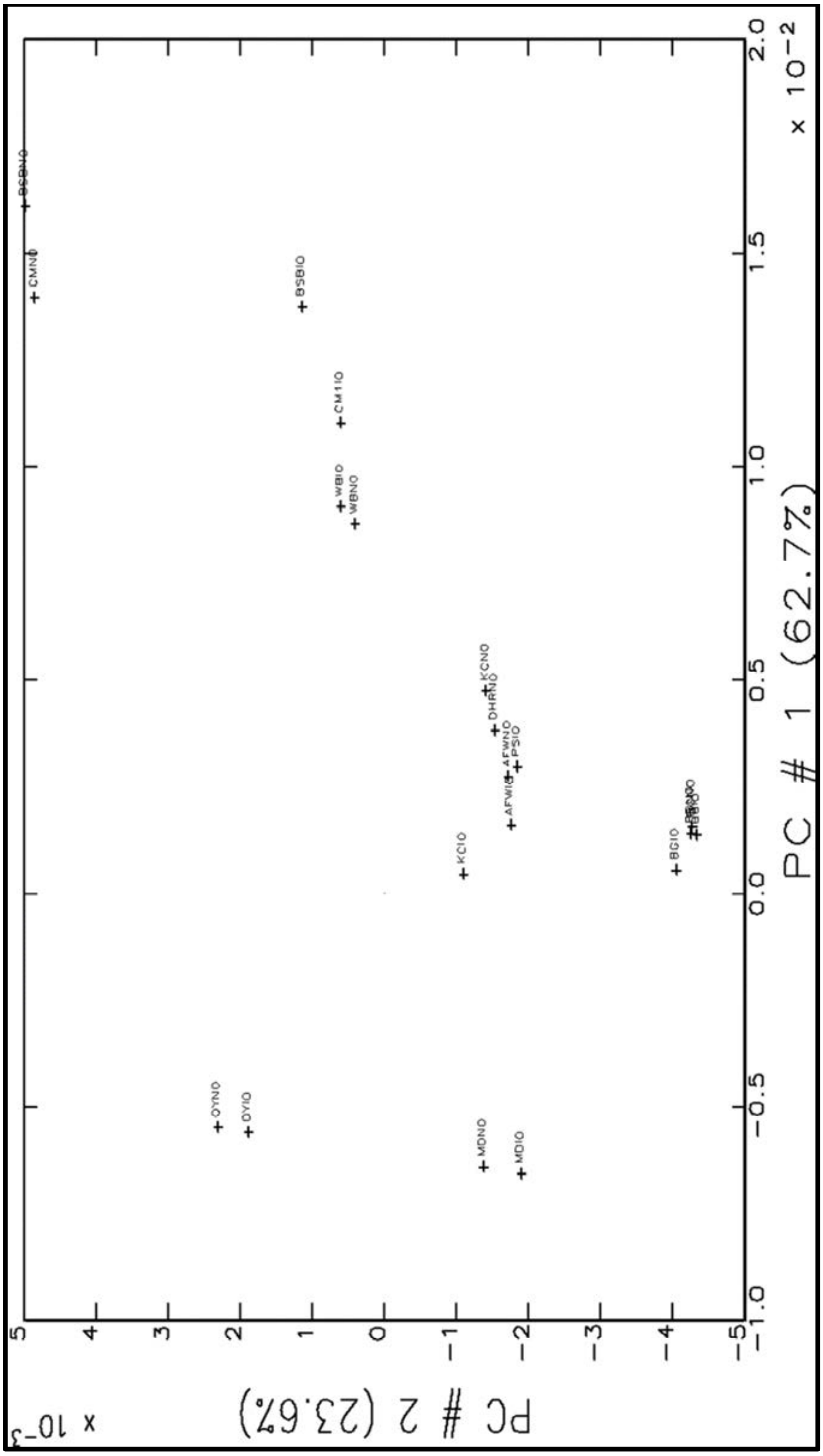

Figure 5.6. Principal Components 1 and 2 of Same Named Obsidian Source Means

Table 5.6 Principal Component Analysis Eigenvalues

PC	Eigenvalue	% of Variance	Cumulative %
1	0.022959	62.7	69.2
2	0.008642	23.6	86.3
3	30.739	5.6	91.9
4	9.977	3.0	94.9
5	7.550	2.3	97.2
6	1.756	1.7	98.9
7	1.316	.8	99.7
8	.809	.3	100

Source group assignment through GAUSS Runtime is determined through group membership probabilities computed using Mahalanobis distance, which measures how much a case's values differ from the average of all cases within a given group or source (Aptech Systems, Inc. 2006). The Mahalanobis distance is used to identify and measure the similarity between an unknown and known sample and is different than Euclidean distance in that it takes into account the correlations within the data set (SPSS 20.0). The benefit of using all or most of the elements for PCA is that the relationship between all or most of the elements can be analyzed whereas with a bi-plot or ternary plot only two or three elements can be used.

According to Glascock (personal communication, 2014), group membership probabilities based on PCA through GAUSS Runtime are ideally applied to ceramic sourcing studies rather than to obsidian sourcing studies, and source group assignments should include those that fall within two standard deviations of the probability mean for the group. Additionally, in using this program to assign sources, there are two requirements: 1) the number of samples included in the analysis must exceed the number of elements under consideration by at least 2 for each group or source, and 2) the source sample size should be at least 2 ½ times the number of elements under consideration. These guidelines require that only eight principal components using the 10 elements in common between labs be used in analysis and that the Browns Bench Area data be dropped from further analysis. Unfortunately, the “best practices” (i.e., sample size at least 2 ½ times the number of elements for each group or source) cannot be completely adhered to in this instance while using the geochemical source profiles provided. It is expected that PCA will not provide a relatively good percentage of artifact-to-source assignments because of the insufficient number of geologic samples characterizing each source.

Another limitation to using PCA for this study is that the GAUSS Runtime program assumes that all existing sources are included in the analysis, not just known sources (Aptech Systems, Inc. 2006). As a result, every individual source profile is assigned to a known group even if it may belong to an as yet unknown group. Therefore, because of the incomplete characterization of known and unknown sources and the huge range of probabilities, only one standard deviation was used to assign obsidian source group membership. Two standard deviations results in all sources being assigned to the source group in which they originated, even though the program assigns a different source. Additionally, two standard deviations includes negative probability values and values greater than 100, which results in all sources being assigned to the source group in which they originated, thus inflating the results of the PCA. One standard deviation was used in the assignments to try to minimize the possible inflation, as noted by Hughes (1984), of the percent correctly classified, because the cases assigned to groups are used to determine the group profile. In theory, PCA is well suited for artifact-to-source assignment with sufficient geologic sample size (Glascock et al. 1998). In this study, PCA is used to confirm source-to-source assignment and to highlight the issues with sample size of the current geologic source.

Hierarchical Cluster Analysis (HCA)

HCA is used to identify groups based on the homogeneity of selected variables (in this instance, elements) by initially pairing like cases, then clusters, until only one is left. Clustering is an exploration tool to evaluate the relationship between artifact samples and sources (Glascock et al. 1998). The Ward's clustering method was applied to the z-scores of the Log-10 transformation of these data. Ward's clustering method minimizes the variance of the squared Euclidean distances among cases within clusters to determine groups (SPSS 20.0). HCA was performed on the sources from both labs and on all artifacts using SPSS 20.0 and GAUSS Runtime 8.0 (Aptech Systems, Inc. 2006; IBM Corp. 2011; MURR 2014).

The results of the HCA exhibit like-named source profiles from both labs in the same cluster, indicating the profiles are not clustering by lab but by source (Appendix Table D). Therefore, artifacts can potentially be sourced on a broad scale, while refinement of sub-source profiles may allow more exact matches. The five most discriminatory elements from the DFA were included in the SPSS HCA of all artifacts and mean source profile values in order to detect any grouping of source profiles by lab. No grouping by lab was present. The GAUSS Runtime HCA was conducted using all 10 elements to analyze all artifacts, mean source profiles from IMNH, and individual source profiles from NWROSL. Artifacts should be reliably classified and grouped with the geochemically closest source profile, assuming that systematic measurement differences between labs do not cause samples to cluster by the lab of measurement. The GAUSS Runtime HCA assigned each source and artifact into an individual cluster, creating visually apparent source assignments as well as highlighting artifacts having unknown source profiles (Aptech Systems, Inc. 2006).

Site versus IMNH and NWROSL Source Profiles

The results of the artifact-to-source assignments using visual analysis, PCA, and HCA suggest that in this instance hierarchical cluster analysis is the most reliable method in assigning sources-to-artifacts with an 86.8% assignment rate (Table 5.8).

Table 5.8 Proportion of Artifacts Assigned to a Source by Method

Site	Visual Assignment		PCA Assignment		HCA Assignment	
10BN23	25/32	78.1%	0/32	0.0%	31/32	96.9%
10BV48	21/24	87.5%	18/24	75.0%	23/24	95.8%
10CN5	4/8	50.0%	6/8	75.0%	7/8	87.5%
10CN6	8/13	61.5%	7/13	53.8%	9/13	69.2%
10CR52	16/22	72.7%	1/22	4.5%	16/22	72.7%
10EL110	13/14	92.9%	3/14	21.4%	14/14	100.0%
10EL215	20/25	80.0%	8/25	32.0%	24/25	96.0%
10EL294	4/5	80.0%	3/5	60.0%	5/5	100.0%
10EL1367	3/5	60.0%	3/5	60.0%	5/5	100.0%
10EL1577	12/12	100.0%	2/12	16.7%	12/12	100.0%
10OE3686	4/14	28.6%	5/14	35.7%	5/14	35.7%
Total	**130/174**	**74.7%**	**56/174**	**32.2%**	**151/174**	**86.8%**

Source versus IMNH and NWROSL Source Profiles

The results of the source-to-source assignments using DFA, PCA, and HCA suggest that in this instance discriminant function analysis and hierarchical cluster analysis are the most reliable in assigning sources at 99.4% and 98.0%, respectively (Table 5.7).

Table 5.7 Source Assignment Results by Method

Source	**DFA Assignment**		**PCA Assignment**		**HCA Assignment**	
American Falls (Walcott)	24/24	100.0%	23/24	95.8%	24/24	100.0%
Bear Gulch	56/56	100.0%	53/56	94.6%	56/56	100.0%
Big Southern Butte	10/10	100.0%	10/10	100.0%	10/10	100.0%
Browns Bench	109/109	100.0%	101/109	92.7%	109/109	100.0%
Browns Bench Area	N=5, therefore dropped from further inclusion in analysis					
Butte Valley A	26/26	100.0%	24/26	92.3%	21/26	80.8%
Cannonball Mountain/ Cannonball Mountain 1	25/25	100.0%	23/25	92.0%	25/25	100.0%
Cannonball Mountain	N=1, therefore dropped from further inclusion in analysis					
Cedar Butte	N=1, therefore dropped from further inclusion in analysis					
Chesterfield	N=1, therefore dropped from further inclusion in analysis					
Conant Creek	N=1, therefore dropped from further inclusion in analysis					
Deadhorse Ridge	9/10	90.0%	10/10	100.0%	9/10	90.0%
Jordan Creek	10/10	100.0%	10/10	100.0%	9/10	90.0%
Kelly Canyon	12/12	100.0%	9/12	75.0%	11/12	91.7%
Malad	25/25	100.0%	22/25	88.0%	25/25	100.0%
Murphy Hot Springs	N=1, therefore dropped from further inclusion in analysis					
Obsidian Cliff	N=1, therefore dropped from further inclusion in analysis					
Owyhee	246/249	98.8%	231/249	92.8%	248/249	99.6%
Pack Saddle	N=1, therefore dropped from further inclusion in analysis					
Reas Pass	22/22	100.0%	16/22	72.7%	17/22	77.3%
Reynolds	24/24	100.0%	24/24	100.0%	24/24	100.0%
Sinker Canyon	39/39	100.0%	39/39	100.0%	39/39	100.0%
Striker Basin Gulch	N=1, therefore dropped from further inclusion in analysis					
Teton Pass 1	N=1, therefore dropped from further inclusion in analysis					
Timber Butte	38/38	100.0%	37/38	97.4%	38/38	100.0%
Wedge Butte	26/26	100.0%	25/26	96.2%	26/26	100.0%
Total	**701/705**	**99.4%**	**657/705**	**93.2%**	**691/705**	**98.0%**

CHAPTER SIX: DISCUSSION AND CONCLUSION

This chapter presents the results of the obsidian source-to-artifact assignment, the role geologic formations can play in obsidian sources, and the theoretical application of obsidian studies.

Discussion of Results

Two sources that have been previously treated as having come from distinct sources may have in fact originated from a singular or geochemically similar geologic source. For example, Pack Saddle (IMNH) and Deadhorse Ridge (NWROSL) may belong to a relatively homogeneous geochemical source (Figure 6.1). The non-statistical assignment of obsidian sources found that both geochemical source profiles could be equally applied to artifact samples. Additionally, PCA and HCA assigned Deadhorse Ridge to Pack Saddle and clustered them in the dendrogram (Appendix Table D). Geologically, while these sources are separated by a valley on the map, they are both from the Basin and Range Province of Southeastern Idaho (Figure 6.2). Due to the potential for spatial location error of the obsidian sources (IMNH = 6 miles and NWROSL = 1 mile) and the unknown geologic sampling methodology, Pack Saddle and Deadhorse Ridge cannot be definitively compared with the current knowledge of these sources. Comparisons between Pack Saddle and Deadhorse Ridge can only be based on the locations in the Basin and Range Province and the age of the geologic obsidian source location. Pack Saddle and Deadhorse Ridge are both located among Pliocene and Upper

Miocene felsic volcanic rocks, rhyolite flows, tuffs, and ignimbrites (Digital Atlas of Idaho Nov. 2002). In further discussions, these sources are treated as a paired source with the caveat that these geologic samples and sources should be further investigated in the future to determine if they are in fact from the same geologic formation.

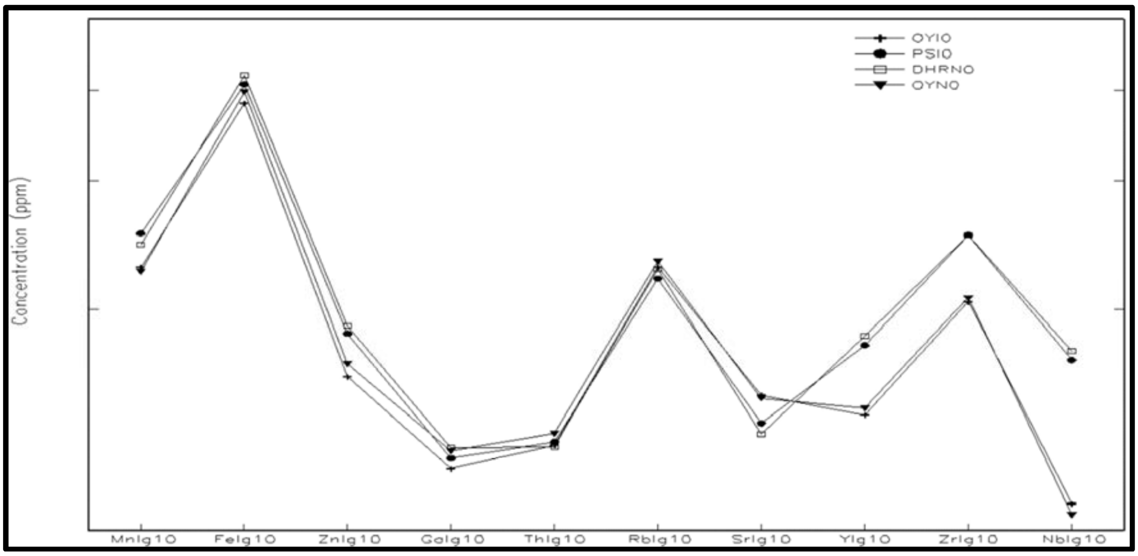

Figure 6.1. Distribution of Element Concentrations for Owyhee, Pack Saddle, and Deadhorse Ridge.

<u>Statistical Analyses</u>

Multiple statistical analyses were applied throughout this study to confirm source assignments and to avoid potential limitations associated with utilizing each approach separately (e.g., Glascock et al. 1998; Hughes 1984; Shackley 2005). As demonstrated in Chapter 4 and other pXRF vs. XRF studies (e.g., Craig et al. 2007; Millhauser et al. 2011), the source profiles and same artifact comparison allowed for pooling transformed data from both labs to attain an increased percentage of artifact source assignments that were not otherwise possible. The ability to assign sources to obsidian artifacts when both labs do not have exhaustive source profiles of the region appears feasible with the caveat to proceed cautiously by applying multiple statistical analyses. Some studies (e.g., Craig et al. 2007) have determined that, while there may be significant differences in element concentration values, these differences had no bearing on consistency of the obsidian source assignment.

The PCA source-to-source assignment resulted in the removal of 64 individual NWROSL cases due to the GAUSS Runtime program assigning those cases to sources other than the named grouping from which they originated. All statistical analyses were performed again with 705 instead of 769 NWROSL cases. All results reported within this thesis are based on 705 NWROSL cases and the means from both NWROSL and IMNH. The incorrect assignment of these 64 source cases could be a direct result of the collection method of obtained geologic samples to characterize the source. In other words, these particular cases may not be representative of the obsidian source to which they are attributed. If these cases are in fact from the obsidian source to which they are attributed, it would suggest that the obsidian source is highly variable.

The source-to-source assignments and artifact-to-source assignments using DFA, PCA, and HCA achieved varying degrees of success in assigning sources, but the combination of all approaches contributed to corroboration of all but four sources. The instances in which PCA was “Unknown” while the other methods resulted in a named source were a direct result of using only one standard deviation for source-to-source assignment because the individual values had such a large range that in some cases two standard deviations in either direction accounted for all the cases — even those assigned to a different source (Appendix Table E). A possible explanation for the wide range of

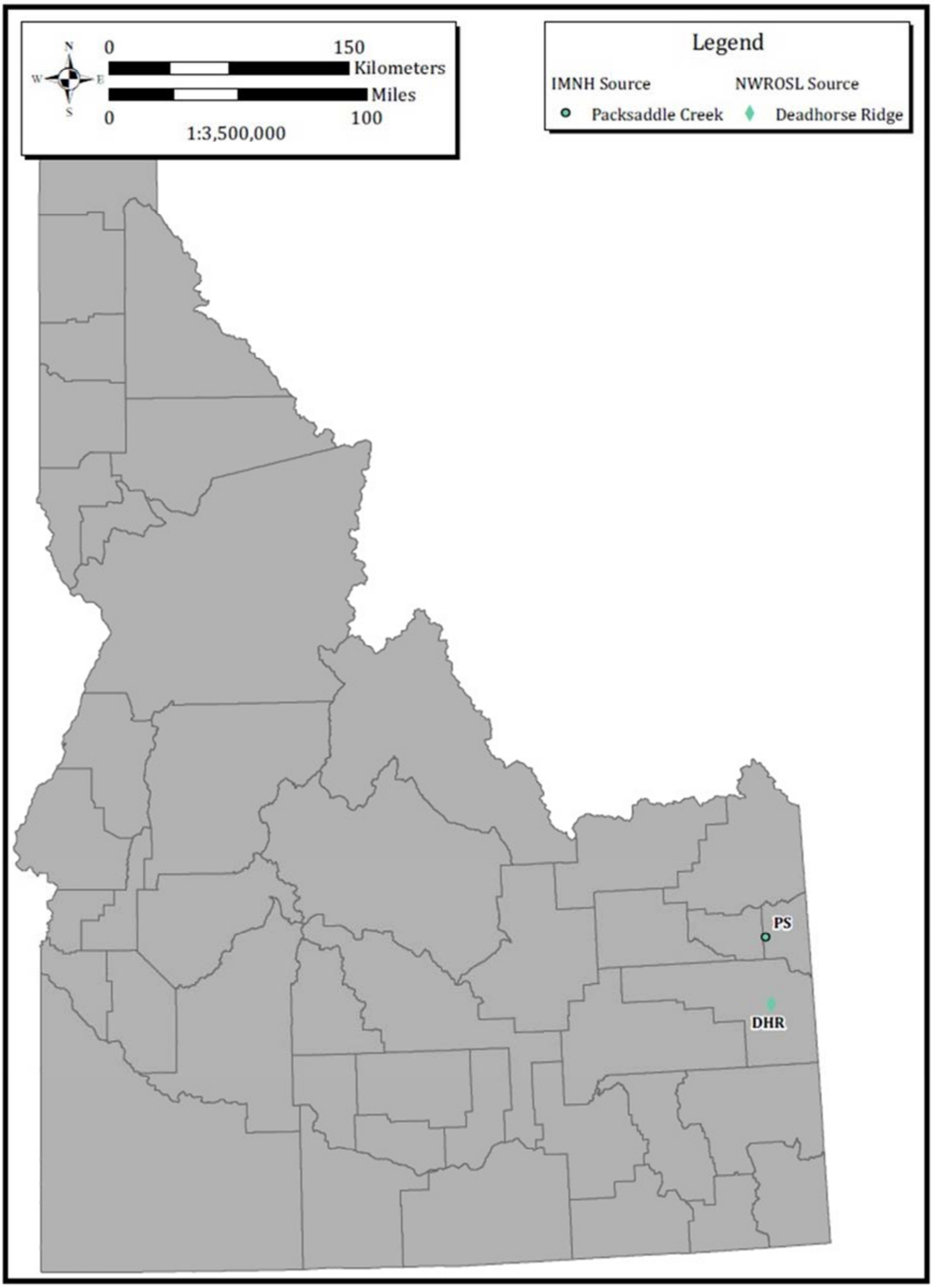

Figure 6.2. Similarly Named Obsidian Sources Including Pack Saddle and Deadhorse Ridge.

source means is likely related to the variation within the geologic source samples, which may or may not have come from the same geologic formation.

Geologic Formation’s Role in Obsidian Sources

An example of an obsidian source and the underlying geologic formation is that of Big Southern Butte. Three buttes rise out of the Snake River Plain: Big Southern Butte, Middle Butte, and East Butte. The obsidian source termed Big Southern Butte coincides with the location of the geologic formation named Big Southern Butte, which rises 2,500 feet above the Snake River Plain covering an area of 12.5 square miles. Both Big Southern Butte and East Butte are rhyolitic domes while Middle Butte is uplifted basalt (Spear and King 1982). The isolated nature of Big Southern Butte would suggest that the likelihood of any obsidian attributed to Big Southern Butte originating at Big Southern Butte is relatively high (King 1982). In reality, at this isolated location, there are in fact one basalt and two rhyolitic domes that have coalesced to create one dome (Figure 6.3).

The western dome is comprised of white rhyolite and black obsidian while the eastern dome is tan to lavender rhyolite. The two rhyolitic domes differ slightly in age and deposition but are mineralogically and chemically homogeneous (Spear and King 1982). XRF detects trace elements that are not usually considered when characterizing geologic formations; therefore, while Big Southern Butte may be geologically homogeneous, the trace elements may be heterogeneous. Although the petrology of Big Southern Butte may be geochemically homogeneous at a geologic scale, it is necessary to consider it from an archaeological perspective as well. It is not known from which rhyolitic dome the obsidian source samples attributed to Big Southern Butte were collected or where they originated.

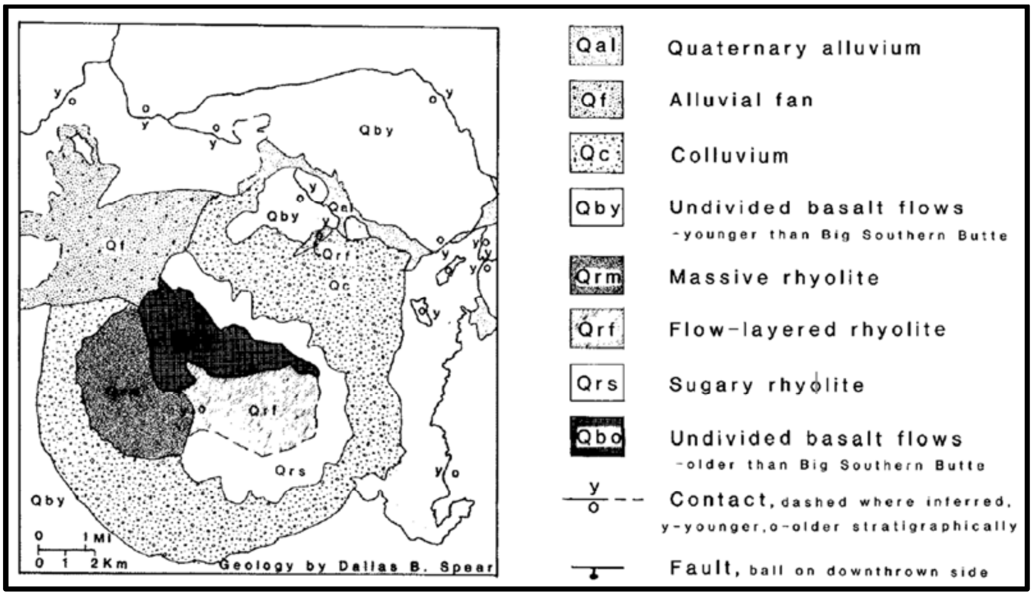

Figure 6.3. Generalized Geologic Map of Big Southern Butte, Idaho (Spear and King 1982).

Another example come from Southwestern Idaho. In perspective, Owyhee County has a wide variety of different geologic formations, including rhyolites dating from the Miocene and Pliocene (Ekren, McIntyre, Bennett, and Malde 1981). Therefore, sources from the Owyhee Mountains might be expected to be diverse when compared to those of Big Southern Butte and other relatively discrete geologic units such as Timber Butte, Cannonball Mountain, and Wedge Butte.

Artifact Source Assignment

The obsidian sources used in this study were restricted to only known sources within Idaho. Therefore, any “Unknown” obsidian sources originate either from outside Idaho or are unknown and uncharacterized sources within Idaho (Willson 2005). A total of 86.8% of artifacts were assigned to a source using all of the statistical approaches. Without the inclusion of the NWROSL sources, only 74.7% of the artifacts would have been assigned to a source. Of the 21 artifacts run between both labs, four were not assigned to the same obsidian source (Appendix Table F). Having obsidian source geochemical profiles for only one state will not account for all the sources represented by the artifact profiles. The other three instances of conflicting source assignments are relatively close spatially, and this emphasizes the need for a geologic re-survey of the sources to increase the geologic sample sizes and to refine the characterization of the sources.

10BN23

No previous obsidian XRF studies had been performed on this artifact collection. Site 10BN23 artifact samples appear to have been conveyed to the site from sources to the south and southeast. The one unknown source may be explained by either the existence of an unknown obsidian source or procurement from a source outside of Idaho (Figure 6.4 and Table 6.1).

Table 6.1 10BN23: All-Method Artifact Source Assignments

AFW	BB	BSB	BVA	CM/1	MD	WB	UNK	Total
9	5	5	3	6	1	2	1	32
28%	**16%**	**16%**	**9%**	**19%**	**3%**	**6%**	**3%**	**100%**

10BV48

No previous obsidian XRF studies had been performed on this artifact collection. Site 10BV48 artifact samples appear to have been conveyed to the site from sources to the north, east, and southwest. The one unknown source may be explained by either the existence of an unknown obsidian source or the procurement from a source outside of Idaho (Figure 6.5 and Table 6.2).

Table 6.2 10BV48: All-Method Artifact Source Assignments

BG	MD	PS/DHR	TP1	UNK	Total
3	1	18	1	1	24
13%	**4%**	**75%**	**4%**	**4%**	**100%**

10CN5

Site 10CN5 artifact samples had been previously analyzed at NWROSL (Hunter, Kennedy, Plager, Plew, and Webb 1998). The results of previous sample analysis indicate the presence of obsidian from sources north of the site and in southeastern Oregon. The samples included in the current analysis appear to have been conveyed to the site from nearby sources to the south. In one instance (10CN5, Artifact 76), analyzed at both labs, the "Unknown" is attributed to a source in Oregon (Figure 6.6 and Table 6.3). The pattern indicated by the analyzed samples from both studies and both labs are in agreement (based on the obsidian sources included).

Table 6.3a 10CN5: Previous Artifact Source Assignments

OY	TB	Oregon	Total
6	1	3	10
60%	**10%**	**30%**	**100%**

Table 6.3b 10CN5: All-Method Artifact Source Assignments

JC	OY	UNK	Total
1	6	1	8
12.5%	**75.0%**	**12.5%**	**100%**

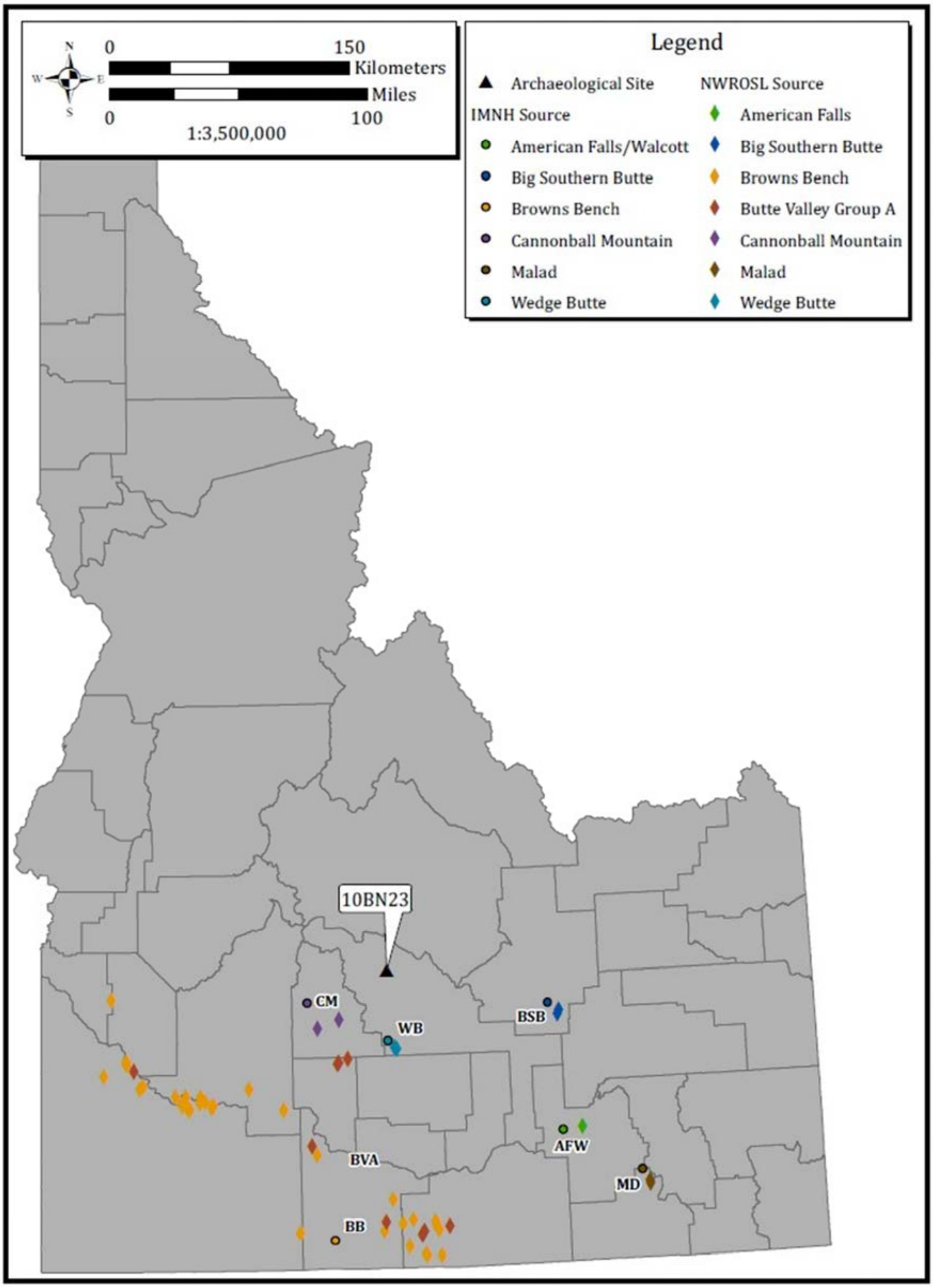

Figure 6.4. Site and Idaho Obsidian Sources Present in Assemblage.

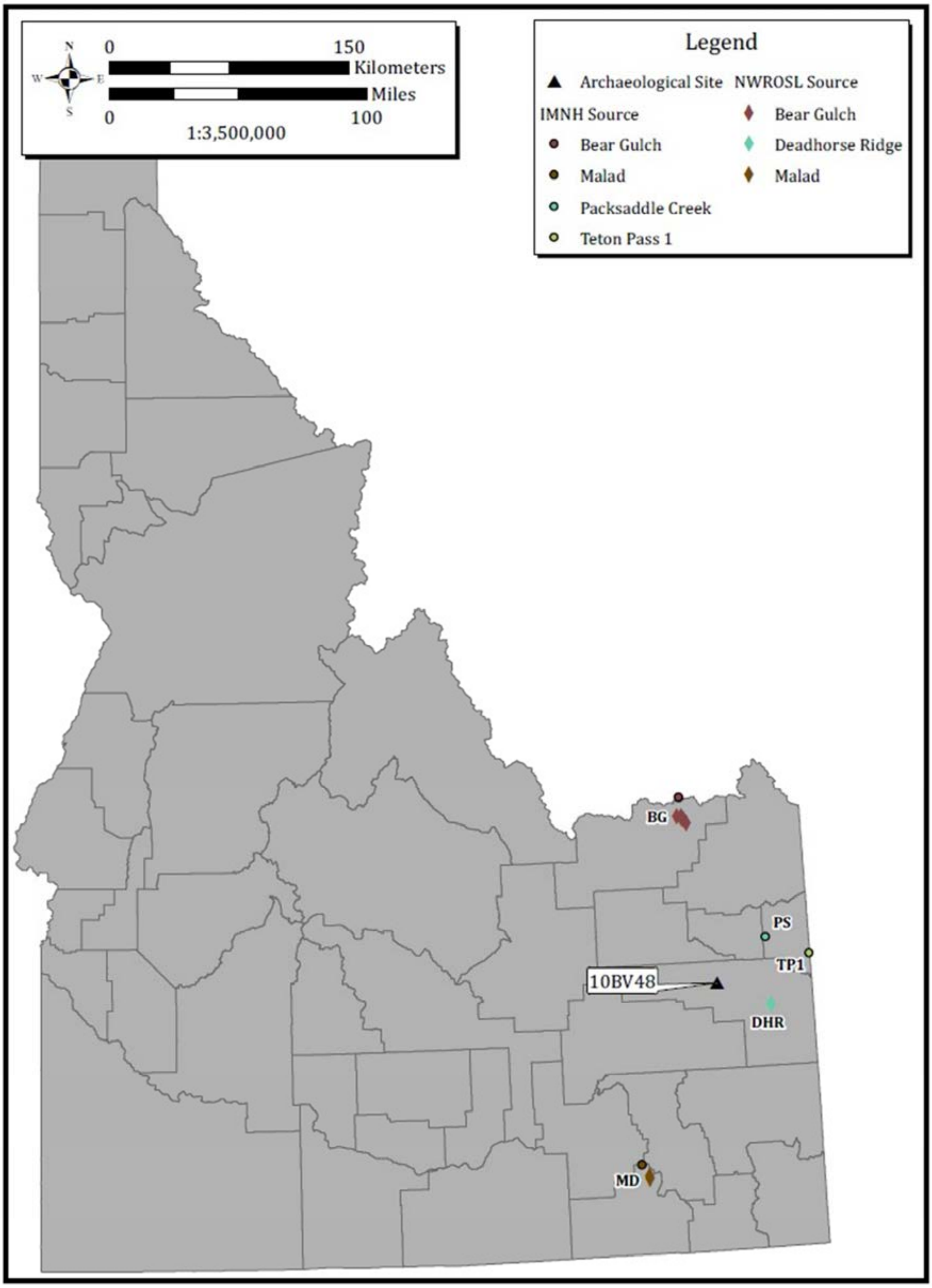

Figure 6.5. Site and Idaho Obsidian Sources Present in Assemblage.

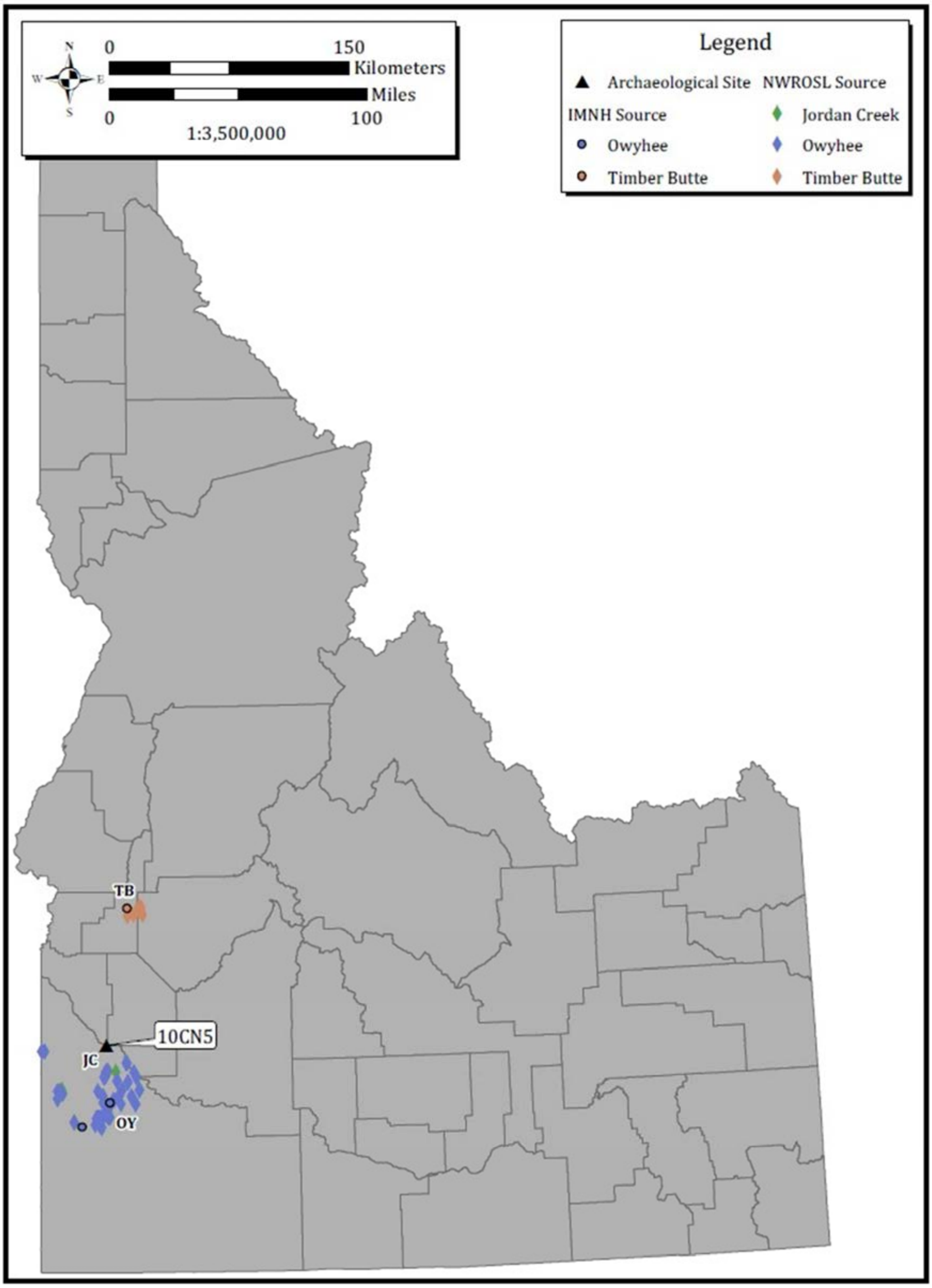

Figure 6.6. Site and Idaho Obsidian Sources Present in Assemblage.

Table 6.3c 10CN5: Comparison of Previous Analysis with Current Study

Specimen	All Methods	NWROSL
A5	N/A	Indian Creek Buttes, Oregon
12	Owyhee	Owyhee
13	Jordan Creek	N/A
A34	N/A	Timber Butte
35	Owyhee	Owyhee
A50	Owyhee	Owyhee
A59	N/A	Sourdough Mountain, Oregon
67	Owyhee	Owyhee
76	Unknown	Coyote Wells, Oregon
161	Owyhee	Owyhee
1134	Owyhee	Owyhee

10CN6

Site 10CN6 artifact samples had been previously analyzed at NWROSL (Plew, Plager, Jacobs, and Willson 2006). The results of previous sample analysis indicate the presence of obsidian in sources from southeastern Oregon. The samples included in the current analysis appear to have been conveyed to the site from sources to the north and south. The three unknown sources may be explained by either the existence of unknown obsidian source(s) or the procurement from source(s) outside of Idaho (Figure 6.7 and Table 6.4). The pattern indicated by the analyzed samples from both studies and both labs are in agreement (based on the obsidian sources included).

Table 6.4a 10CN6: Previous Artifact Source Assignments

OY	SC	TB	Oregon	UNK	Total
12	1	5	3	1	22
54.5%	**4.5%**	**22.8%**	**13.7%**	**4.5%**	**100%**

Table 6.4b 10CN6: All-Method Artifact Source Assignments

OY	SC	TB	UNK	Total
8	1	1	3	13
61.5%	**7.7%**	**7.7%**	**23.1%**	**100%**

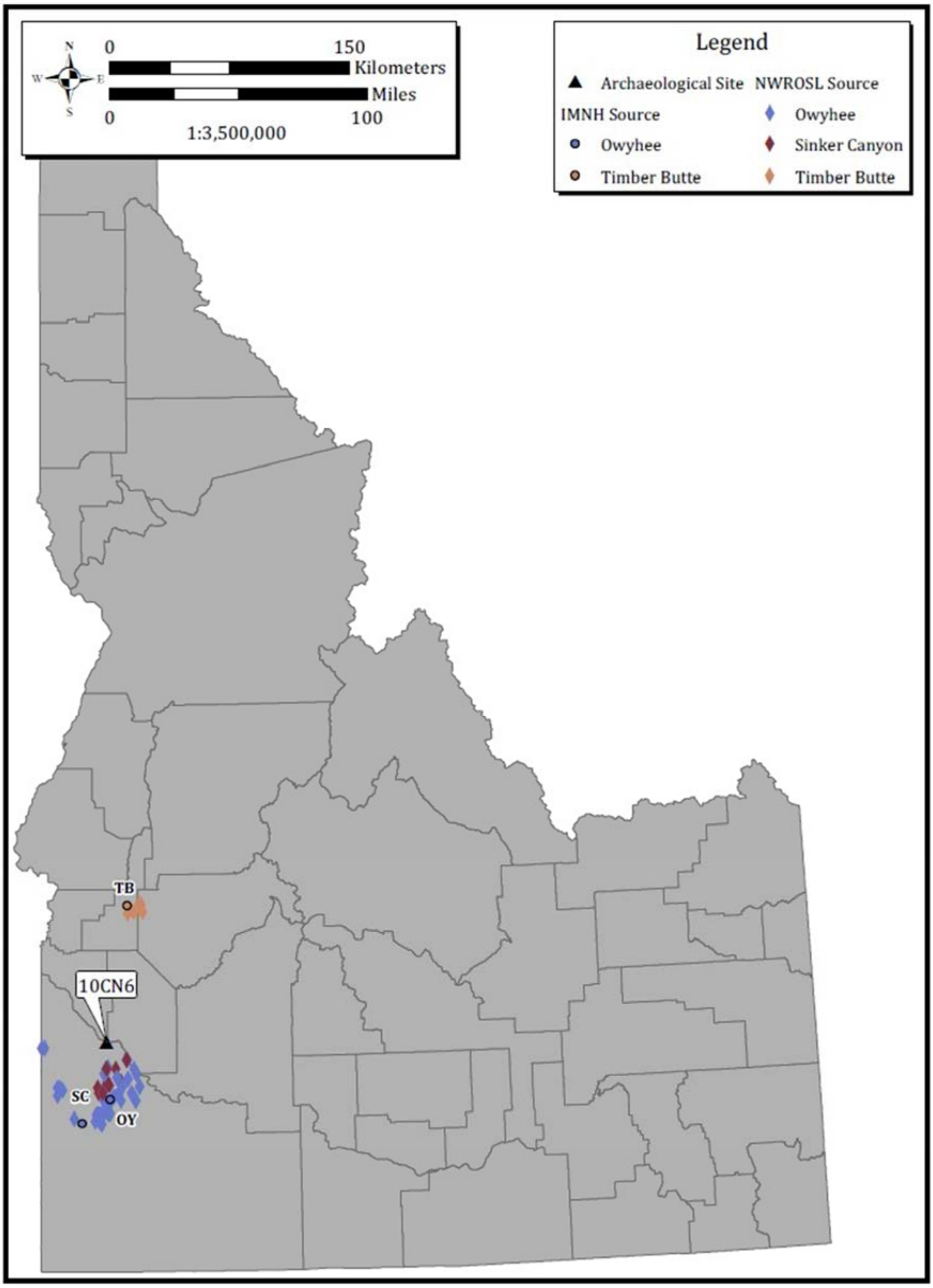

Figure 6.7. Site and Idaho Obsidian Sources Present in Assemblage.

Table 6.4c 10CN6: Comparison of Previous Analysis with Current Study

Specimen	All Methods	NWROSL
1	N/A	Owyhee
2	N/A	Coyote Well, Oregon
3	N/A	Unknown
4	N/A	Timber Butte
5	Timber Butte	Timber Butte
6	Owyhee	Owyhee
31	Unknown	N/A
32	Unknown	N/A
A34	N/A	Owyhee
A35	N/A	Timber Butte
45	N/A	Owyhee
A46	N/A	Coyote Well, Oregon
A48	Owyhee	Owyhee
56	Owyhee	N/A
A57	N/A	Venator, Oregon
A60	Owyhee	Owyhee
74	Unknown	N/A
77	N/A	Owyhee
A78	Owyhee	Owyhee
79	N/A	Owyhee
92	N/A	Owyhee
95	N/A	Timber Butte
96	N/A	Owyhee
100	Owyhee	N/A
A110	N/A	Timber Butte
A116	Owyhee	Owyhee
117	Owyhee	N/A
A121	Sinker Canyon	Sinker Canyon

10CR52

No previous obsidian XRF studies had been performed on this artifact collection. Site 10CR52 artifact samples appear to have been conveyed to the site from sources to the south and east. The six unknown sources are perhaps explained by either the existence of unknown obsidian source(s) or procurement from source(s) outside of Idaho (Figure 6.8 and Table 6.5).

Table 6.5 10CR52: All-Method Artifact Source Assignments

AFW	BG	BSB	CM/1	PS/DHR	UNK	Total
7	5	1	2	1	6	22
31.8%	**22.7%**	**4.6%**	**9.0%**	**4.6%**	**27.3%**	**100%**

10EL110

Site 10EL110 artifact samples had been previously analyzed at NWROSL (Willson and Plew 2007). The pattern indicated by the analyzed samples from both studies and both labs are in agreement and expanded to the east and south (based on the obsidian sources included). The samples included in the current analysis appear to have been conveyed to the site from sources to the north, west, and south with the majority originating from the east. There are no unknown sources (Figure 6.9 and Table 6.6).

Table 6.6a 10EL110: Previous Artifact Source Assignments

BB	BBA	BSB	CM/1	OY	SC	Total
1	2	1	2	2	1	9
11.1%	**22.2%**	**11.1%**	**22.2%**	**22.2%**	**11.1%**	**100%**

Table 6.6b 10EL110: All-Method Artifact Source Assignments

AFW	BB	BG	BVA	CM/1	CM2	MHS	OY	Total
1	2	1	1	6	1	1	1	14
7%	**15%**	**7%**	**7%**	**43%**	**7%**	**7%**	**7%**	**100%**

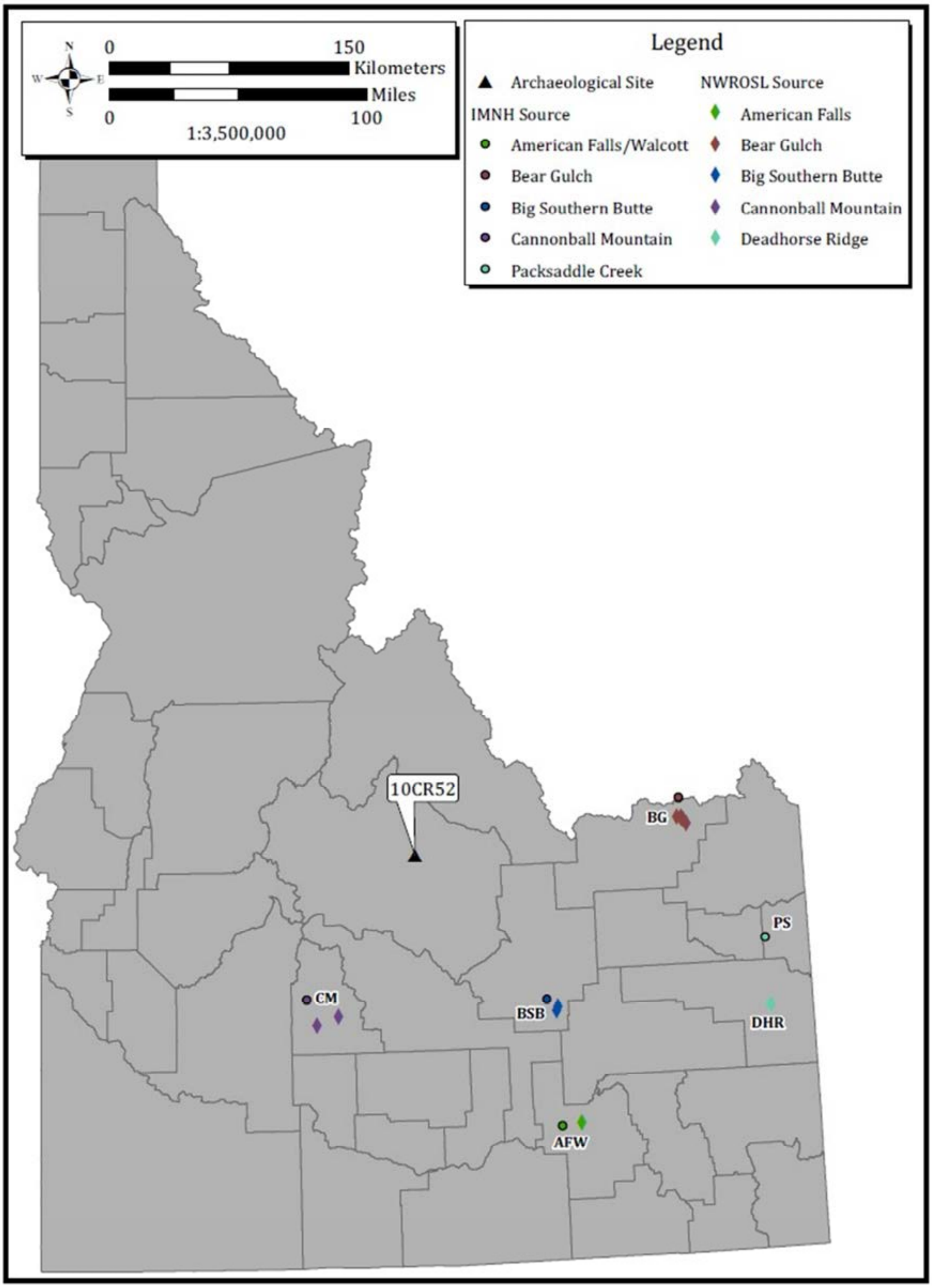

Figure 6.8. Site and Idaho Obsidian Sources Present in Assemblage.

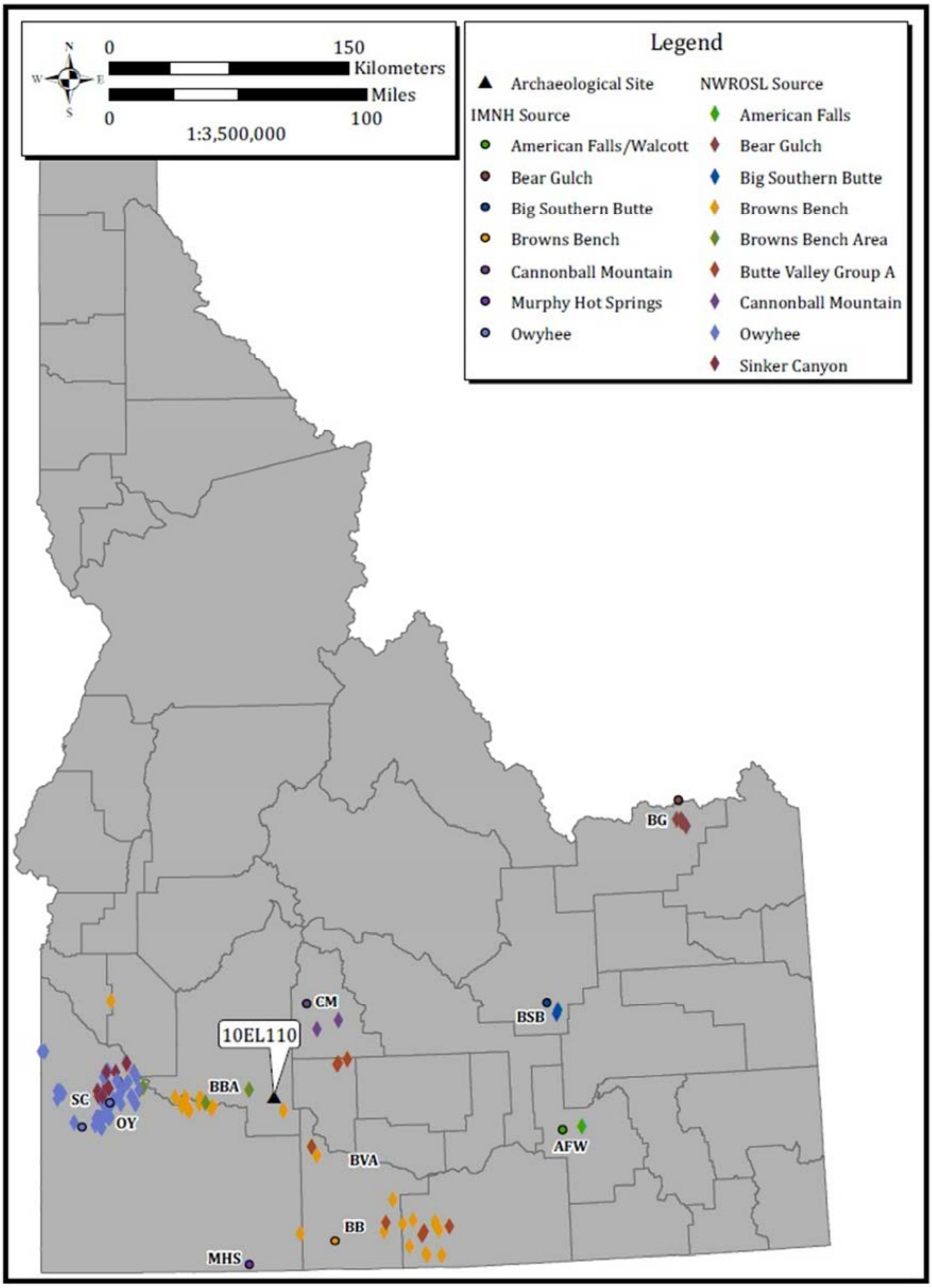

Figure 6.9. Site and Idaho Obsidian Sources Present in Assemblage.

Table 6.6c 10EL110: Comparison of Previous Analysis with Current Study

Specimen	All Methods	NWROSL
1	Cannonball Mountain 2	N/A
A9	N/A	Sinker Canyon
A21	Murphy Hot Springs	Browns Bench Area
A42	N/A	Big Southern Butte
A52	N/A	Browns Bench Area
A67	N/A	Cannonball Mountain/1
82	Cannonball Mountain/1	N/A
89	Cannonball Mountain/1	N/A
A93	Owyhee	Cannonball Mountain/1
96	Cannonball Mountain/1	N/A
A99	Browns Bench	Browns Bench
A118	N/A	Owyhee
191	Butte Valley A	N/A
A208	N/A	Owyhee
A216	American Falls/Walcott	N/A
228	Bear Gulch	N/A
234	Browns Bench	N/A
247	Cannonball Mountain/1	N/A
259	Cannonball Mountain/1	N/A
261	Cannonball Mountain/1	N/A

10EL215

Site 10EL215 artifact samples had been previously analyzed at NWROSL (Plew and Willson 2011). The patterns indicated by the analyzed samples from both studies and both labs are in agreement and have expanded the number of sources originating from the west and south (based on the obsidian sources included). The samples included in the current analysis appear to have been conveyed to the site from sources to the north, southeast, and west. The one unknown source is perhaps explained by either the existence of an unknown obsidian source or the procurement from a source outside of Idaho. There are four instances of disagreement; the PCA results were not the same as the non-statistical or HCA assignment. Therefore, a source could not be confidently assigned (Figure 6.10 and Table 6.7).

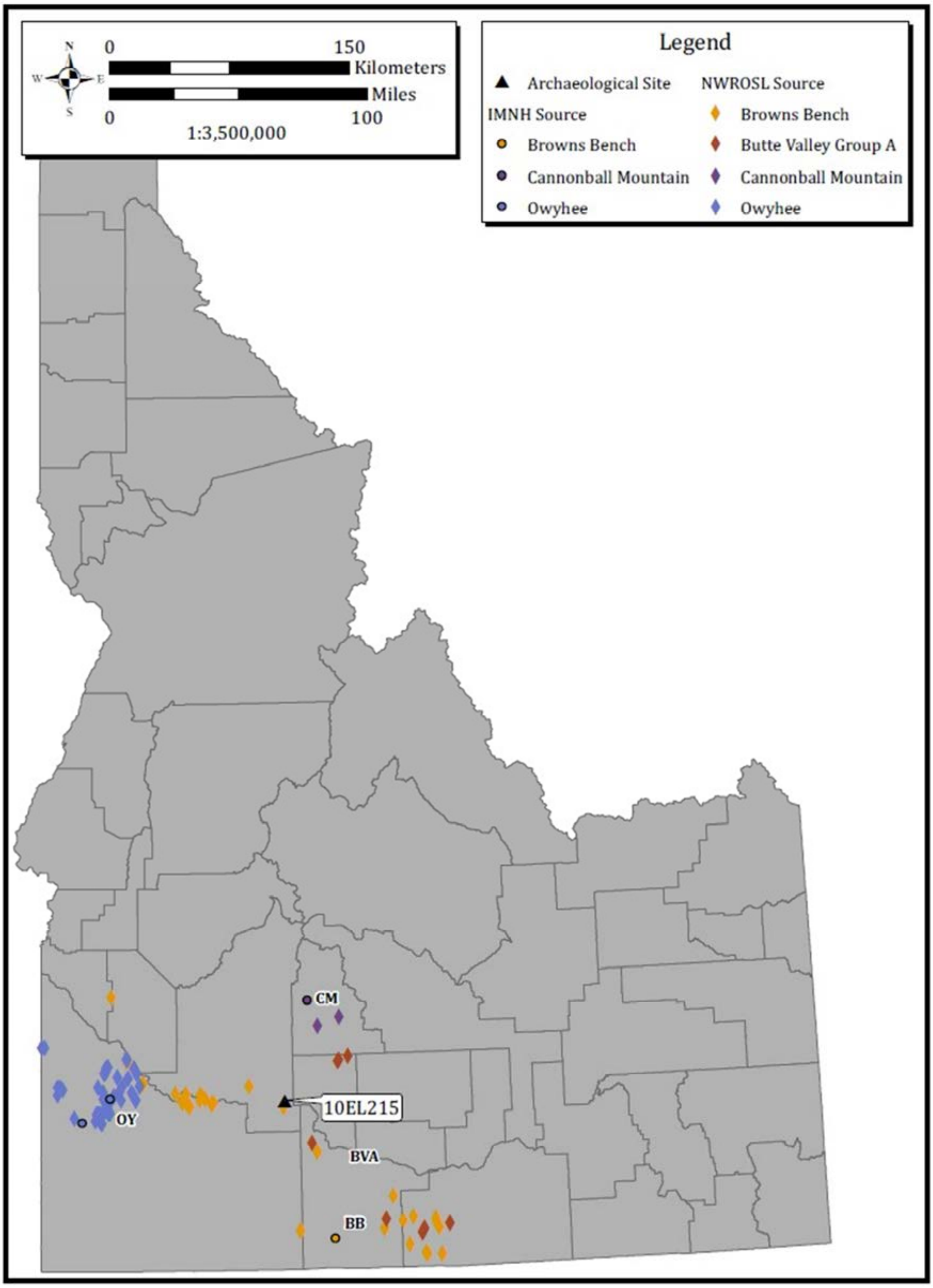

Figure 6.10. Site and Idaho Obsidian Sources Present in Assemblage.

Table 6.7a 10EL215: Previous Artifact Source Assignments

BB	CM/1	Total
9	3	12
75%	**25%**	**100%**

Table 6.7b 10EL215: All-Method Artifact Source Assignments

BB	BVA	CM/1	CM2	OY	UNK	UNK-C	Total
7	1	7	1	4	1	4	25
28%	**4%**	**28%**	**4%**	**16%**	**4%**	**16%**	**100%**

Table 6.7c 10EL215: Comparison of Previous Analysis with Current Study

Specimen	All Methods	NWROSL
1	N/A	Browns Bench
2	N/A	Browns Bench
3	N/A	Cannonball Mountain/1
4	Unknown-Conflict	Browns Bench
5	N/A	Browns Bench
6	N/A	Cannonball Mountain/1
7	Browns Bench	Browns Bench
8	Browns Bench	Browns Bench
9	Browns Bench	Browns Bench
10	N/A	Browns Bench
11	Cannonball Mountain/1	Cannonball Mountain/1
12	N/A	Browns Bench
29	Browns Bench	N/A
37	Unknown-Conflict	N/A
42	Unknown	N/A
78	Browns Bench	N/A
88	Butte Valley A	N/A
95	Cannonball Mountain/1	N/A
117	Browns Bench	N/A
118	Cannonball Mountain/1	N/A
131	Cannonball Mountain/1	N/A
158	Cannonball Mountain/1	N/A
172	Cannonball Mountain/1	N/A
179	Unknown-Conflict	N/A
180	Owyhee	N/A
193	Cannonball Mountain 2	N/A
216	Browns Bench	N/A
225	Cannonball Mountain/1	N/A
252	Browns Bench	N/A
270	Owyhee	N/A
280	Owyhee	N/A
289	Owyhee	N/A

10EL294

Site 10EL294 artifact samples had been previously analyzed at NWROSL (Gould and Plew 2001). The pattern indicated by the previously analyzed samples and the current study are in agreement and the current study has added an obsidian source (based on the obsidian sources included). The samples included in the current analysis appear to have been conveyed to the site from sources to the north and south. There are no unknown sources. One PCA result did not agree with the non-statistical or HCA assignment and therefore could not be confidently assigned to a source (Figure 6.11 and Table 6.8a).

Table 6.8a 10EL294: Previous Artifact Source Assignments

AFW	BB	BBA	BG	OY	TB	Total
2	6	1	4	2	1	16
12.5%	**37.5%**	**6.25%**	**25.0%**	**12.5%**	**6.25%**	**100%**

Table 6.8b 10EL294: All-Method Artifact Source Assignments

BB	CM/1	UNK-C	Total
3	1	1	5
60%	**20%**	**20%**	**100%**

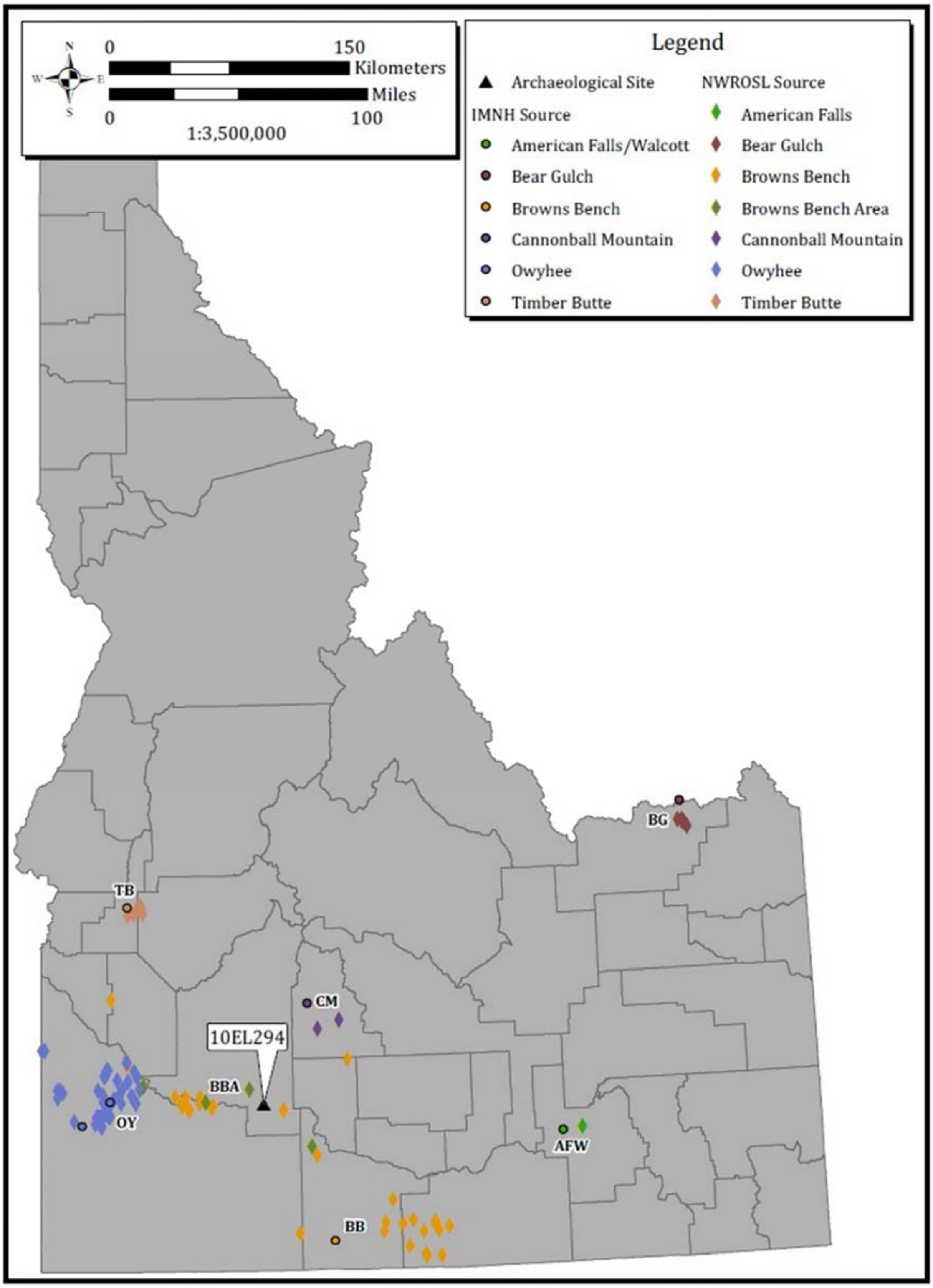

Figure 6.11. Site and Idaho Obsidian Sources Present in Assemblage.

Table 6.8c 10EL294: Comparison of Previous Analysis with Current Study

Specimen	All Methods	NWROSL
1	N/A	Bear Gulch
2	N/A	Browns Bench Area
3	N/A	Browns Bench
4	N/A	Bear Gulch
5	N/A	American Falls/Walcott
6	N/A	American Falls/Walcott
7	N/A	Bear Gulch
8	N/A	Browns Bench
9	N/A	Owyhee
10	N/A	Browns Bench
74	Browns Bench	N/A
88	Browns Bench	N/A
109	Browns Bench	N/A
116	Unknown-Conflict	N/A
158	Cannonball Mountain/1	N/A
381	N/A	Browns Bench
382	N/A	Bear Gulch
569	N/A	Browns Bench
970	N/A	Browns Bench
972	N/A	Timber Butte
1173	N/A	Owyhee

10EL1367

Site 10EL1367 artifact samples had been previously analyzed at NWROSL (Plew and Willson 2005). The patterns indicated by the previously analyzed samples and the current study are in agreement (based on the obsidian sources included). The samples included in the current analysis appear to have been conveyed to the site from sources to the northeast and southeast. There are no unknown sources. (Figure 6.12 and Table 6.9).

Table 6.9a 10EL1367: Previous Artifact Source Assignments

BB	BBA	CM/1	OY	Total
4	1	2	2	9
44.5%	**11.1%**	**22.2%**	**22.2%**	**100%**

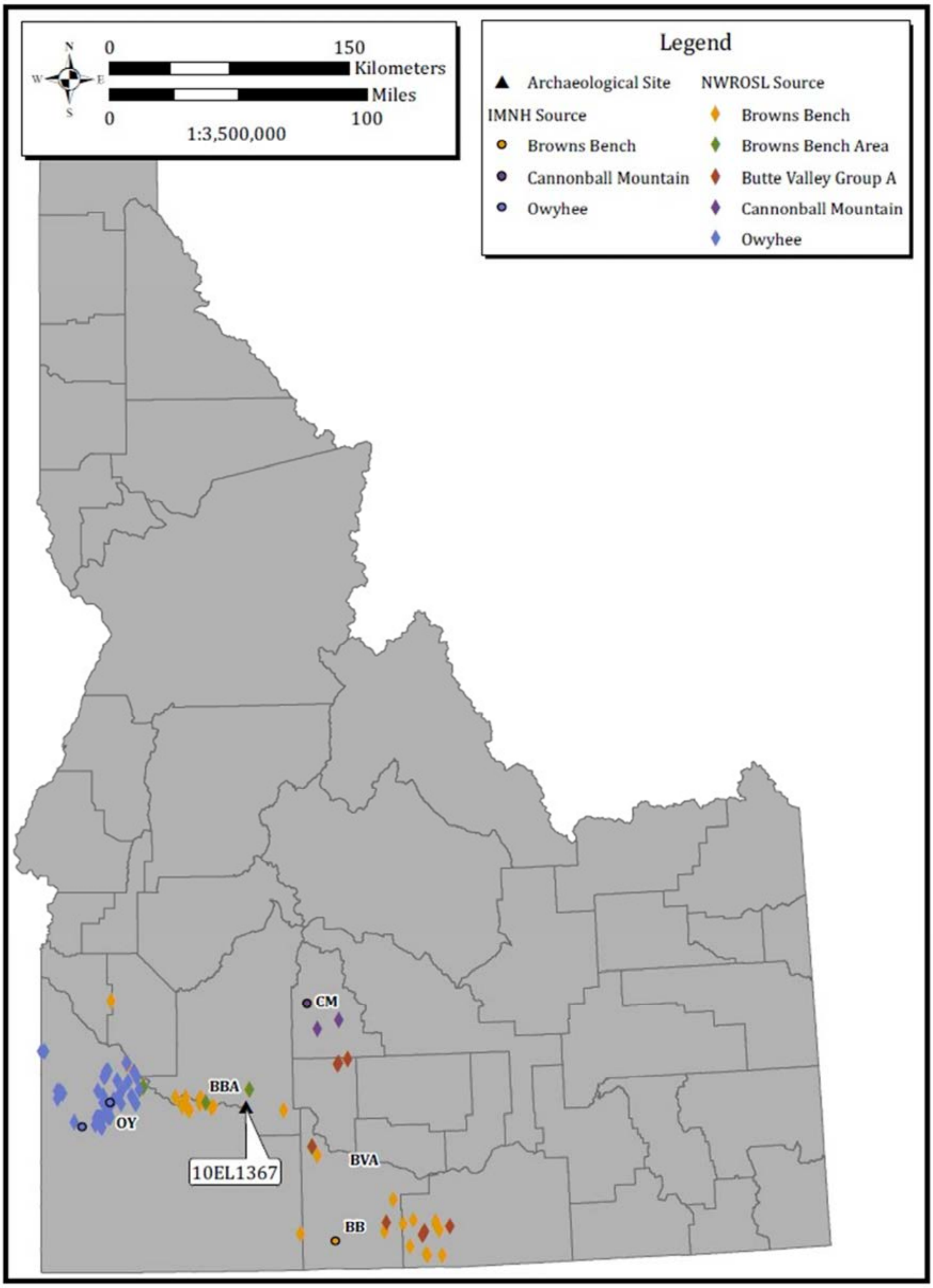

Figure 6.12. Site and Idaho Obsidian Sources Present in Assemblage.

Table 6.9b 10EL1367: All-Method Artifact Source Assignments

BB	BVA	CM/1	Total
2	2	1	5
40%	**40%**	**20%**	**100%**

Table 6.9c 10EL1367: Comparison of Previous Analysis with Current Study

Specimen	All Methods	NWROSL
1	N/A	Owyhee
2	N/A	Browns Bench
3	N/A	Cannonball Mountain/1
4	N/A	Browns Bench
5	N/A	Owyhee
9	Butte Valley A	N/A
A10	N/A	Browns Bench
11	Browns Bench	N/A
19	Butte Valley A	N/A
22	Browns Bench	N/A
26	Cannonball Mountain/1	N/A
A29	N/A	Browns Bench Area
A30	N/A	Cannonball Mountain/1
A34	N/A	Browns Bench

10EL1577

Site 10EL1577 artifact samples had been previously analyzed at NWROSL (Plew, Hunter, and Benedict 2002). The patterns indicated by the previously analyzed samples and the current study are in agreement and the current study has and have expanded the number of sources originating from the east and south (based on the obsidian sources included). The samples included in the current analysis appear to have been conveyed to the site from sources to the north, east, and south with the majority from the east. There are no unknown sources in this site sample (Figure 6.13 and Table 6.10).

Table 6.10a 10EL1577: Previous Artifact Source Assignments

BB	BG	CM/1	OY	UNK	Total
3	1	1	2	12	19
15.8%	**5.3%**	**5.3%**	**10.5%**	**63.1%**	**100%**

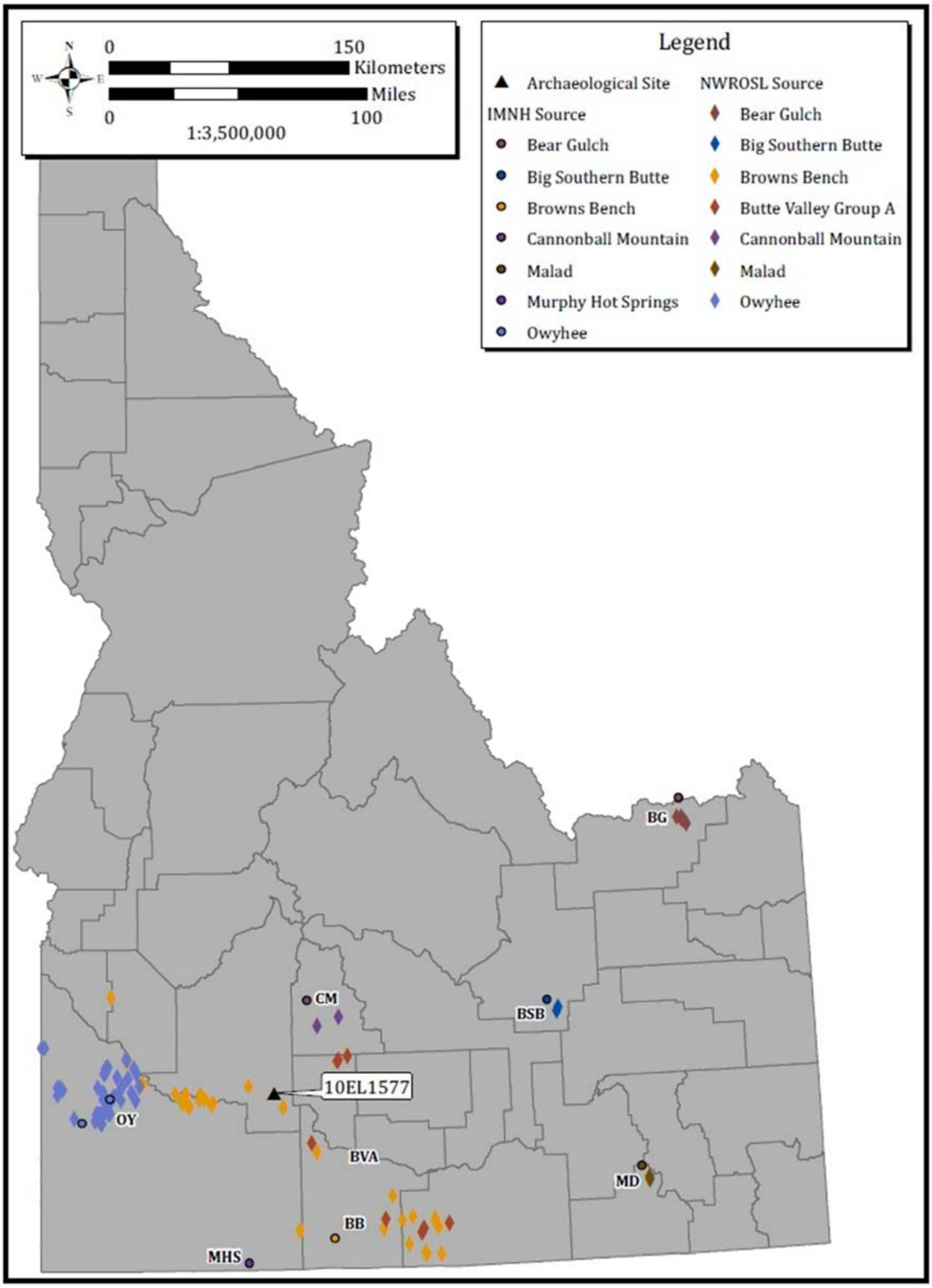

Figure 6.13. Site and Idaho Obsidian Sources Present in Assemblage.

Table 6.10b 10EL1577: All-Method Artifact Source Assignments

BB	BG	BSB	BVA	CM/1	MD	MHS	OY	Total
2	2	1	1	3	1	1	1	12
17.0%	**17.0%**	**8.2%**	**8.2%**	**25.0%**	**8.2%**	**8.2%**	**8.2%**	**100%**

Table 6.10c 10EL1577: Comparison of Previous Analysis with Current Study

Specimen	All Methods	NWROSL
3	N/A	Unknown
5	N/A	Unknown
10	N/A	Unknown
16	N/A	Bear Gulch
25	N/A	Unknown
30	N/A	Unknown
42	N/A	Owyhee
54	N/A	Unknown
60	N/A	Unknown
63	N/A	Browns Bench
86	N/A	Browns Bench
91	Bear Gulch	N/A
92	N/A	Cannonball Mountain/1
173	Browns Bench	N/A
226	Bear Gulch	N/A
246	Big Southern Butte	N/A
267	Malad	N/A
274	Owyhee	N/A
282	N/A	Unknown
320	N/A	Unknown
335	N/A	Unknown
361	N/A	Unknown
371	N/A	Unknown
412	Browns Bench	N/A
457	Butte Valley A	N/A
476	Cannonball Mountain/1	N/A
501	Cannonball Mountain/1	N/A
522	N/A	Owyhee
532	Cannonball Mountain/1	N/A
537	N/A	Browns Bench
564	Murphy Hot Springs	N/A

10OE3686

No previous obsidian XRF studies had been performed on this artifact collection. Site 10OE3686 artifact samples appear to have been conveyed to the site from sources to

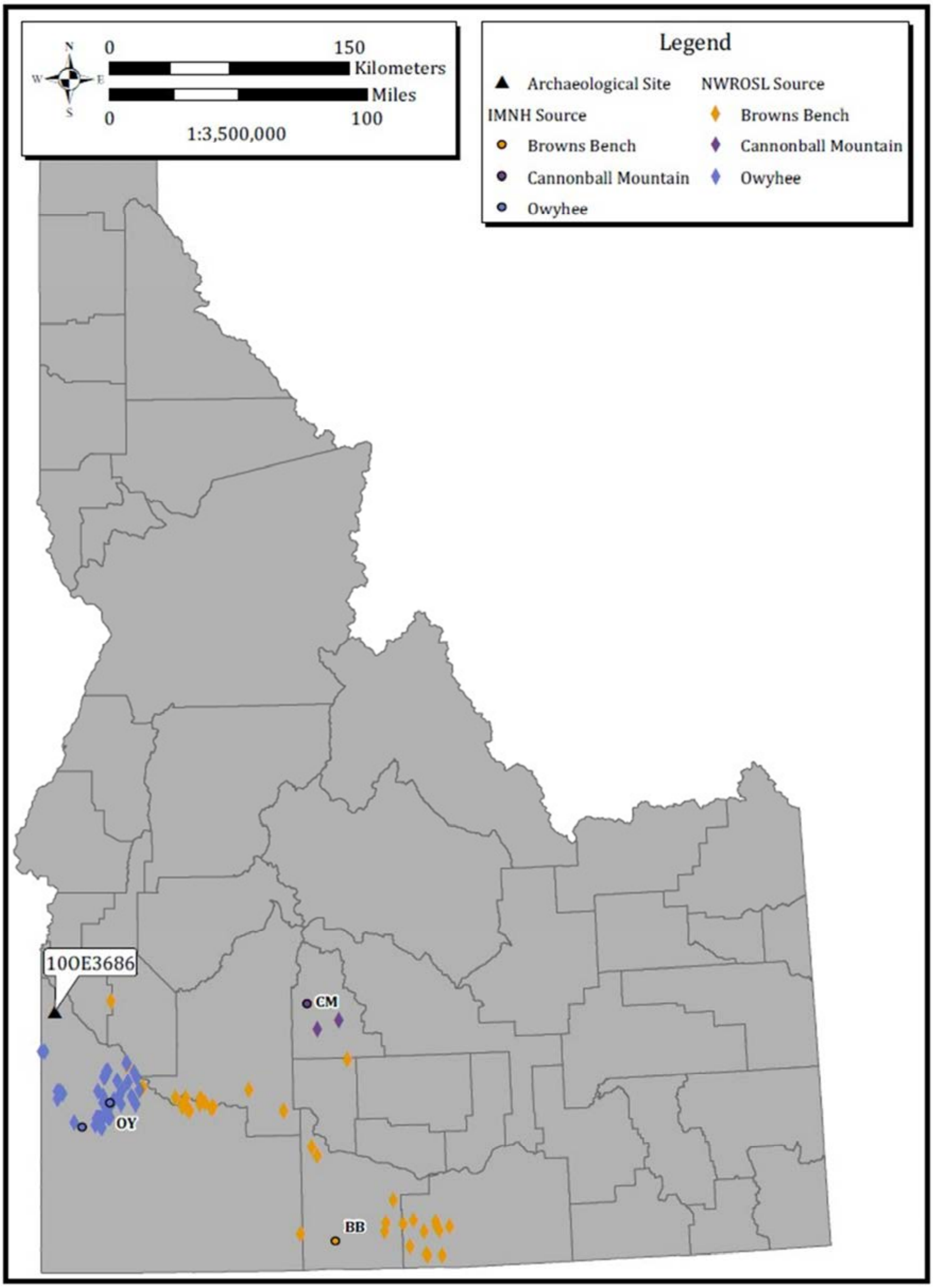

Figure 6.14. Site and Idaho Obsidian Sources Present in Assemblage.

the east, southeast, and south. However, the majority of artifacts appear to be from unknown source(s). The nine unknown sources are perhaps explained by either the existence of unknown obsidian source(s) or by procurement from source(s) outside of Idaho (Figure 6.14 and Table 6.11).

Table 6.11 10OE3686: All-Method Artifact Source Assignments

BB	CM/1	OY	UNK	Total
1	1	3	9	14
7.1%	**7.1%**	**21.5%**	**64.3%**	**100%**

Theoretical Application

To determine the relative frequencies of obsidian artifacts and the distances between sites and sources, it is necessary to statistically and systematically determine the obsidian sources represented at a site. In theory, the sources reflected in a site’s assemblage might have a higher relative frequency of smaller or later stage debitage at sites farther from a source (e.g., obsidian), while at sites closer to the source, all sizes and stages of lithic reduction may be present (Metcalfe and Barlow 1992; Renfrew 1977). The expectation is that obsidian sources closer to the site should exhibit a higher relative frequency of obsidian artifacts in a site’s assemblage, while obsidian sources farther from the site should result in a lower relative frequency of obsidian artifacts.

Geography of Lithic Procurement

Geographical applications of distance decay (fall-off) models in the United States arose in the 1970s. The theory of distance decay originated from Christaller’s Central Place Theory (CPT) with the intent to study the movement of contemporary people in regards to land use, transportation, and economics (Christaller 1933; Fotheringham 1981; Olsson 1970). The idea that the frequency of artifacts decreases with increasing distance from a source was first formalized by Colin Renfrew in 1977 with the law of monotonic decrement:

> In circumstances of uniform loss or deposition, and in the absence of highly organized directional (i.e., preferential, nonhomogeneous) exchange, the curve of frequency or abundance of occurrence of an exchanged commodity against effective distance from a localised source will be a monotonic decreasing one. (Renfrew 1977: 72)

Distance decay parameters measure the relationship between observed interaction patterns and distance, assuming all other determinants are held constant and that any variants observed are a result of decision making on the part of the agent (Fotheringham 1981). Logistical foragers move across the landscape relatively frequently compared to residential collectors (Binford 1980). This behavior may be reflected in the site assemblage as more or less variety in the obsidian sources found in the site. In theory, the farther a site is from a lithic source, the lower the relative abundance of that lithic source when compared to the relative abundance of a lithic source closer to a site. However, this does not take into account preference, quality, spatial relationship to other sources, or physical and social boundaries or constraints, all of which impact the validity of a simple distance decay model.

Distance decay models focus on the pattern of resources found in archaeological sites as the distance from the resource increases. An alternate way to look at the problem is to assess the appeal of the resource to the agent because this would explain why the “decision” would be made to travel a farther distance to obtain a particular resource. Renfrew (1977) cautioned that this Law of Monotonic Decrement is frequently violated due to the presence of a commodity from farther away at a greater frequency than that of a commodity in closer proximity. When the law is violated, the pattern of resource distribution is directional and is best explained by a gravity model (Wilson 2007). This disagreement with the hypothetical distance decay model outcome may be explained by a gravity model that assumes that additional attractiveness variables are substantial factors in lithic resource procurement. The gravity model explains the presence of a commodity from farther away at a greater frequency than a commodity in closer proximity. Gravity models are applicable to the study of directional resource distribution and the attraction to competing resources. In essence, the opposite viewpoint of a distance decay model is a gravity model (Wilson 2007, 2011).

The first experiments with distance decay and gravity models in archaeology were performed by archaeologists from the United Kingdom: Renfrew, Hodder, and Orton. The first explicit use of a gravity model in archaeology is performed by Hodder and Orton (1976), while the first use of a distance decay model in archaeology is performed by Renfrew (1977). The study performed by Hodder and Orton found that there are distance decay gradients in terms of how steeply the abundance of a given good falls off in relation to its size and value, wherein heavier less valuable items (cores, etc.) fall off more steeply than do lighter more valuable goods (bifaces, projectile points, etc.) (Hodder and Orton 1976). Renfrew found that in addition to the expectations of a distance decay model, resources would be distributed in an extremely localized fashion and that distance between a central place and a resource should be considered three-dimensionally (Renfrew 1977).

The gravity model applied by Lucy Wilson's study to flint sources in southeastern France is an innovative application wherein she ranks the attractiveness of particular flint resources according to the quality of the raw material, the size and ease of the packages that can be extracted from the source, as well as the abundance of usable pieces per square meter (Elston 1992; Wilson 2007). Factors that could detract from the attractiveness of a resource include the difficulty of the terrain in accessing the resource and the cost (in time) of extracting the resource (Wilson 2007). In addition to the attractiveness of a flint resource, Wilson also recognizes that no matter how attractive a lithic resource is, distance will always play a role in the distribution of the resource (Wilson 2007). The creation of a gravity model allows for directly comparing sources, and calculating the attractiveness of sources, as well as the areas of influence for a particular resource (Wilson 2007, 2011).

Conclusion

Hughes and Bennyhoff (1986:238) caution that “it is one thing to determine the geographic source area for a commodity, but it is quite another matter to infer the social mechanism responsible for the occurrence of that material at an archaeological site.”

The comparison of obsidian source profiles between labs, the discrepancy in names, and the low between-lab reliability for some elements of these source profiles suggests that interpretations of prehistoric human activity in Southern Idaho should be evaluated with skepticism due to the incomplete knowledge of obsidian sources. A systematic survey and re-survey of geologic obsidian sources and a sampling strategy to address variation within and between obsidian sources may provide an opportunity to develop more reliable inferences. A survey of the sources should incorporate information on the geologic context, petrogenesis, and geochemical character of the obsidian sources. A more detailed, centralized, and accessible regional database of geologic obsidian sources that goes beyond state boundaries would provide researchers with access to the same source geochemical profiles and allow for more direct comparison(s). The preceding recommendations would increase the validity of source and artifact assemblage geochemical characterizations and provide a foundation for more useful interpretations of past human behavior.

REFERENCES

Aptech Systems, Inc.

2006 GAUSS Runtime Module for Windows. http://archaeometry.missouri.edu/datasets/GAUSS_Download.html, accessed February 1, 2014.

Armstrong, R. L.

1975 The Geochemistry of Idaho: Isochron. *West* 14:50.

Bailey, Jeff

1992 X-Ray Fluorescence Characterization of Volcanic Glass Artifacts from Wilson Butte Cave, Idaho. Unpublished Master's Thesis, Department of Anthropology, University of Alberta, Edmonton, Alberta, Canada.

Beck, Charlotte, and George T. Jones

1988 Western Pluvial Lakes Tradition Occupation in Butte Valley, Eastern Nevada. In *Early Human Occupation in Far Western North America: The Clovis-Archaic Interface*, edited by J. A. Willig, C. M. Aikens, and J. L. Fagan, pp. 273-301. Nevada State Museum Anthropological Papers 21. Carson City.

1990a The Late Pleistocene/Early Holocene Archaeology of Butte Valley, Nevada: Three Seasons' Work. *Journal of California and Great Basin Anthropology* 12(2):231-261.

1990b Toolstone Selection and Lithic Technology in Early Great Basin Prehistory. *Journal of Field Archaeology* 17:283-299.

1997 The Terminal Pleistocene/Early Holocene Archaeology of the Great Basin. *Journal of World Prehistory* 11(2):161-236.

Beck, Charlotte, Amanda K. Taylor, George T. Jones, Cynthia M. Fadem, Caitlyn R. Cook, and Sara A. Millward

2002 Rocks are Heavy: Transport Costs and Paleoarchaic Quarry Behavior in the Great Basin. *Journal of Anthropological Archaeology* 21:481-507.

Binford, Lewis. R.

1973 Inter-assemblage Variability- the Mousterian and the “Functional Argument”. In *The Explanation of Culture Change: Models in Prehistory*, edited by C. Renfrew, pp. 227-254, Duckworth, London.

1977 Forty-seven Trips. In *Stone Tools as Cultural Markers: Change, Continuity, and Complexity*, edited by R. V. S. Wright, pp. 24-36. Australian Institute of Aboriginal Studies, Canberra, ACT.

1979 Organization and Formation Processes: Looking at Curated Technologies. *Journal of Anthropological Research* 35:255-273.

1980 Willow Smoke and Dogs' Tails: Hunter-Gatherer Settlement Systems and Archaeological Site Formation. *American Antiquity* 45:4-20.

Bonnichsen, Bill

1982 The Bruneau-Jarbidge Eruptive Center, Southwestern Idaho. In *Cenozoic Geology of Idaho*, edited by B. Bonnichsen and R. M. Breckenridge, pp. 237-254. Idaho Bureau of Mines and Geology Bulletin 26.

Brott, Charles A., David D. Blackwell, and John C. Mitchell

1978 Tectonic Implications of the Heat Flow of the Western Snake River Plain, Idaho. Geological Society of America Bulletin 89(12).1697-1707.

Brown, Patricia E.

1982 Tracing Prehistoric Sources of Obsidian. In *Granite Reef: A Study in Desert Archaeology*, edited by Patricia E. Brown and Connie L. Stone, pp.227-241. Arizona State University Anthropological Research Papers No. 28 and Arizona State University Anthropological Field Studies No. 3. Arizona State University, Tempe.

Bruker Corporation

2014 http://www.bruker.com/products/x-ray-diffraction-and-elemental-analysis/handheld-xrf.html, accessed February 1, 2014.

Burley, David, Peter J. Sheppard, and Maia Simonin

2011 Tongan and Samoan Volcanic Glass: pXRF Analysis and Implications for Constructs of Ancestral Polynesian Society. *Journal of Archaeological Science* 38:2625-2632.

Cann, Johnson R., and Colin Renfrew

1964 The Characterization of Obsidian and its Application to the Mediterranean Region. In *Proceedings of the Prehistoric Society* 30(1):1.

Christaller, Walter

1933 Central Places in Southern Germany. Translated by Carlisle W. Baskin. 1966, Prentice-Hall, Englewood Cliffs, NJ.

Clemens, Drew M.

1993 Tectonics and Silicic Volcanic Stratigraphy of the Western Snake River Plain, Southwestern Idaho. Unpublished MA thesis, Department of Anthropology, Arizona State University, Phoenix, Arizona.

Corn, Tyrone L.

2006 Timber Butte Obsidian Source Survey: Geology, Prehistory, Chemical Sourcing, and Debitage Analysis. Unpublished MA thesis, Department of Anthropology, University of Idaho, Moscow, Idaho.

Craig, Nathan, Robert J. Speakman, Rachel S. Popelka-Filcoff, Michael D. Glascock, J. David Robertson, M. Steven Shackley, and Mark S. Aldenderfer

2007 Comparison of XRF and PXRF for Analysis of Archaeological Obsidian from Southern Peru. *Journal of Archaeological Science* 34(12):2012-2024.

Davis, M. Kathleen, Thomas L. Jackson, M. Steven Shackley, Timothy Teague, and Joachim H. Hampel

2011 Factors Affecting the Energy-Dispersive X-ray Fluorescence (EDXRF) Analysis of Archaeological Obsidian. In *Archaeological Obsidian Studies: Method and Theory*, edited by M. S. Shackley, pp. 83-102. Kluwer Academic/Plenum Press, New York and Amsterdam.

Digital Atlas of Idaho

2002 Compiled by Paul K. Link, Idaho State University, Geosciences Department. http://imnh.isu.edu/digitalatlas, accessed February 1, 2014.

Ebinger, Michael H.

1984 An X-ray Fluorescence Analysis of Hohokam Lithics. In *Hohokam Archaeology Along the Salt-Gila Aqueduct Central Arizona Project: 8. Material Culture*, edited by L. S. Teague and P. L. Crown, pp. 445-452. Archaeological Series No.

150. Cultural Resource Management Division, Arizona State Museum, University of Arizona, Tucson.

Eerkens, Jelmer W., Jeffrey R. Ferguson, Michael D. Glascock, Craig E. Skinner, and Sharon A. Waechter

2007 Reduction Strategies and Geochemical Characterization of Lithic Assemblages: A Comparison of Three Case Studies from Western North America. *American Antiquity* 72:585-597.

Ekren, Einar B., McIntyre, D. H., Bennett, E. H., and H. E. Malde

1981 Geologic Map of Owyhee County, Idaho West of Longitude 116^{O} W. Miscellaneous Investigation Series Map I-1256 (SHEET 2 OF 2). Department of the Interior United States Geological Survey.

Elston, Robert G.

1992 Modeling the Economics and Organization of Lithic Procurement. In *Archaeological Investigations at Tosawihi, A Great Basin Quarry, Part 1: The Periphery, Volume 1*. Report prepared for the Bureau of Land Management, Elko Resource Area, Nevada. Edited by R. G. Elston and C. Raven. Intermountain Research and Bureau of Land Management, Silver City, Nevada.

Forster, Nicola, and Peter Grave

2012 Non-Destructive PXRF Analysis of Museum-Curated Obsidian from the Near East. *Journal of Archaeological Science* 39:728-736.

Forster, Nicola, Peter Grave, Nancy Vickery, and Lisa Kealhofer

2011 Non-Destructive Analysis Using PXRF: Methodology and Application to Archaeological Ceramics. *X-ray Spectrometry* 40:389-398.

Fotheringham, A. Stewart

1981 Spatial Structure and Distance-Decay Parameters. *Annals of the Association of American Geographers* 71: 425-436.

Frahm, Ellery

2013a Validity of “Off-the-Shelf” Handheld Portable XRF for Sourcing Near Eastern Obsidian Chip Debris. *Journal of Archaeological Science* 40(2):1080-1092.

2013b Is Obsidian Sourcing About Geochemistry or Archaeology? A Reply to Speakman and Shackley. *Journal of Archaeological Science* 40(2):1444-1448.

Freeman, Otis W., J. D. Forrester, and R. L. Lupher

1945 Physiographic Divisions of the Columbia Intermountane Province. *Association of American Geographers Annuals* 35(2):53-75.

Gallagher, Joseph G.

1979 *Archaeology of Sheepeater Battleground and Redfish Overhang Sites: Settlement Model for Central Idaho*. U.S. Forest Service, Intermountain Region, Archaeological Report 5. Ogden.

GAUSS Runtime Version 8.0

2014 University of Missouri Research Reactor, Archaeometry Laboratory. http://archaeometry.missouri.edu/datasets/GAUSS_Download.html, accessed February 1, 2014.

Giauque, Robert D., Frank Asaro, Fred H. Stross, and Thomas R. Hester

1993 High-Precision Non-Destructive X-ray Fluorescence Method Applicable to Establishing the Provenance of Obsidian Artifacts. *X-ray Spectrometry* 22(1):44-53.

Glascock, Michael D., Geoffrey E. Braswell, and Robert H. Cobean

1998 A Systematic Approach to Obsidian Source Characterization. In *Archaeological Obsidian Studies: Method and Theory,* edited by M. S. Shackley, pp. 83-102. Kluwer Academic/Plenum Press, New York and Amsterdam.

Glascock, Michael D.

2002 Introduction: Geochemical Evidence for Long-Distance Exchange. In *Geochemical Evidence for Long-Distance Exchange*, edited by M. D. Glascock, pp. 1-12. Bergin and Garvey, Westport, Conn.

Goffer, Zui

1980 *Archaeological Chemistry: A Sourcebook on the Applications of Chemistry to Archaeology*. John Wiley and Sons, New York.

Goodale, Nathan, David G. Bailey, George T. Jones, Catherine Prescott, Elizabeth Scholz, Nick Stagliano, and Chelsea Lewis

2012 pXRF: A Study of Inter-instrument Performance. *Journal of Archaeological Science* 39:875-883.

Goodyear, Albert C.

1979 *A Hypothesis for the Use of Cryptocrystalline Raw Materials Among Paleo-Indian Groups of North America*. Research Manuscript Series No. 156. Institute of Archaeology and Anthropology, University of South Carolina, Columbia.

Gould, Russell T., and Mark G. Plew

2001 *Archaeological Excavations at Three Island Crossing*. Boise State University. Boise, Idaho.

Green, James P.

1982 XRF Trace Element Analysis and Hydration Measurement of Archaeological and Source Obsidians from the Northeastern Great Basin. Paper presented at the 18th Biennial Meeting of the Great Basin Anthropological Conference, Reno.

1983 Obsidian Hydration Chronology: The Early Owl Cave Remains. Paper Presented at the 11th Annual Conference of the Idaho Archaeological Society, Boise.

1984 Obsidian Hydration Chronology of Three Upland Sites from the Northeastern Great Basin. Paper presented at the 19th Biennial Meeting of the Great Basin Anthropological Conference, Boise.

Hodder, Ian and Clive Orton

1976 *Spatial Analysis in Archaeology*. Cambridge University Press, Cambridge.

Holmer, Richard N.

1997 Volcanic Glass Utilization in Eastern Idaho. *Tebiwa* 26(2):186-194.

Hughes, Richard E.

1984 Obsidian Sourcing Studies in the Great Basin: Problems and Prospects. In *Contributions of the University of California Archaeological Research Facility: Obsidian studies in the Great Basin, No. 45*. Editor Richard E. Hughes, pp. 1-20. Berkeley: Archaeological Research Facility, Dept. of Anthropology, University of California.

1986 Exploring Diachronic Variability in Obsidian Procurement Patterns in Northeast California and Southcentral Oregon. *University of California Publications in Anthropology* 17. Berkeley.

1998 Reliability, Validity, and Scale in Obsidian Sourcing Research. In *Unit Issues in Archaeology: Measuring Time, Space, and Material*, edited by A. F. Ramenofsky and A. Steffen. University of Utah Press, Salt Lake City, Utah.

2012 *Perspectives on Prehistoric Trade and Exchange in California and the Great Basin*. University of Utah Press.

Hughes, Richard E. and James A. Bennyhoff

1986 Early Trade. In *Handbook of North American Indians Great Basin Vol. 11*, edited by W. L. D'Azevedo, pp. 238-255. Smithsonian Institution, Washington D.C.

Hughes, Richard E. and Max G. Pavesic

2009 Geochemical Analysis of Obsidian from the DeMoss Site, Western Idaho: Implications for the Western Idaho Archaic Burial Complex. *Journal of Northwest Anthropology* 43(1):117-124.

Hughes, Richard E. and Robert L. Smith

1993 Archaeology, Geology, and Geochemistry in Obsidian Provenance Studies. In *Scale on Archaeological and Geoscientific Perspectives*, edited by J. K. Stein and A. R. Linse, pp.79-91. Geological Society of America Special Paper No. 283. The Society, Boulder, Colorado.

Hunter, Pamela, John Kennedy, Sharon Plager, Mark Plew, and Trisha Webb

1998 *Archaeological Test Excavations at 10CN5, Southwest Idaho.* Technical Reports No. 10. Boise State University. Boise, Idaho.

IBM Corp.

2011 IBM SPSS Statistics for Windows, Version 20.0. Armonk, NY: IBM Corp.

Idaho State University

2014 Idaho State University, Geology Department. http://geology.isu.edu/dml/maps/Idaho_latlong.jpg, accessed April 4, 2014.

Jack, Robert N., and Ian Carmichael

1969 The Chemical “Fingerprinting” of Acid Volcanic Rocks. *California Division of Mines and Geology Special Report* 100:17-32.

Jack, Robert N., and Heizer, Robert F.

1968 “Finger-Printing” of Some Mesoamerican Obsidian Artifacts. *Contributions of the University of California Archaeological Research Facility* 5:81-100.

Jenkins, Ron

1974 *Introduction to X-ray Spectrometry*. Heyden, London.

Jones, George T. and Charlotte Beck

1999 Paleoarchaic Archaeology in the Great Basin. In *Models for the Millennium*, edited by C. Beck, pp. 83-95. University of Utah Press, Salt Lake City.

Jones, George T., Charlotte Beck, Eric E. Jones, and Richard E. Hughes

2003 Lithic Source Use and Paleoarchaic Foraging Territories in the Great Basin. *American Antiquity* 68:5-38.

Kelly, Robert L.

1983 Hunter-Gatherer Mobility Strategies. *Journal of Anthropological Research* 39:277-306.

1988 The Three Sides of a Biface. *American Antiquity* 53:717-734.

1992 Mobility/Sedentism: Concepts, Archaeological Measures, and Effects. *Annual Review of Anthropology* 21:43-66.

2001 Prehistory of the Carson Desert and Stillwater Mountains: Environment, Mobility and Subsistence in a Great Basin Wetland. *University of Utah Anthropological Papers Number 123*. Salt Lake City.

Kelly, Robert L. and Lawrence C. Todd

1988 Coming into the Country: Early Paleoindian Hunting and Mobility. *American Antiquity* 53:231-244.

King, J. S.

1982 Selected Volcanic Features of the South-Central Snake River Plain, Idaho. In *Cenozoic Geology of Idaho*, edited by B. Bonnichsen and R. M. Breckenridge, pp. 439-451. Idaho Bureau of Mines and Geology Bulletin 26.

Kuhn, Steven L.

1995 *Mousterian Lithic Technology: An Ecological Perspective*. Princeton University Press.

Kuntz, Mel A., Duane E. Champion, Elliott C. Spiker, Richard H. Lefebvre, and Lisa A. McBroome

1982 The Great Rift and the Evolution of the Craters of the Moon Lava Field, Idaho. In *Cenozoic Geology of Idaho: Idaho Bureau of Mines and Geology Bulletin* 26, edited by B. Bonnichsen and R. M. Breckenridge, pp. 423 - 438.

Liritzis, Ioannis, and Nikolaos Zacharias

2011 Portable XRF of Archaeological Artifacts: Current Research, Potentials and Limitations. In *X-Ray Fluorescence Spectrometry (XRF) in Geoarchaeology*, edited by M. S. Shackley, pp. 109-142. Springer Science + Business Media, LLC. New York.

Lundblad, Steven P., Peter R. Mills, and Ken Hon

2008 Analysing Archaeological Basalt Using Non-Destructive Energy-Dispersive X-ray Fluorescence (EDXRF): Effects of Post-Depositional Chemical Weathering and Sample Size on Analytical Precision. *Archaeometry* 50:1-11.

Malde, Harold E.

1965 Snake River Plain. *The Quaternary of the United States*, edited by H. E. Wright, Jr. and David G. Frey, pp. 255-263. Princeton University Press, Cambridge.

1991 Quaternary Geology and Structural History of the Snake River Plain, Idaho and Oregon. *The Geology of North America* 2:251-281.

Metcalfe, Duncan, and K. Renee Barlow

1992 A Model for Exploring the Optimal Trade-off Between Field Processing and Transport. *American Anthropologist* 94:340-356.

Millhauser, John K., Enrique Rodrigues-Alegria, and Michael D. Glascock

2011 Testing the Accuracy of Portable X-ray Fluorescence to Study Aztec and Colonial Obsidian Supply at Xaltocan, Mexico. *Journal of Archaeological Science* 38:3141-3152.

Nazaroff, Adam, Keith M. Prufer, and Brandon L. Drake

2010 Assessing the Applicability of Portable X-ray Fluorescence Spectrometry for Obsidian Provenance Research in the Maya Lowlands. *Journal of Archaeological Science* 37:885-895.

Nazaroff, Adam, and M. Steven Shackley

2009 Testing the Size Dimension Limitation of Portable XRF Instrumentation for Obsidian Provenance. In *2009 Portland GSA Annual Meeting.*

Neff, Hector

2001 Neutron Activation Analysis for Provenance Determination in Archaeology. In *Modern Analytical Methods in Art and Archaeology,* edited by Enrico Ciliberto and Guiseppe Spoto. Chemical Analysis Series, Volume 155. John Wiley & Sons, New York.

Nelson Jr, Fred W.

1984 X-ray Fluorescence Analysis of Some Western North American Obsidians. In *Contributions of the University of California Archaeological Research Facility: Obsidian studies in the Great Basin, No. 45,* edited by Richard E. Hughes, pp. 27-62. University of California. Berkeley.

O’Connor, Jim E.

1993 *Hydrology, Hydraulics, and Geomorphology of the Bonneville Flood.* Geological Society of America Special Paper 274. Boulder, Colorado.

Olsson, Gunnar

1970 Explanation, Prediction and Meaning Variance: An Assessment of Distance Interaction Models. *Economic Geography* 46:223.

Parry, William J., and Robert L. Kelly

1987 Expedient Core Technology and Sedentism. In *The Organization of Core Technology,* edited by J. K. Johnson and C. A. Morrow, pp. 285-304. Westview Press, Boulder, Colorado.

Perkins, Michael E., William P. Nash, Francis H. Brown, and Robert J. Fleck

1995 Fallout Tuffs of Trapper Creek, Idaho: A Record of Miocene Explosive Volcanism in the Snake River Plain Volcanic Province. *Geological Society of America Bulletin* 107(12):1484-1506.

Pessanha, S., A. Guilherme, and M.L. Carvalho

2009 Comparison of Matrix Effects on Portable and Stationary XRF Spectrometers for Cultural Heritage Samples. *Applied Physics A 97*:497-505.

Phillips, S. Colby, and Robert J. Speakman

2009 Initial Source Evaluation of Archaeological Obsidian from the Kuril Islands of the Russian Far East Using Portable XRF. *Journal of Archaeological Science* 36:1256-1263.

Pierce, Kenneth L. and Lisa A. Morgan

1992 The Track of the Yellowstone Hot Spot: Volcanism, Faulting, and Uplift. In *Regional Geology of Eastern Idaho and Western Wyoming*, edited by P. K. Link, M. A. Kuntz, and L. B. Platt. Geological Society of America Memoir 179:1-53.

Plager, Sharon R.

2001 Patterns in the Distribution of Volcanic Glass Across Southern Idaho. Unpublished MA thesis, Department of Anthropology, Idaho State University, Pocatello, Idaho.

Plew, Mark G., Pamela Hunter, and Richard Benedict

2002 *Archaeological Test Excavations at 10EL1577 Near King Hill, Idaho.* Boise State University. Boise, Idaho.

Plew, Mark G., Sharon Plager, Tedd D. Jacobs, and Christopher A. Willson

2006 *Archaeological Excavations at 10CN6, Middle Snake River Idaho.* Monographs in Archaeology No. 3. Boise State University. Boise, Idaho.

Plew, Mark G., and Christopher A. Willson

2005 *Archaeological Test Excavations at the Medbury Site (10-EL-1367), Southwest Idaho.* Idaho Archaeologist 28(2):15-22.

2011 *Archaeological Excavations at 10-EL-215, Near King Hill, Idaho.* Monographs in Archaeology No. 5. Boise State University. Boise, Idaho.

Reed, William G.

1985 An Approach to the Archaeological Identification of Shoshonean Subsistence Territories in Southern Idaho. . Unpublished MA thesis, Department of Anthropology, Idaho State University, Pocatello, Idaho.

Renfrew, Colin.

1977 Alternative Models for Exchange and Spatial Distribution. In *Exchange Systems in Prehistory,* edited by T.K. Earle and J.E. Ericson, pp. 71-90. Academic Press, New York.

Sappington, Robert L.

1981a A Progress Report on the Obsidian and Vitrophyre Sourcing Project. *Idaho Archaeologist* 4(4):4-17.

1981b Additional Obsidian and Vitrophyre Source Descriptions from Idaho and Adjacent Areas. *Idaho Archaeologist* 5(1):4-8.

Shackley, M. Steven

1990 Early Hunter-Gatherer Procurement Ranges in the Southwest: Evidence for Obsidian Geochemistry and Lithic Technology. Unpublished Ph.D. dissertation, Arizona State University.

1992 The Upper Gila River Gravels as an Archaeological Obsidian Source Region: Implications for Models of Exchange and Interaction. *Geoarchaeology* 7:315-326.

1996 Range and Mobility in the Early Hunter-Gatherer Southwest. In *Early Formative Adaptations in the Southern Southwest,* edited by B. J. Rother, pp. 5-16. Prehistory Press, Madison, Wisconsin.

1998a Current Issues and Future Directions in Archaeological Volcanic Glass Studies: An Introduction. In *Archaeological Obsidian Studies: Method and Theory*, edited by M. S. Shackley, pp. 83-102. Kluwer Academic/Plenum Press, New York and Amsterdam.

1998b Geochemical Differentiation and Prehistoric Procurement of Obsidian in the Mount Taylor Volcanic Field, Northwest New Mexico. *Journal of Archaeological Science* 25:1073-1082.

1998c Intrasource Chemical Variability and Secondary Depositional Processes in Sources of Archaeological Obsidian: Lessons from the American Southwest. In *Archaeological Obsidian Studies: Method and Theory,* edited by M. S. Shackley, pp. 83-102. Kluwer Academic/Plenum Press, New York and Amsterdam.

2002 Precision Versus Accuracy in the XRF Analysis of Archaeological Obsidian: Some Lessons for Archaeometry and Archaeology. In *Proceedings of the 31st Symposium on Archaeometry, Budapest, Hungary*, edited by E. Jerem and K. T. Biro, pp. 805-810. BAR International Series 1043 (II), Oxford.

2005 *Obsidian: Geology and Archaeology in the North American Southwest*. University of Arizona Press, Tucson, Arizona.

2011 An Introduction to X-Ray Fluorescence Spectrometry (XRF) in Archaeology. In *X-Ray Fluorescence Spectrometry (XRF) in Geoarchaeology*, edited by M. S. Shackley, pp. 7-44. Springer Science + Business Media, LLC. New York.

Sheppard, Peter, Barbara Trichereau, and Cristany Milicich

2010 Pacific Obsidian Sourcing by Portable XRF. *Archaeology in Oceania* 45:21-30.

Shott, Michael J.

1989 On Tool-class Use Lives and the Formation of Archaeological Assemblages. American Antiquity 54(1):9-30.

Skinner, Craig E., M. Kathleen Davis, and Thomas M. Origer

1995 *X-Ray Fluorescence Analysis and Obsidian Hydration Rim Measurements of Artifact Obsidian from 10-CU-170, Caribou County, Idaho*. BioSystems Analysis, Inc., Obsidian Studies Laboratory, Corvallis, Oregon. Prepared for Science Applications International Corporation, Golden, Colorado, Report 1995-71.

Skinner, Craig E. and Jennifer J. Thatcher

2013 *X-Ray Fluorescence Analysis of Artifact Obsidian from 10-CW-30, 10-IH-453, 10-ID-1009, and 10-IH-2737, Clearwater and Idaho Counties, Idaho*. Northwest Research Obsidian Studies Laboratory, Corvallis, Oregon. Prepared for the University of Idaho, Moscow, Idaho, Report 2013-107.

Smith, Geoffrey M.

2005a The Paleoarchaic Occupation of Moonshine Spring South and Moonshadow Spring, Pershing County, Nevada: Implications for Early-Period Mobility in the Great Basin. *Nevada Archaeologist* 20/21:57-70.

2005b Pre-Archaic Mobility at the Parman Localities, Humboldt County, Nevada. *Current Research in the Pleistocene* 22:64-66.

Smith, Robert B. and Lawrence W. Braile

1994 The Yellowstone Hotspot. *Journal of Volcanology and Geothermal Research* 61(3-4):121-129,135-187.

Speakman, Robert J.

2012 Evaluation of Bruker's Tracer Family Factory Obsidian Calibration for Handheld Portable XRF Studies of Obsidian. Centre for Applied Isotope Studies, University of Georgia, Athens Georgia. Report prepared for Bruker AXS, Kennewick, WA. Available on-line: http://www.bruker-axs.com/fileadmin/user_upload/PDFse/handhelds/Bruker_Obsidian_Report.pdf.

Speakman, Robert J. and M. Steven Shackley

2013 Silo Science and Portable XRF in Archaeology: A Response to Frahm. *Journal of Archaeological Science* 40(2):1435-1443.

Spear, Dallas B. and John S. King

1982 The Geology of Big Southern Butte, Idaho. In *Cenozoic Geology of Idaho: Idaho Bureau of Mines and Geology Bulletin* 26, edited by B. Bonnichsen and R. M. Breckenridge, pp. 395-403.

Stevenson, D. P., F. H. Stross, and R. F. Heizer

1971 An Evaluation of X-ray Fluorescence Analysis as a Method for Correlating Obsidian Artifacts with Source Location. *Archaeometry* 13(1):17-25.

Thompson, Randy A.

2004 Trade or Transport Occurrence of Obsidian from the Malad, Idaho, Source in the Great Plains. Unpublished MA thesis, Department of Anthropology, Idaho State University, Pocatello, Idaho.

Thornbury, William D.

1965 *Regional Geomorphology of the United States*. John Wiley and Sons, New York.

Weigand, Phil C., Garman Harbottle, and Edward V. Sayre

1977 Turquoise Sources and Source Analysis: Mesoamerica and Southwestern U.S.A. In Exchange Systems in Prehistory, edited by T. K. Earle and J. E. Ericson, pp.15-34. Academic Press, New York.

Williams-Thorpe, Olwyn

2008 The Application of Portable X-ray Fluorescence Analysis to Archaeological Lithic Provenancing. Portable X-ray Fluorescence Spectrometry: Capabilities for in Situ Analysis, edited by Philip J. Potts and Margaret West, pp. 174-205. Royal Society of Chemistry.

Willson, Christopher A.

2005 X-ray Fluorescence Analysis of Obsidian Associated with Late Archaic Sites in Southwestern Idaho and Southeastern Oregon, Issues in Addressing Mobility. Unpublished MA thesis, Department of Anthropology, University of Idaho, Moscow, Idaho.

Willson, Christopher A., Mark G. Plew

2007 *Archaeological Excavations at the King Hill Creek Site (10EL110): A Late Archaic Occupation Near King Hill, Idaho.* Monographs in Archaeology No. 4. Boise State University. Boise, Idaho.

Wilson, Lucy

2007 Understanding Prehistoric Lithic Raw Material Selection: Application of a Gravity Model. *Journal of Archaeological Method and Theory* 14:388-411.

2011 The Role of Geoarchaeology in Extending Our Perspective. In *Human Interactions with the Geosphere: the Geoarchaeological Perspective,* edited by L. Wilson, pp. 1-9. The Geological Society of London. MPG Books, Ltd. Bodmin, UK.

APPENDIX A

Table A Idaho Obsidian Source Name Variants by XRF Lab

Source Name	**IMNH & Holmer 1997 Name(s)**	**NWROSL Name(s)**
American Falls (Walcott)*	American Falls; *Walcott; Snake River*	American Falls
Bear Gulch*	Bear Gulch; *Big Table Mountain; Centennial; Camas-Dry Creek; Spring Creek; Warm Creek Spring; West Camas Creek*	Bear Gulch
Big Southern Butte*	Big Southern Butte	Big Southern Butte
Browns Bench*	Browns Bench; *Rock Creek; Mahogany Butte*	Browns Bench; *Monument Peak, Hudson Ridge 1, 2 & 3; McMullen Basin; Shoshone Creek; Cassias Ridge View; Indian Springs/ Road; Snake River Area; Snake River 1 & 2; Schooler Creek Area; Timmerman Hills; Twin Falls Area; Sinker Creek Area B; Oakley Area; Sawtooth NF; CJ Strike Reservoir/ Area; Cold Springs Creek; Salmon Falls Creek Area 1 & 2; Coal Bank; Bruneau Dunes Area; Pasadena Valley Area; Devils Creek; New York Canal*
Browns Bench Area*	--	Browns Bench Area; *Salmon Falls Creek Area 2; Snake River Area; CJ Strike Reservoir*
Butte Valley A*	Butte Valley A	Browns Bench/Butte Valley Group A; *Hudson Ridge 1, 2 & 3; McMullen Basin; Snake River 2; Canyon Creek 1 & 2; Schooler Creek Area; Oakley Area; Twin Falls Area*
Camas Prairie	Camas Prairie; *Camas Prairie A; Camas Prairie 1*	--
Cannonball Mountain (Cannonball Mountain 1)*	Cannonball Mountain 1; *Camas Prairie 2*	Cannonball Mountain; *Simon Site*

Cannonball Mountain 2*	Cannonball Mountain 2	--
Cedar Butte*	Cedar Butte; *Cedar Creek; House Creek*	--
Chesterfield*	Chesterfield; *Smith Creek*	--
Coal Bank Spring	Coal Bank Spring	Browns Bench
Conant Creek*	Conant Creek; *Buggy Springs*	--
Deadhorse Ridge*	--	Deadhorse Ridge
Deep Creek	Deep Creek	--
Dry Creek	Dry Creek	--
Fish Creek	Fish Creek; *Upper Fish Creek Road; Partridge Creek; South Partridge Creek; Lower Fish Creek Road*	--
Jasper Flats	Jasper Flats	--
Jordan Creek*	--	Jordan Creek
Kelly Canyon*	Kelly Canyon	Kelly Canyon
Malad*	Malad; *Hawkins; Oneida; Dairy Creek; Garden Creek Gap*	Malad; *Wright Creek*
Medicine Lodge Canyon	Medicine Lodge Canyon	--
Murphy Hot Springs*	Murphy Hot Springs; *Murphy Springs*	--
Obsidian Cliff*	Obsidian Cliff	--
Owyhee*	Owyhee; *Owyhee 2; Browns Castle; Oreana; Toy Pass*	Owyhee; *Toy Pass A; Antelope Spring; Meadow Creek; Browns Creek; Brown Owyhee; Gray Owyhee; Owyhee Area; Jordan Creek; Snake River/ Area; Sinker Creek Area A, B & C; Stateline Area; Castle Creek*
Ozone	Ozone	--
Pack Saddle*	Pack Saddle; *Pack Saddle Creek; Gibson Creek*	--
Picabo Hills	Picabo Hills	--
Pine Mountain	Pine Mountain	--
Reas Pass*	Reas Pass	Reas Pass; *Yale Creek*
Rock Creek	Rock Creek	--
Reynolds*	Reynolds	Reynolds; *Jordan Creek*
Sinker Canyon*	--	Sinker Canyon; *Owyhee Area; Snake River 1*
Striker Basin Gulch*	--	Striker Basin Gulch
Teton Pass 1*	Teton Pass 1; *Teton Pass 2; Fish Creek; Mosquito Creek*	--
Three Creek 1 & 2	Three Creek 1 & 2	--
Timber Butte*	Timber Butte; *Squaw Butte*	Timber Butte

Walcott (American Falls)*	Walcott; *American Falls*	American Falls
Wedge Butte*	Wedge Butte; *Snowflake*	Wedge Butte
Yale Creek	Yale Creek	Reas Pass

Table B **IMNH Bear Gulch Library Standard**

Tile Runs	Mn Avg	Mn SD	Fe Avg	Fe SD	Zn Avg	Zn SD	Ga Avg	Ga SD	Th Avg	Th SD
0	308.0556	51.6170	11229.1100	178.0180	63.2105	4.0490	17.2086	0.4190	19.7930	1.2110
1	301.6899	1.2183	11187.7040	27.6930	58.9569	1.7651	16.7860	0.8015	17.8320	1.8731
2	277.7233	1.1713	11119.7911	27.5106	60.3947	1.7956	16.9521	0.8154	20.2177	2.0416
3	318.6624	1.2559	11524.7367	28.6023	65.9841	1.9043	17.3165	0.8146	21.2675	2.1296
4	235.4368	1.0795	10594.3098	26.1076	53.5358	1.6616	16.4873	0.8129	19.5633	1.9959
5	249.9132	1.1133	10907.3030	26.9414	65.1524	1.9234	17.4363	0.8255	19.2518	1.9768
6	360.1193	1.3263	11188.6531	27.6956	58.0929	1.7112	16.7887	0.8456	20.0556	2.0261
7	308.7230	1.2317	11191.8240	27.7041	67.4887	1.8428	17.7791	0.9844	20.7963	2.0951
8	334.4300	1.2785	11130.2510	27.5387	62.8795	1.8050	17.2845	0.8859	18.3588	1.8968
9	299.0019	1.2180	11475.3266	28.4686	65.1485	1.7754	17.4585	0.9690	18.6864	1.9215
10	321.3271	1.2553	11190.5630	27.7007	58.5598	1.7817	16.6661	0.7652	18.7704	1.9269
11	349.9044	1.3116	11410.9623	28.2946	66.1555	1.8168	17.5719	0.9526	19.7664	2.0122
12	277.2888	1.1724	11243.4957	27.8431	62.0121	1.8180	17.0834	0.8275	22.1076	2.1803
13	257.0990	1.1354	11400.2166	28.2656	65.7566	1.8811	17.4151	0.8519	18.5437	1.9204
14	414.2979	1.4221	11198.4456	27.7219	58.1919	1.7102	16.8000	0.8494	21.0015	2.1030
15	315.0228	1.2465	11371.2216	28.1873	57.4037	1.7387	16.5392	0.7673	18.4849	1.9113
16	239.8248	1.0977	11200.0162	27.7261	63.4982	1.8295	17.2949	0.8665	17.4419	1.8392
17	263.3350	1.1413	11002.1251	27.1951	62.8835	1.8567	17.2227	0.8288	19.2065	1.9756
18	263.4038	1.1479	11406.9609	28.2838	61.6359	1.8044	16.9890	0.8170	19.2412	1.9757

Tile Runs	Rb Avg	Rb SD	Sr Avg	Sr SD	Y Avg	Y SD	Zr Avg	Zr SD	Nb Avg	Nb SD
0	165.2724	4.6950	49.6528	1.5860	42.4712	1.8290	300.3661	1.9900	52.1023	1.3940
1	161.6525	12.3859	47.8731	4.1251	40.9152	7.0642	297.4689	34.4221	52.4739	9.1149
2	167.0527	12.7841	49.5181	4.2522	43.0193	7.3571	296.1723	34.2924	51.2670	8.9817
3	160.7211	12.3171	49.2488	4.2314	42.3147	7.2051	298.8480	34.5956	50.6059	8.8830
4	165.2427	12.6507	46.6987	4.0343	44.2154	7.4651	299.3202	34.6206	52.6363	9.1686
5	162.7280	12.4652	52.1057	4.4522	40.7500	7.0591	303.7152	35.1851	52.8310	9.1609
6	169.2543	12.9463	53.7516	4.5795	40.1893	7.0761	308.4909	35.7503	49.5893	8.7394
7	160.4046	12.2937	48.6351	4.1840	45.1974	7.5138	302.5878	35.0166	49.4568	8.7579
8	171.3435	13.1000	48.7767	4.1949	39.1992	6.9933	294.8198	34.1291	53.5356	9.2470
9	171.1233	13.0838	52.0278	4.4462	44.5548	7.5717	312.6338	36.2046	55.5717	9.5568
10	171.6249	13.1207	46.3847	4.0100	40.5431	7.1428	307.0598	35.5027	51.4393	8.9867
11	164.4616	12.5931	50.9161	4.3603	45.1435	7.5562	307.2988	35.5816	52.3462	9.1383
12	168.0619	12.8585	51.7923	4.4280	43.9292	7.4676	299.5587	34.7059	53.6912	9.3056
13	165.1452	12.6435	50.2142	4.3060	43.6102	7.3984	300.6620	34.8142	52.0657	9.0890
14	165.0091	12.6335	45.5018	3.9418	44.0636	7.4459	303.6304	35.1002	52.5703	9.1585
15	168.1038	12.8616	48.5651	4.1786	43.2382	7.3933	299.0311	34.6087	51.0760	8.9597
16	164.7660	12.6156	48.8745	4.2025	43.2419	7.3540	297.7586	34.4666	51.8227	9.0538
17	161.3634	12.3645	46.4074	4.0118	43.1064	7.2987	301.1726	34.8293	52.8704	9.1855
18	162.9371	12.4807	48.9814	4.2107	39.3500	6.9092	310.8501	35.9659	50.5435	8.8507

Table C.1 Idaho Obsidian Source Geochemical Profiles by Name and Lab

Source	Mn Avg	Mn SD	Fe Avg	Fe SD	Zn Avg	Zn SD	Ga Avg	Ga SD	Th Avg	Th SD
American Falls/ Walcott (IMNH)	303.3613	30.7860	8744.9437	608.6239	54.0474	5.2829	16.9513	0.5352	20.8687	1.5206
American Falls/ Walcott (NWROSL)	266.0833	22.5039	11750.0000	1003.9054	69.2917	7.9645	19.8750	2.7554	30.7500	3.9370
Bear Gulch (IMNH)	290.2491	44.8612	10935.3420	481.9229	59.8492	4.2790	17.0210	0.4763	19.2041	1.5486
Bear Gulch (NWROSL)	295.0645	25.5612	15920.9677	1220.6068	62.1129	8.7817	20.9032	2.7324	27.1935	2.9300
Big Southern Butte (IMNH)	301.2221	42.1819	12074.8905	656.9405	174.9565	9.9679	30.9612	1.2614	29.9397	2.2540
Big Southern Butte (NWROSL)	264.9000	32.9088	15700.0000	2458.5452	281.8000	21.3479	40.5000	3.9791	24.8000	2.7406
Browns Bench (IMNH)	290.7551	49.2551	15671.3582	1283.5866	110.4861	62.9207	19.8504	4.5306	24.8232	2.2403
Browns Bench (NWROSL)	278.2035	88.1122	19137.1681	2506.1779	60.0885	14.6193	19.9381	4.8500	25.1441	6.3301
Browns Bench Area (NWROSL)	297.6000	107.2185	15360.0000	1006.4790	52.4000	8.4735	20.4000	4.1593	27.2000	3.0332
Butte Valley A (IMNH)	450.4200	71.8400	36036.0000	0.3500	90.0500	9.4000	17.0600	0.6900	No Data	No Data
Butte Valley A (NWROSL)	374.4444	81.4467	24892.5926	2614.7402	82.8148	14.3849	21.2963	4.4877	17.0909	5.7645

Source	Rb Avg	Rb SD	Sr Avg	Sr SD	Y Avg	Y SD	Zr Avg	Zr SD	Nb Avg	Nb SD
American Falls/ Walcott (IMNH)	173.9705	7.5724	28.2255	2.6855	54.9399	1.9360	226.5974	9.6992	44.5763	1.7646
American Falls/ Walcott (NWROSL)	200.5833	7.6835	27.3333	1.7611	63.9167	1.9763	234.2083	5.0215	49.9583	1.6011
Bear Gulch (IMNH)	164.6071	6.6555	47.9367	2.2147	42.0590	2.3077	293.3805	11.8457	50.5899	1.9408
Bear Gulch (NWROSL)	187.1290	5.9519	46.8548	2.0232	46.5161	1.8795	301.6935	9.7553	60.2903	2.0991
Big Southern Butte (IMNH)	265.7938	9.1533	7.7723	1.0560	209.0336	8.6229	317.6467	11.3928	338.6152	16.0973
Big Southern Butte (NWROSL)	311.2000	11.8958	4.8000	0.4472	223.2000	5.1381	311.6000	9.2760	309.9000	6.7239
Browns Bench (IMNH)	188.4035	9.3190	54.4236	3.6136	58.0257	3.8559	444.0334	23.1997	42.8185	1.9959
Browns Bench (NWROSL)	216.9669	13.3116	48.8347	6.0337	65.4463	5.2757	421.5702	36.0476	47.2727	4.3436
Browns Bench Area (NWROSL)	234.6000	5.1284	25.4000	2.6077	59.6000	1.6733	350.8000	25.5480	44.8000	1.7889
Butte Valley A (IMNH)	155.4400	4.1300	72.9000	3.1100	66.6600	3.2800	518.5400	27.1000	49.7200	0.7800
Butte Valley A (NWROSL)	188.8889	7.3607	70.0741	4.4109	71.2593	2.7117	537.1111	21.3079	53.5926	2.0050

Source	Ba Avg	Ba SD	Pb Avg	Pb SD	Ti Avg	Ti SD
American Falls/ Walcott (IMNH)	No Data	No Data	No Data	No Data	No Data	No Data
American Falls/ Walcott (NWROSL)	915.2917	53.8327	32.2917	3.4450	1165.5417	96.5802
Bear Gulch (IMNH)	No Data	No Data	No Data	No Data	No Data	No Data
Bear Gulch (NWROSL)	644.0806	27.8493	28.0484	2.9941	1569.3710	138.4544
Big Southern Butte (IMNH)	No Data	No Data	No Data	No Data	No Data	No Data
Big Southern Butte (NWROSL)	4.3000	5.2292	87.0000	5.6765	413.8000	44.4492
Browns Bench (IMNH)	No Data	No Data	No Data	No Data	No Data	No Data
Browns Bench (NWROSL)	987.7603	108.5234	27.9381	5.2632	1649.4159	207.3431
Browns Bench Area (NWROSL)	494.4000	40.2467	29.6000	2.9665	1425.4000	88.0528
Butte Valley A (IMNH)	No Data	No Data	No Data	No Data	No Data	No Data
Butte Valley A (NWROSL)	1112.1111	43.1244	25.7407	5.7015	1973.7407	186.7424

Table C.2 Idaho Obsidian Source Geochemical Profiles by Name and Lab

Source	Mn Avg	Mn SD	Fe Avg	Fe SD	Zn Avg	Zn SD	Ga Avg	Ga SD	Th Avg	Th SD
Cannonball Mountain/1 (IMNH)	429.7113	51.6718	22223.1048	238.0860	232.0098	11.0889	28.6086	1.0769	42.4785	2.0084
Cannonball Mountain/1 (NWROSL)	396.7456	66.9766	33431.1111	3168.1289	230.2923	18.5880	30.4740	6.1572	40.1763	10.4851
Cannonball Mountain 2 (IMNH)	514.8948	81.1271	27676.4252	1477.6692	297.2463	35.3728	28.3491	2.0886	35.8124	3.2301
Cedar Butte (IMNH)	545.1288	66.3004	18261.4649	917.1663	216.4342	13.8612	30.6166	1.5332	29.4327	1.6692
Chesterfield (IMNH)	329.4497	38.1831	12324.4417	927.7469	58.2651	9.9899	16.3877	0.7305	9.3311	1.0725
Conant Creek (IMNH)	269.3977	31.0383	10148.0336	1380.2408	68.8270	7.9971	18.1888	0.5095	20.3874	1.5002
Deadhorse Ridge (NWROSL)	292.3000	79.5935	15730.0000	1952.2352	80.7000	17.5629	19.9000	3.2128	20.5000	6.2583
Jordan Creek (NWROSL)	146.1000	45.9600	10890.0000	2137.7298	40.3000	6.7007	16.6000	3.7771	14.8000	1.8738
Kelly Canyon (IMNH)	269.5153	92.7284	9186.4379	1808.4926	59.1840	18.9355	17.4069	1.5045	20.1014	0.9093
Malad (IMNH)	262.4188	93.0932	6891.6431	1059.7479	35.6390	3.7145	15.6083	0.1958	16.2624	1.0135
Malad (NWROSL)	171.5600	32.8254	7608.0000	1523.1327	38.0000	4.7258	17.1200	3.1665	23.6400	4.0299

Source	**Rb Avg**	**Rb SD**	**Sr Avg**	**Sr SD**	**Y Avg**	**Y SD**	**Zr Avg**	**Zr SD**	**Nb Avg**	**Nb SD**
Cannonball Mountain/1 (IMNH)	336.3349	10.2157	9.9621	1.6657	112.9192	3.2656	1052.0643	31.8985	114.6530	4.0270
Cannonball Mountain/1 (NWROSL)	385.1848	19.7977	5.5124	1.3699	118.3573	5.8459	1090.3944	51.4740	124.0403	6.5439
Cannonball Mountain 2 (IMNH)	293.6539	21.9703	9.3267	1.3131	103.3163	7.1714	664.7917	37.3767	105.0200	7.0362
Cedar Butte (IMNH)	219.1403	8.7584	9.8644	1.1929	213.3920	9.6167	668.3967	30.6952	298.2692	16.7603
Chesterfield (IMNH)	78.2290	1.4463	218.3279	8.1955	23.1869	0.9101	181.0992	2.9552	12.4482	1.2003
Conant Creek (IMNH)	160.8058	3.6961	30.7369	9.2782	64.5423	2.9315	186.7848	6.5943	53.9236	1.7279
Deadhorse Ridge (NWROSL)	186.2000	8.8040	22.4000	1.7764	69.1000	3.5730	335.7000	10.1986	56.6000	2.8363
Jordan Creek (NWROSL)	175.9000	8.8122	79.9000	4.9092	26.9000	2.2336	178.2000	21.4880	10.4000	1.7127
Kelly Canyon (IMNH)	179.0205	19.4781	29.4316	7.1774	48.4496	23.4217	187.5217	77.5008	34.6121	23.7443
Kelly Canyon (NWROSL)	182.6000	6.9775	21.4667	1.1255	81.8000	3.0048	267.4000	5.1381	64.8667	2.5033
Malad (IMNH)	119.2974	3.1812	77.7570	3.8481	30.5930	1.5314	95.3299	6.4640	15.4707	1.0095
Malad (NWROSL)	130.2400	8.6037	74.5200	3.6185	33.8800	1.5631	98.4400	4.0526	14.4400	1.9166

Source	Ba Avg	Ba SD	Pb Avg	Pb SD	Ti Avg	Ti SD
Cannonball Mountain/1 (IMNH)	No Data	No Data	No Data	No Data	No Data	No Data
Cannonball Mountain/1 (NWROSL)	2.9289	4.6537	58.8464	6.8319	978.2993	107.8481
Cannonball Mountain 2 (IMNH)	No Data	No Data	No Data	No Data	No Data	No Data
Cedar Butte (IMNH)	No Data	No Data	No Data	No Data	No Data	No Data
Chesterfield (IMNH)	No Data	No Data	No Data	No Data	No Data	No Data
Conant Creek (IMNH)	No Data	No Data	No Data	No Data	No Data	No Data
Deadhorse Ridge (NWROSL)	811.4000	30.9846	25.1000	6.3149	1096.9000	153.1567
Jordan Creek (NWROSL)	1451.1000	169.6922	22.0000	2.4944	773.7000	270.2102
Kelly Canyon (IMNH)	No Data	No Data	No Data	No Data	No Data	No Data
Kelly Canyon (NWROSL)	753.0000	23.9255	29.8667	2.3258	790.9333	63.4344
Malad (IMNH)	No Data	No Data	No Data	No Data	No Data	No Data
Malad (NWROSL)	1530.7600	98.6527	31.4800	3.6414	305.0800	61.0095

Table C.3 Idaho Obsidian Source Geochemical Profiles by Name and Lab

Source	Mn Avg	Mn SD	Fe Avg	Fe SD	Zn Avg	Zn SD	Ga Avg	Ga SD	Th Avg	Th SD
Murphy Hot Springs (IMNH)	241.4075	28.7655	13288.0789	382.9507	75.6210	1.5819	17.8631	0.1560	27.9480	1.8282
Obsidian Cliff (IMNH)	314.1300	20.0400	14962.0000	0.0750	79.7000	6.6600	20.2300	0.2600	No Data	No Data
Owyhee (IMNH)	192.1464	22.0696	6931.8040	265.7502	41.2570	5.3392	16.2113	0.5549	20.0792	2.0047
Owyhee (NWROSL)	186.1037	49.2216	9703.3333	1078.2524	49.4176	16.0999	19.3788	4.6888	22.2051	4.3022
Pack Saddle (IMNH)	349.0912	42.7824	11861.8184	737.4290	70.8518	4.5797	17.8022	0.4292	20.7108	1.4485
Reas Pass (NWROSL)	231.3929	30.2891	14289.2857	2245.2154	66.1429	5.9982	21.2500	2.5477	28.4643	4.0413
Reynolds (NWROSL)	150.3043	55.9468	10665.2174	2049.0815	133.7500	10.9475	24.6250	3.3207	29.3333	6.0409
Sinker Canyon (NWROSL)	197.5714	51.8333	14623.8095	1015.4440	150.2143	21.9195	25.8095	4.9151	25.2619	3.4786
Striker Basin Gulch (NWROSL)	No Data	No Data	No Data	No Data	No Data	No Data	36.0000	No Data	34.0000	No Data
Teton Pass 1 (IMNH)	348.1724	35.7900	7720.7545	411.5382	41.4137	4.4576	15.9641	0.4380	12.5288	1.7608
Timber Butte (IMNH)	526.1300	17.1430	7902.0000	0.0320	59.3300	6.0500	17.5300	0.2900	No Data	No Data
Timber Butte (NWROSL)	684.1750	75.2207	4455.0000	661.3700	60.7500	5.5320	22.8462	3.4909	14.0750	3.6961

Source	Rb Avg	Rb SD	Sr Avg	Sr SD	Y Avg	Y SD	Zr Avg	Zr SD	Nb Avg	Nb SD
Murphy Hot Springs (IMNH)	214.6707	6.8705	27.2290	0.9003	60.2512	2.2982	365.9203	10.6823	43.7049	1.6501
Obsidian Cliff (IMNH)	237.3400	6.3400	7.4700	0.3200	77.9200	2.2400	163.5900	3.2200	42.2000	1.5600
Owyhee (IMNH)	193.3054	7.4507	33.4208	2.3558	27.0878	0.6760	111.7736	4.4749	12.1640	0.4959
Owyhee (NWROSL)	211.5165	12.9867	34.9744	10.3655	29.0586	2.8252	120.4505	11.6663	11.1612	1.9953
Pack Saddle (IMNH)	159.4906	6.4641	24.8431	2.1232	60.7424	3.0068	338.9246	12.4668	50.4030	2.0219
Reas Pass (NWROSL)	188.1786	6.0373	26.0357	2.9374	66.2857	2.2910	292.5000	8.7242	55.5000	2.6458
Reynolds (NWROSL)	334.4583	19.8275	6.2857	2.5912	113.0417	4.3885	184.2083	6.8269	40.7083	2.8814
Sinker Canyon (NWROSL)	254.9762	4.2912	23.0952	2.9780	92.9762	3.4464	218.3810	7.7647	40.5000	2.0030
Striker Basin Gulch (NWROSL)	361.0000	No Data	34.0000	No Data	100.0000	No Data	355.0000	No Data	48.0000	No Data
Teton Pass 1 (IMNH)	112.9595	6.2588	129.3229	5.5024	24.6617	1.8620	80.9843	3.1414	14.4150	1.0161
Timber Butte (IMNH)	176.2700	3.9800	17.4800	0.7000	41.1400	2.2900	49.7600	2.7800	27.9200	0.8800
Timber Butte (NWROSL)	191.4500	5.3491	18.0000	1.2403	44.1500	2.1430	62.7000	2.0903	36.3250	1.5589

Source	Ba Avg	Ba SD	Pb Avg	Pb SD	Ti Avg	Ti SD
Murphy Hot Springs (IMNH)	No Data	No Data	No Data	No Data	No Data	No Data
Obsidian Cliff (IMNH)	No Data	No Data	No Data	No Data	No Data	No Data
Owyhee (IMNH)	No Data	No Data	No Data	No Data	No Data	No Data
Owyhee (NWROSL)	294.4444	224.2107	24.9927	3.4289	550.8444	147.5131
Pack Saddle (IMNH)	No Data	No Data	No Data	No Data	No Data	No Data
Reas Pass (NWROSL)	858.0357	57.7937	29.0714	2.7207	1005.3929	137.9341
Reynolds (NWROSL)	0.1250	0.6124	53.7500	5.1605	303.0870	74.0908
Sinker Canyon (NWROSL)	207.0000	34.7668	37.7381	3.7938	577.9286	96.8805
Striker Basin Gulch (NWROSL)	No Data	No Data	64.0000	No Data	No Data	No Data
Teton Pass 1 (IMNH)	No Data	No Data	No Data	No Data	No Data	No Data
Timber Butte (IMNH)	No Data	No Data	No Data	No Data	No Data	No Data
Timber Butte (NWROSL)	42.6000	8.5778	35.3250	2.7492	222.6500	42.4122

Table C.4 Idaho Obsidian Source Geochemical Profiles by Name and Lab

Source	Mn Avg	Mn SD	Fe Avg	Fe SD	Zn Avg	Zn SD	Ga Avg	Ga SD	Th Avg	Th SD
Wedge Butte (IMNH)	291.5028	38.6112	8187.1496	274.6380	95.2719	5.0775	22.4476	0.7031	52.1151	2.1744
Wedge Butte (NWROSL)	291.8077	62.0639	10461.5385	963.3595	121.1538	13.9762	32.8077	4.9962	38.8846	4.7017

Source	Rb Avg	Rb SD	Sr Avg	Sr SD	Y Avg	Y SD	Zr Avg	Zr SD	Nb Avg	Nb SD
Wedge Butte (IMNH)	490.7559	17.0880	12.5822	1.0560	171.6608	4.9663	154.9058	9.1998	122.0986	3.8799
Wedge Butte (NWROSL)	532.6154	26.7224	13.8077	1.4702	177.0385	6.9136	143.0000	6.8235	113.1154	8.0911

Source	**Ba Avg**	**Ba SD**	**Pb Avg**	**Pb SD**	**Ti Avg**	**Ti SD**
Wedge Butte (IMNH)	No Data	No Data	No Data	No Data	No Data	No Data
Wedge Butte (NWROSL)	5.2692	8.3501	63.6923	5.7045	596.7308	236.7683

Table D HCA Dendrogram

Page 14/1

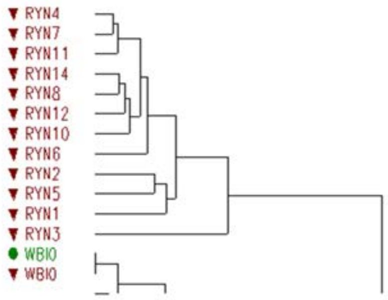

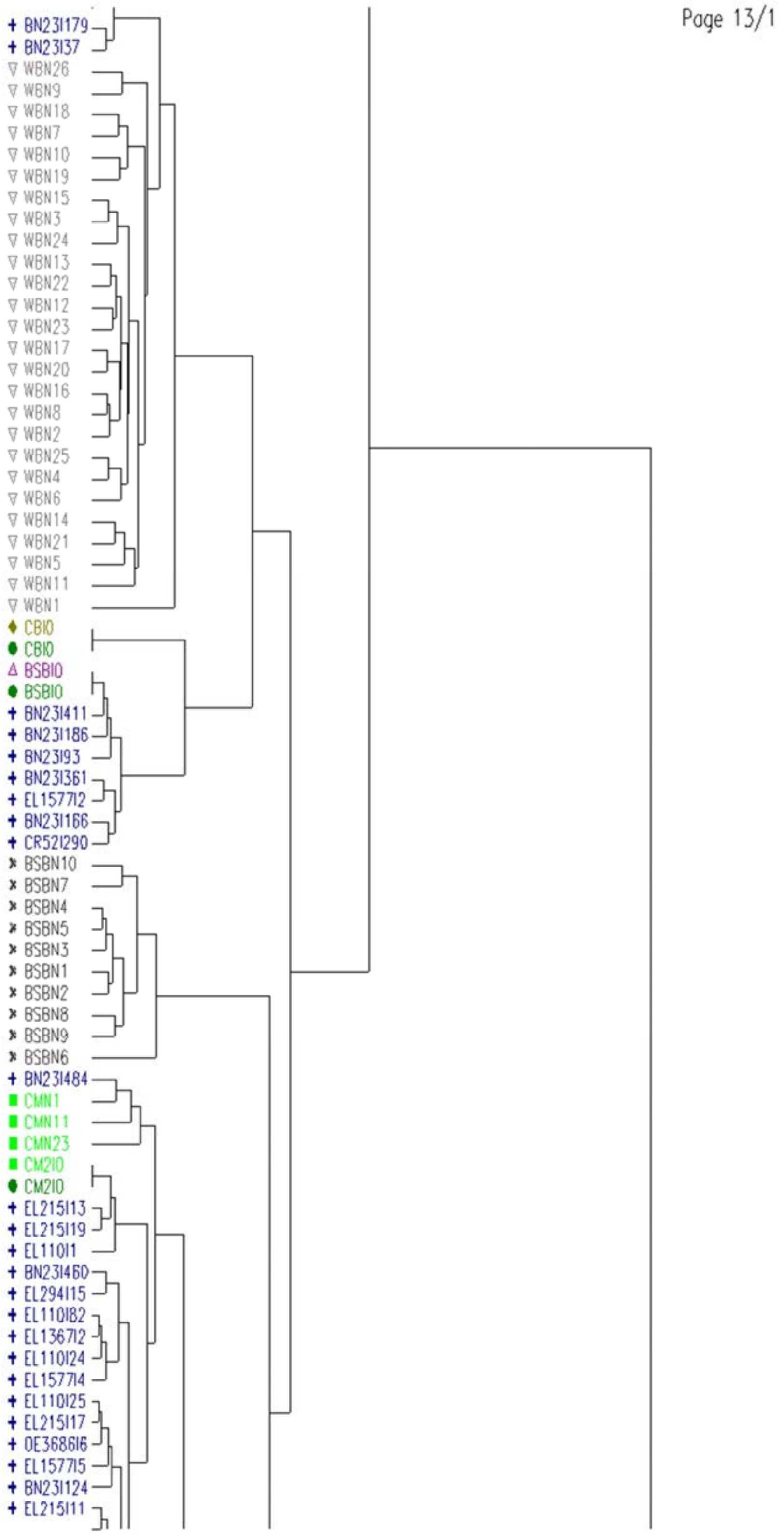
Page 13/1
BN231179
BN23137
WBN26
WBN9
WBN18
WBN7
WBN10
WBN19
WBN15
WBN3
WBN24
WBN13
WBN22
WBN12
WBN23
WBN17
WBN20
WBN16
WBN8
WBN2
WBN25
WBN4
WBN6
WBN14
WBN21
WBN5
WBN11
WBN1
CB10
CB10
BSB10
BSB10
BN231411
BN231186
BN23193
BN231361
EL157712
BN231166
CR521290
BSBN10
BSBN7
BSBN4
BSBN5
BSBN3
BSBN1
BSBN2
BSBN8
BSBN9
BSBN6
BN231484
CMN1
CMN11
CMN23
CM210
CM210
EL215113
EL215119
EL11011
BN231460
EL294115
EL110182
EL136712
EL110124
EL157714
EL110125
EL215117
0E368616
EL157715
BN231124
EL215111

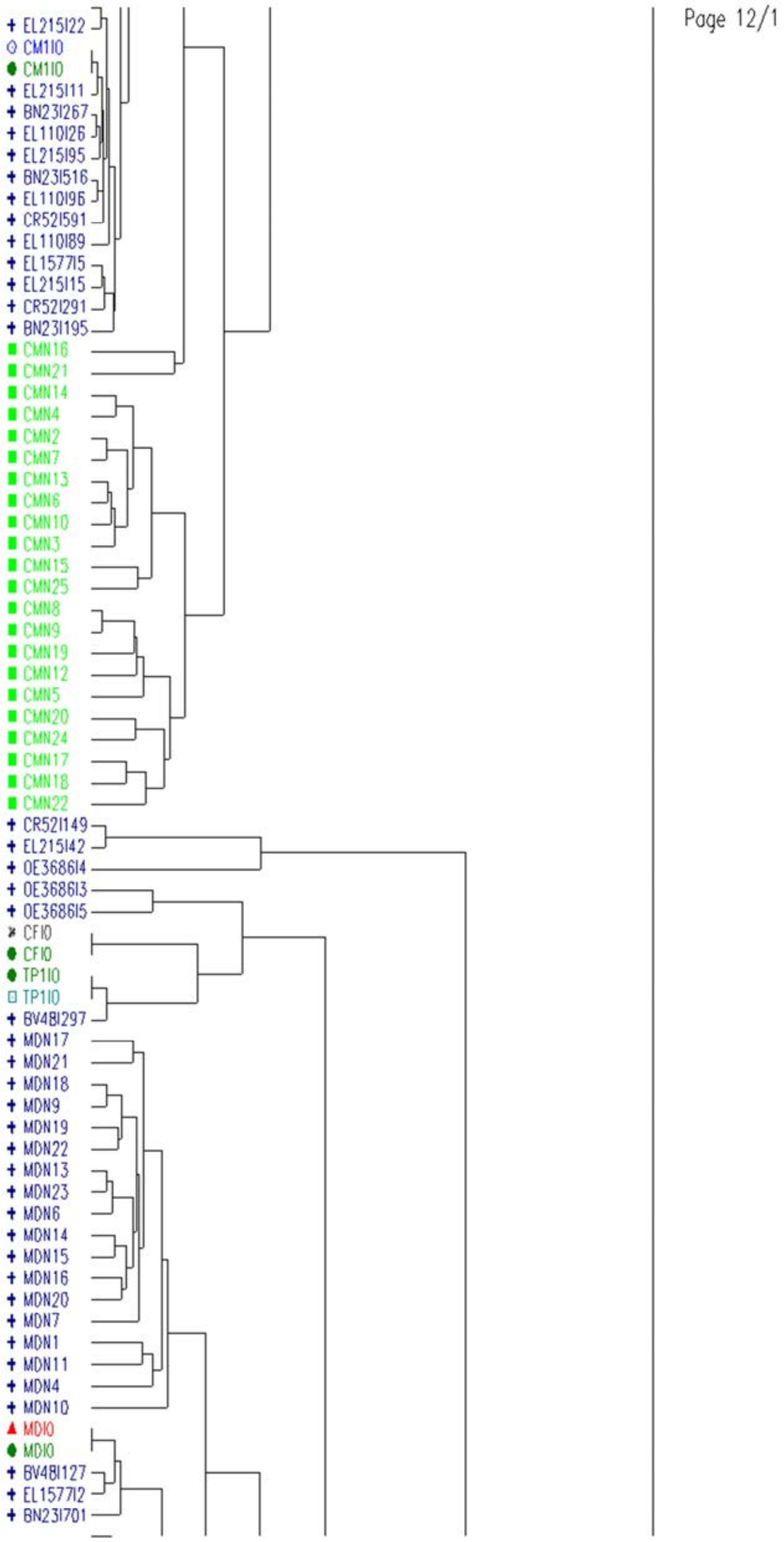
Page 12/1
+ EL215I22
○ CM1I0
● CM1I0
+ EL215I11
+ BN23I267
+ EL110I26
+ EL215I95
+ BN23I516
+ EL110I96
+ CR52I591
+ EL110I89
+ EL1577I5
+ EL215I15
+ CR52I291
+ BN23I195
■ CMN16
■ CMN21
■ CMN14
■ CMN4
■ CMN2
■ CMN7
■ CMN13
■ CMN6
■ CMN10
■ CMN3
■ CMN15
■ CMN25
■ CMN8
■ CMN9
■ CMN19
■ CMN12
■ CMN5
■ CMN20
■ CMN24
■ CMN17
■ CMN18
■ CMN22
+ CR52I149
+ EL215I42
+ OE3686I4
+ OE3686I3
+ OE3686I5
✻ CFI0
● CFI0
● TP1I0
□ TP1I0
+ BV48I297
+ MDN17
+ MDN21
+ MDN18
+ MDN9
+ MDN19
+ MDN22
+ MDN13
+ MDN23
+ MDN6
+ MDN14
+ MDN15
+ MDN16
+ MDN20
+ MDN7
+ MDN1
+ MDN11
+ MDN4
+ MDN10
▲ MDI0
● MDI0
+ BV48I127
+ EL1577I2
+ BN23I701

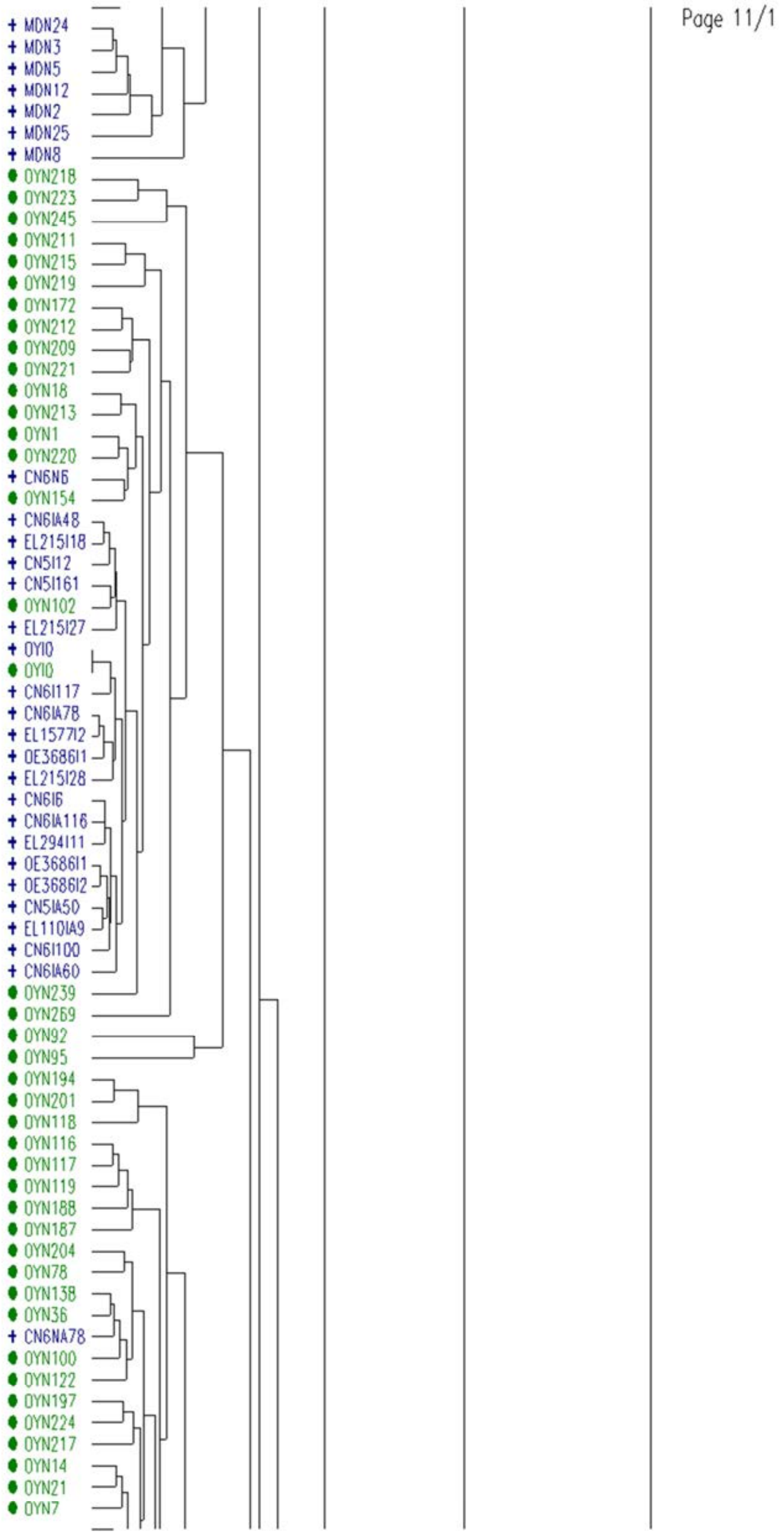
Page 11/1
+ MDN24
+ MDN3
+ MDN5
+ MDN12
+ MDN2
+ MDN25
+ MDN8
● OYN218
● OYN223
● OYN245
● OYN211
● OYN215
● OYN219
● OYN172
● OYN212
● OYN209
● OYN221
● OYN18
● OYN213
● OYN1
● OYN220
+ CN6N6
● OYN154
+ CN6IA48
+ EL215I18
+ CN5I12
+ CN5I161
● OYN102
+ EL215I27
+ OYI0
● OYI0
+ CN6I117
+ CN6IA78
+ EL157I2
+ OE3686I1
+ EL215I28
+ CN6I6
+ CN6IA116
+ EL294I11
+ OE3686I1
+ OE3686I2
+ CN5IA50
+ EL110IA9
+ CN6I100
+ CN6IA60
● OYN239
● OYN269
● OYN92
● OYN95
● OYN194
● OYN201
● OYN118
● OYN116
● OYN117
● OYN119
● OYN188
● OYN187
● OYN204
● OYN78
● OYN138
● OYN36
+ CN6NA78
● OYN100
● OYN122
● OYN197
● OYN224
● OYN217
● OYN14
● OYN21
● OYN7

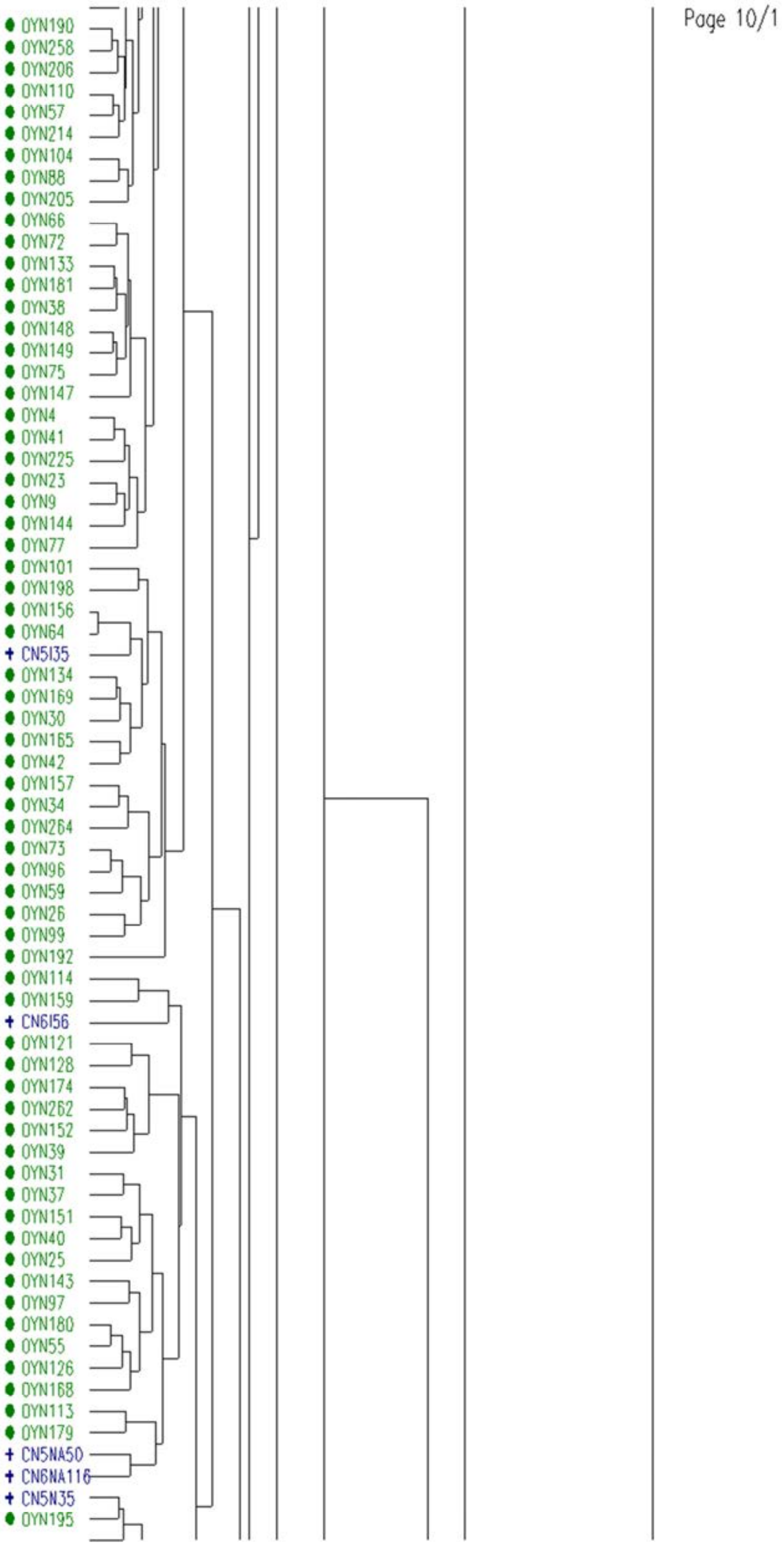
Page 10/1
● OYN190
● OYN258
● OYN206
● OYN110
● OYN57
● OYN214
● OYN104
● OYN88
● OYN205
● OYN66
● OYN72
● OYN133
● OYN181
● OYN38
● OYN148
● OYN149
● OYN75
● OYN147
● OYN4
● OYN41
● OYN225
● OYN23
● OYN9
● OYN144
● OYN77
● OYN101
● OYN198
● OYN156
● OYN64
+ CN5I35
● OYN134
● OYN169
● OYN30
● OYN165
● OYN42
● OYN157
● OYN34
● OYN264
● OYN73
● OYN96
● OYN59
● OYN26
● OYN99
● OYN192
● OYN114
● OYN159
+ CN6I56
● OYN121
● OYN128
● OYN174
● OYN262
● OYN152
● OYN39
● OYN31
● OYN37
● OYN151
● OYN40
● OYN25
● OYN143
● OYN97
● OYN180
● OYN55
● OYN126
● OYN168
● OYN113
● OYN179
+ CN5NA50
+ CN6NA116
+ CN5N35
● OYN195

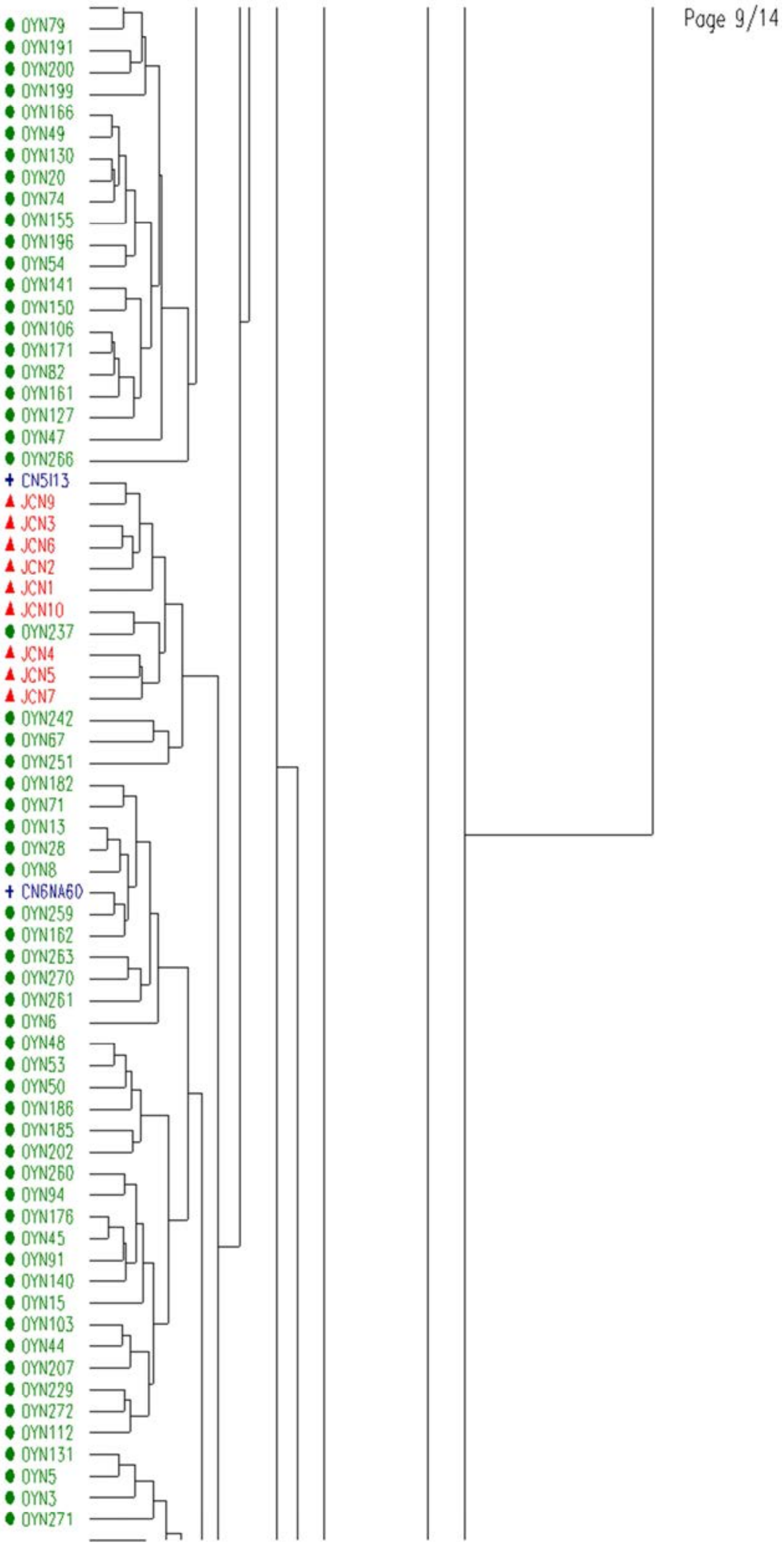
Page 9/14
● OYN79
● OYN191
● OYN200
● OYN199
● OYN166
● OYN49
● OYN130
● OYN20
● OYN74
● OYN155
● OYN196
● OYN54
● OYN141
● OYN150
● OYN106
● OYN171
● OYN82
● OYN161
● OYN127
● OYN47
● OYN266
+ CN5I13
▲ JCN9
▲ JCN3
▲ JCN6
▲ JCN2
▲ JCN1
▲ JCN10
● OYN237
▲ JCN4
▲ JCN5
▲ JCN7
● OYN242
● OYN67
● OYN251
● OYN182
● OYN71
● OYN13
● OYN28
● OYN8
+ CN6NA60
● OYN259
● OYN162
● OYN263
● OYN270
● OYN261
● OYN6
● OYN48
● OYN53
● OYN50
● OYN186
● OYN185
● OYN202
● OYN260
● OYN94
● OYN176
● OYN45
● OYN91
● OYN140
● OYN15
● OYN103
● OYN44
● OYN207
● OYN229
● OYN272
● OYN112
● OYN131
● OYN5
● OYN3
● OYN271

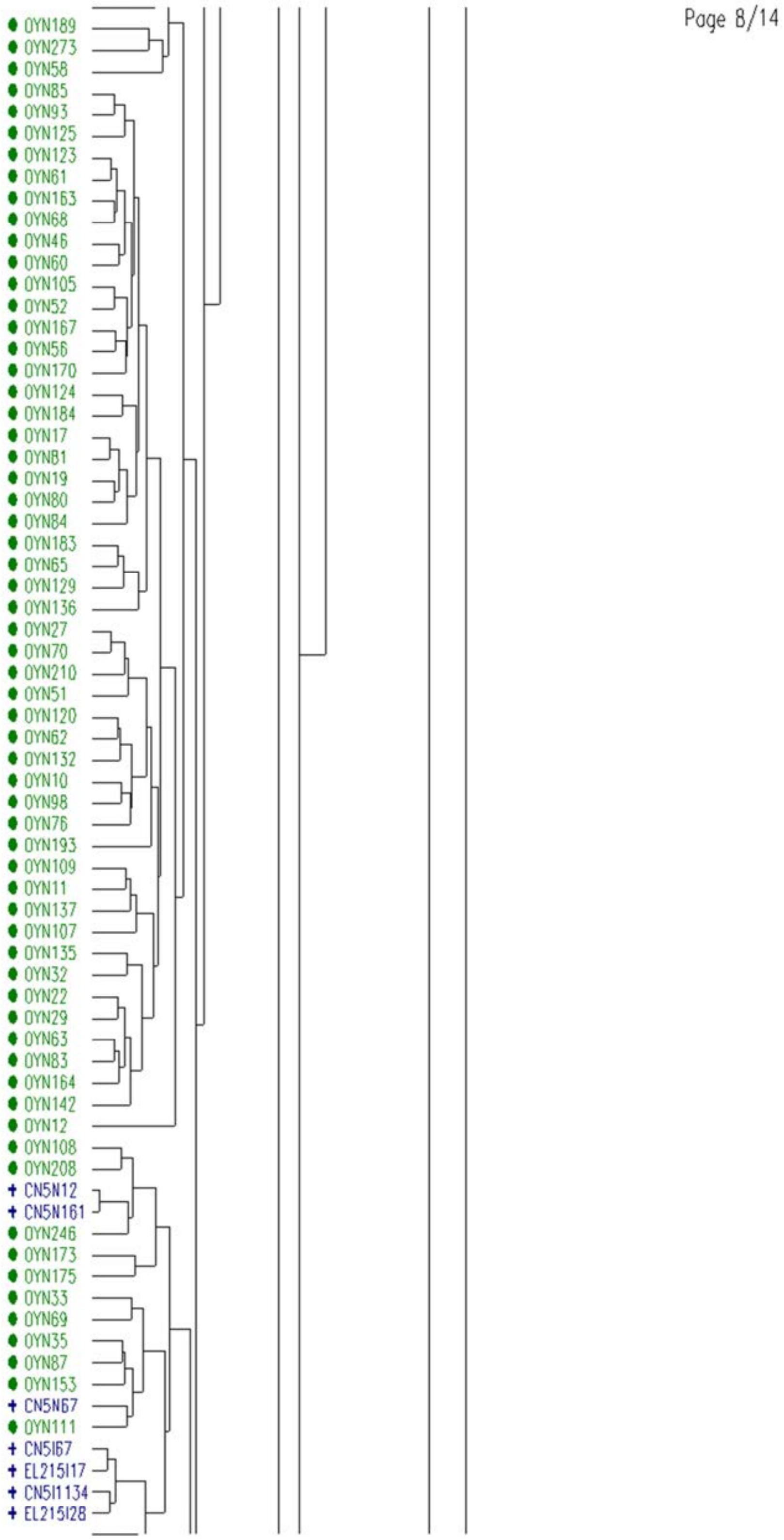
Page 8/14
OYN189
OYN273
OYN58
OYN85
OYN93
OYN125
OYN123
OYN61
OYN163
OYN68
OYN46
OYN60
OYN105
OYN52
OYN167
OYN56
OYN170
OYN124
OYN184
OYN17
OYN81
OYN19
OYN80
OYN84
OYN183
OYN65
OYN129
OYN136
OYN27
OYN70
OYN210
OYN51
OYN120
OYN62
OYN132
OYN10
OYN98
OYN76
OYN193
OYN109
OYN11
OYN137
OYN107
OYN135
OYN32
OYN22
OYN29
OYN63
OYN83
OYN164
OYN142
OYN12
OYN108
OYN208
CN5N12
CN5N161
OYN246
OYN173
OYN175
OYN33
OYN69
OYN35
OYN87
OYN153
CN5N67
OYN111
CN5I67
EL215I17
CN5I1134
EL215I28


Page 7/14
OYN232
OYN236
OYN216
OYN89
OYN146
OYN2
OYN203
OYN268
OYN86
OYN139
OYN255
OYN90
OYN177
OYN158
OYN254
CN5N1134
OYN115
OYN43
OYN230
OYN234
OYN160
OYN178
OYN145
OE368615
JCN8
SCN6
SCN8
SCN1
SCN7
SCN13
SCN15
SCN23
SCN2
SCN39
SCN17
SCN32
SCN19
SCN26
SCN22
SCN31
SCN28
SCN36
SCN40
SCN11
SCN34
SCN3
SCN9
SCN29
SCN16
SCN21
SCN37
SCN5
SCN35
SCN4
SCN18
SCN24
SCN12
SCN10
SCN41
SCN27
SCN14
SCN30
SCN20
CN6IA121
SCN25
KCN12
KCN13
KCN3
KCN5
KCN2

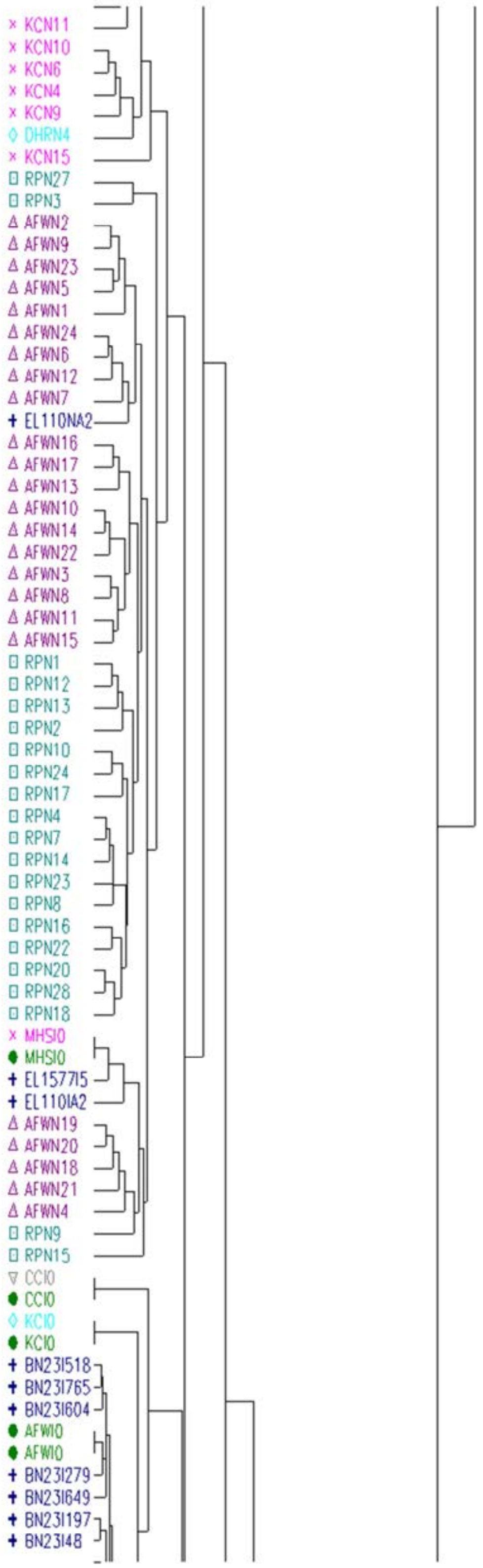
× KCN11
× KCN10
× KCN6
× KCN4
× KCN9
◊ DHRN4
× KCN15
□ RPN27
□ RPN3
△ AFWN2
△ AFWN9
△ AFWN23
△ AFWN5
△ AFWN1
△ AFWN24
△ AFWN6
△ AFWN12
△ AFWN7
+ EL110NA2
△ AFWN16
△ AFWN17
△ AFWN13
△ AFWN10
△ AFWN14
△ AFWN22
△ AFWN3
△ AFWN8
△ AFWN11
△ AFWN15
□ RPN1
□ RPN12
□ RPN13
□ RPN2
□ RPN10
□ RPN24
□ RPN17
□ RPN4
□ RPN7
□ RPN14
□ RPN23
□ RPN8
□ RPN16
□ RPN22
□ RPN20
□ RPN28
□ RPN18
× MHSI0
● MHSI0
+ EL157715
+ EL110IA2
△ AFWN19
△ AFWN20
△ AFWN18
△ AFWN21
△ AFWN4
□ RPN9
□ RPN15
▽ CCI0
● CCI0
◊ KCI0
● KCI0
+ BN231518
+ BN231765
+ BN231604
● AFWI0
● AFWI0
+ BN231279
+ BN231649
+ BN231197
+ BN23148

Page 6/14

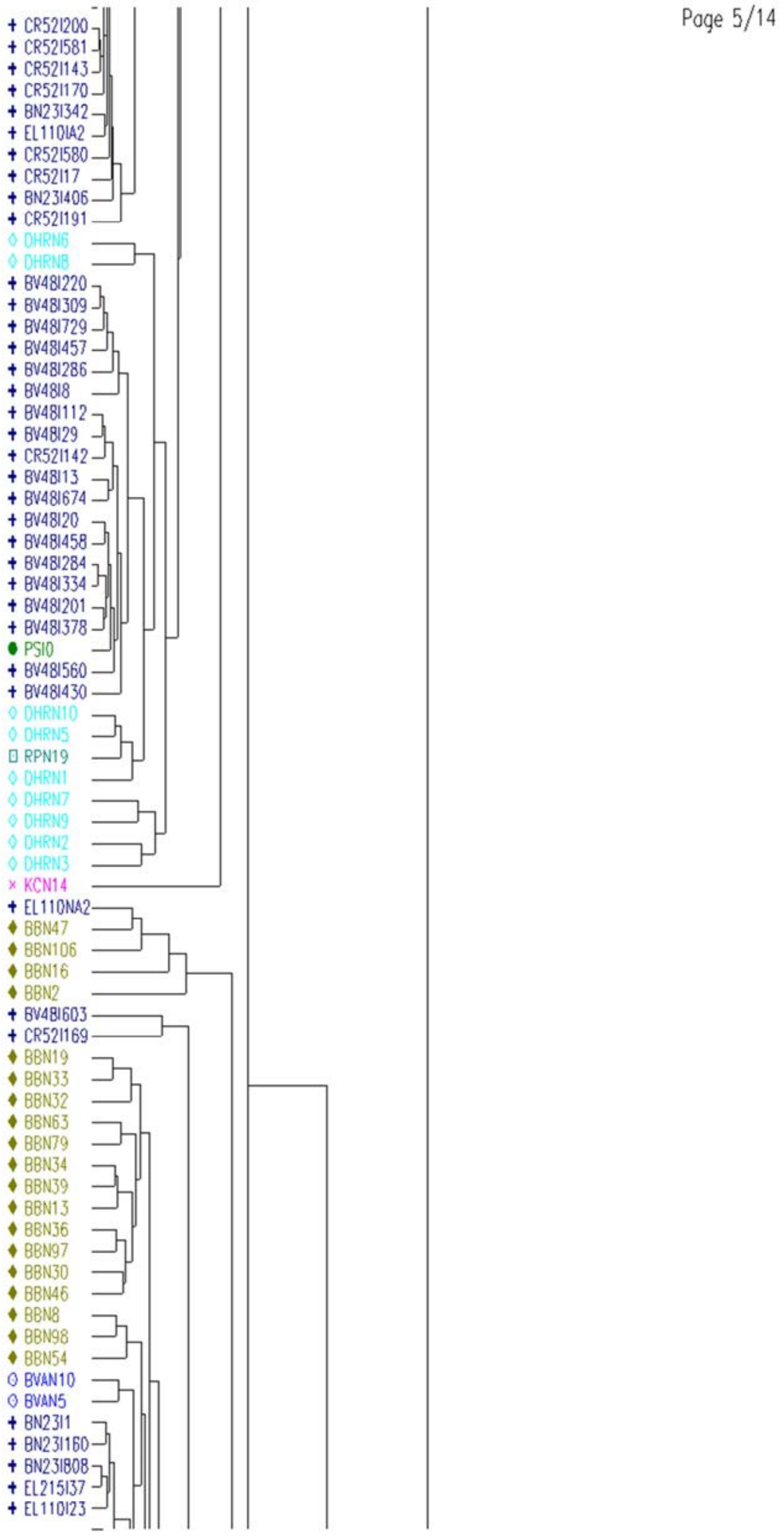
Page 5/14
CR52I200
CR52I581
CR52I143
CR52I170
BN23I342
EL110IA2
CR52I580
CR52I17
BN23I406
CR52I191
DHRN6
DHRN8
BV48I220
BV48I309
BV48I729
BV48I457
BV48I286
BV48I8
BV48I112
BV48I29
CR52I142
BV48I13
BV48I674
BV48I20
BV48I458
BV48I284
BV48I334
BV48I201
BV48I378
PSI0
BV48I560
BV48I430
DHRN10
DHRN5
RPN19
DHRN1
DHRN7
DHRN9
DHRN2
DHRN3
KCN14
EL110NA2
BBN47
BBN106
BBN16
BBN2
BV48I603
CR52I169
BBN19
BBN33
BBN32
BBN63
BBN79
BBN34
BBN39
BBN13
BBN36
BBN97
BBN30
BBN46
BBN8
BBN98
BBN54
BVAN10
BVAN5
BN23I1
BN23I160
BN23I808
EL215I37
EL110I23

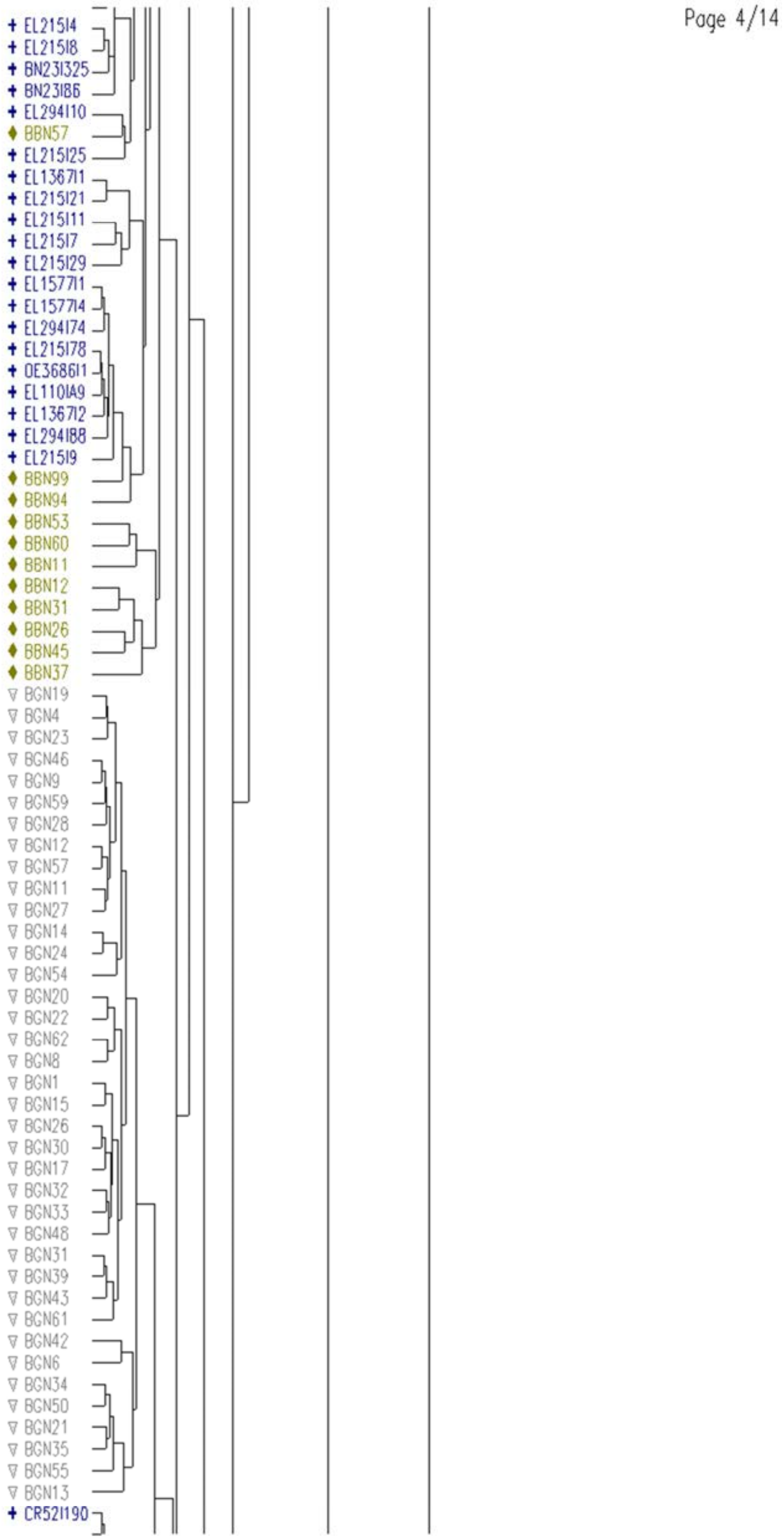
Page 4/14
+ EL215I4
+ EL215I8
+ BN23I325
+ BN23I86
+ EL294I10
♦ BBN57
+ EL215I25
+ EL1367I1
+ EL215I21
+ EL215I11
+ EL215I7
+ EL215I29
+ EL1577I1
+ EL1577I4
+ EL294I74
+ EL215I78
+ OE3686I1
+ EL110IA9
+ EL1367I2
+ EL294I88
+ EL215I9
♦ BBN99
♦ BBN94
♦ BBN53
♦ BBN60
♦ BBN11
♦ BBN12
♦ BBN31
♦ BBN26
♦ BBN45
♦ BBN37
▽ BGN19
▽ BGN4
▽ BGN23
▽ BGN46
▽ BGN9
▽ BGN59
▽ BGN28
▽ BGN12
▽ BGN57
▽ BGN11
▽ BGN27
▽ BGN14
▽ BGN24
▽ BGN54
▽ BGN20
▽ BGN22
▽ BGN62
▽ BGN8
▽ BGN1
▽ BGN15
▽ BGN26
▽ BGN30
▽ BGN17
▽ BGN32
▽ BGN33
▽ BGN48
▽ BGN31
▽ BGN39
▽ BGN43
▽ BGN61
▽ BGN42
▽ BGN6
▽ BGN34
▽ BGN50
▽ BGN21
▽ BGN35
▽ BGN55
▽ BGN13
+ CR52I190

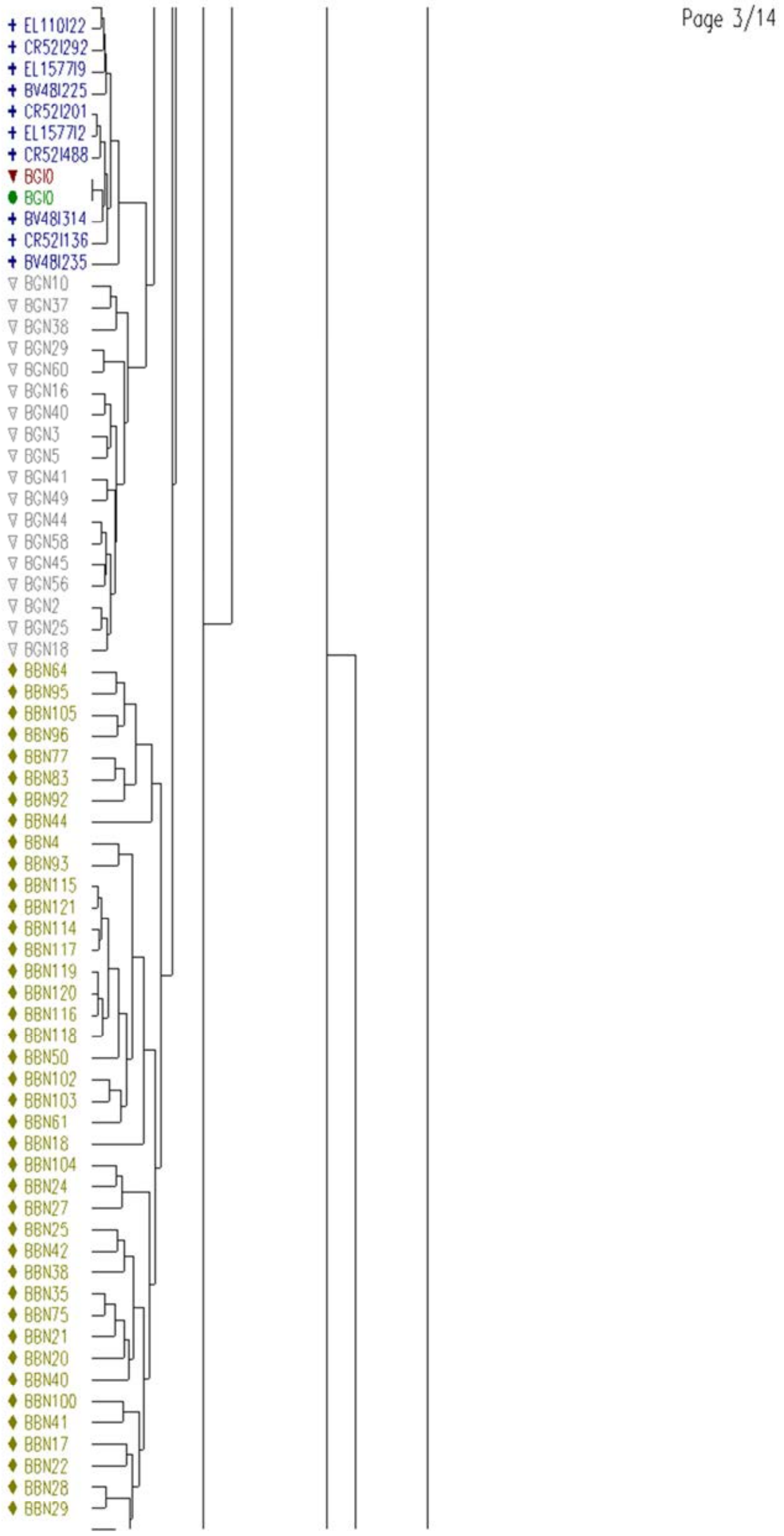
Page 3/14
EL110I22
CR52I292
EL157719
BV48I225
CR52I201
EL157712
CR52I488
BGI0
BGI0
BV48I314
CR52I136
BV48I235
BGN10
BGN37
BGN38
BGN29
BGN60
BGN16
BGN40
BGN3
BGN5
BGN41
BGN49
BGN44
BGN58
BGN45
BGN56
BGN2
BGN25
BGN18
BBN64
BBN95
BBN105
BBN96
BBN77
BBN83
BBN92
BBN44
BBN4
BBN93
BBN115
BBN121
BBN114
BBN117
BBN119
BBN120
BBN116
BBN118
BBN50
BBN102
BBN103
BBN61
BBN18
BBN104
BBN24
BBN27
BBN25
BBN42
BBN38
BBN35
BBN75
BBN21
BBN20
BBN40
BBN100
BBN41
BBN17
BBN22
BBN28
BBN29

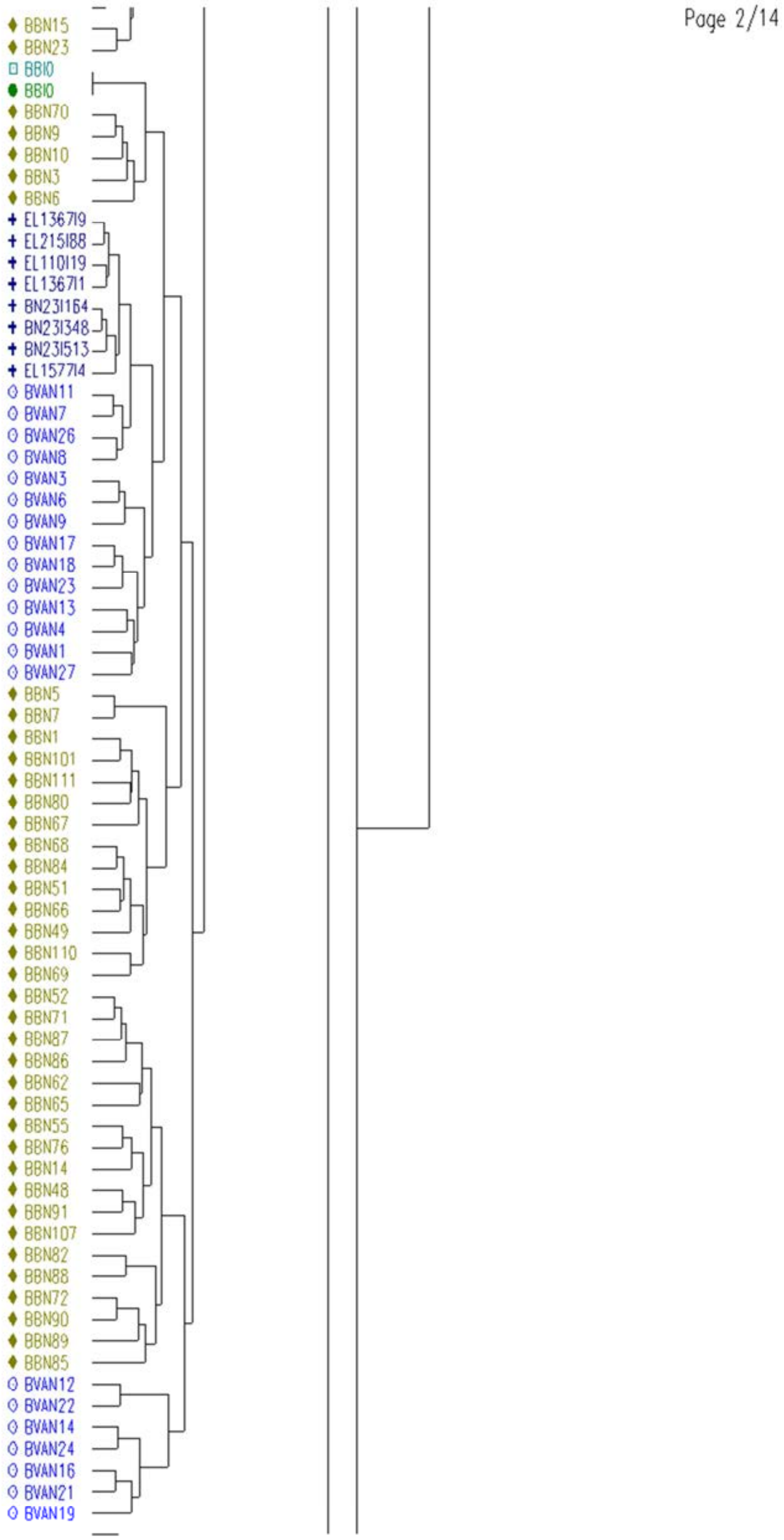
Page 2/14
◆ BBN15
◆ BBN23
□ BBI0
● BBI0
◆ BBN70
◆ BBN9
◆ BBN10
◆ BBN3
◆ BBN6
+ EL136719
+ EL215188
+ EL110119
+ EL136711
+ BN231164
+ BN231348
+ BN231513
+ EL157714
○ BVAN11
○ BVAN7
○ BVAN26
○ BVAN8
○ BVAN3
○ BVAN6
○ BVAN9
○ BVAN17
○ BVAN18
○ BVAN23
○ BVAN13
○ BVAN4
○ BVAN1
○ BVAN27
◆ BBN5
◆ BBN7
◆ BBN1
◆ BBN101
◆ BBN111
◆ BBN80
◆ BBN67
◆ BBN68
◆ BBN84
◆ BBN51
◆ BBN66
◆ BBN49
◆ BBN110
◆ BBN69
◆ BBN52
◆ BBN71
◆ BBN87
◆ BBN86
◆ BBN62
◆ BBN65
◆ BBN55
◆ BBN76
◆ BBN14
◆ BBN48
◆ BBN91
◆ BBN107
◆ BBN82
◆ BBN88
◆ BBN72
◆ BBN90
◆ BBN89
◆ BBN85
○ BVAN12
○ BVAN22
○ BVAN14
○ BVAN24
○ BVAN16
○ BVAN21
○ BVAN19

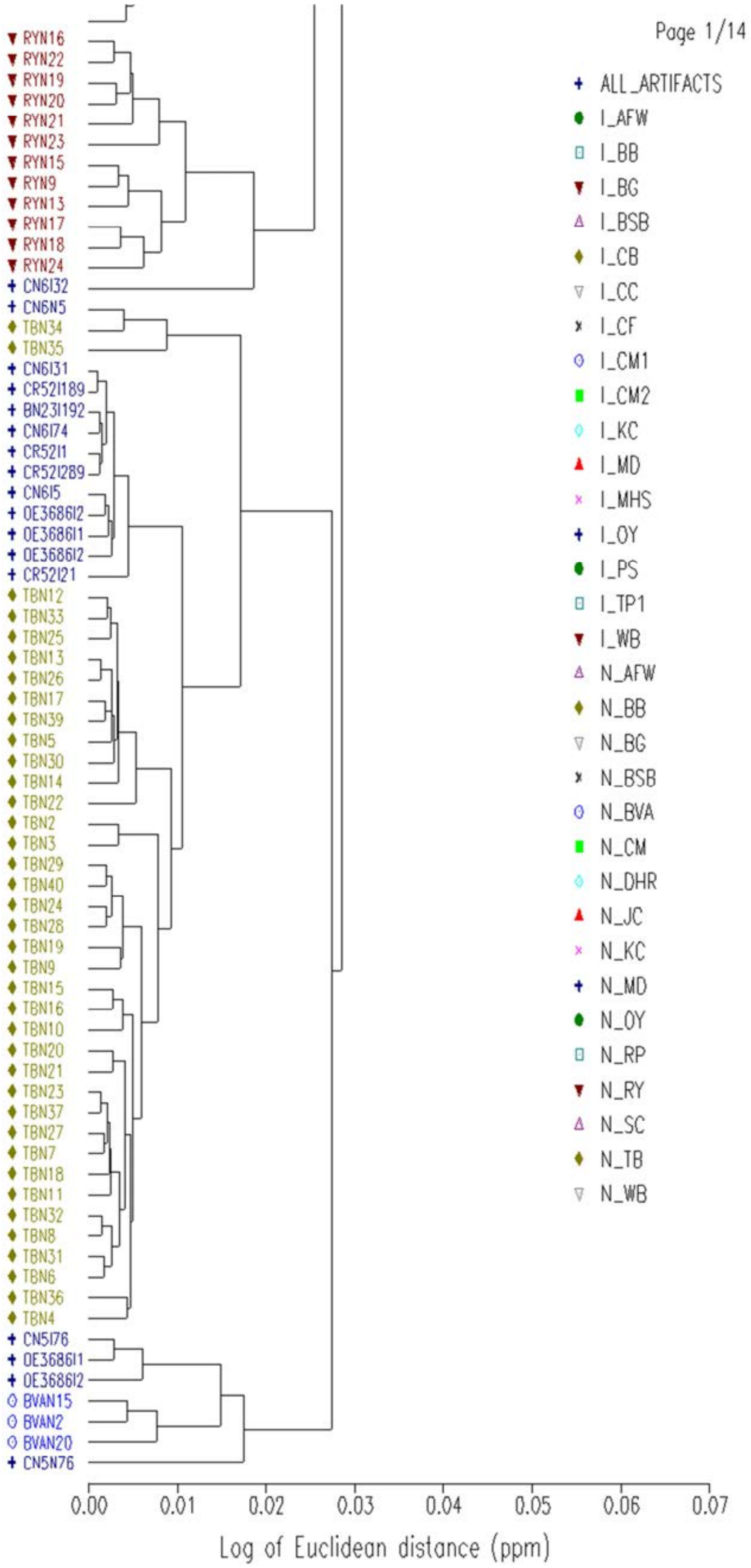
Page 1/14
RYN16
RYN22
RYN19
RYN20
RYN21
RYN23
RYN15
RYN9
RYN13
RYN17
RYN18
RYN24
CN6I32
CN6N5
TBN34
TBN35
CN6I31
CR52I189
BN23I192
CN6I74
CR52I1
CR52I289
CN6I5
OE3686I2
OE3686I1
OE3686I2
CR52I21
TBN12
TBN33
TBN25
TBN13
TBN26
TBN17
TBN39
TBN5
TBN30
TBN14
TBN22
TBN2
TBN3
TBN29
TBN40
TBN24
TBN28
TBN19
TBN9
TBN15
TBN16
TBN10
TBN20
TBN21
TBN23
TBN37
TBN27
TBN7
TBN18
TBN11
TBN32
TBN8
TBN31
TBN6
TBN36
TBN4
CN5I76
OE3686I1
OE3686I2
BVAN15
BVAN2
BVAN20
CN5N76
0.00
0.01
0.02
0.03
0.04
0.05
0.06
0.07
Log of Euclidean distance (ppm)
ALL_ARTIFACTS
I_AFW
I_BB
I_BG
I_BSB
I_CB
I_CC
I_CF
I_CM1
I_CM2
I_KC
I_MD
I_MHS
I_OY
I_PS
I_TP1
I_WB
N_AFW
N_BB
N_BG
N_BSB
N_BVA
N_CM
N_DHR
N_JC
N_KC
N_MD
N_OY
N_RP
N_RY
N_SC
N_TB
N_WB

Table E Artifact Source Assignment Results by Method

Site	Artifact	Visual Assignment	PCA Assignment	HCA Assignment
10BN23	1	Unknown	Unknown	Browns Bench
10BN23	37	Wedge Butte	Unknown	Wedge Butte
10BN23	48	Unknown	Unknown	American Falls/Walcott
10BN23	86	Browns Bench	Unknown	Browns Bench
10BN23	93	Big Southern Butte	Unknown	Big Southern Butte
10BN23	124	Cannonball Mountain 1	Unknown	Cannonball Mountain 1
10BN23	160	Browns Bench	Unknown	Browns Bench
10BN23	164	Unknown	Unknown	Butte Valley A
10BN23	166	Unknown	Unknown	Big Southern Butte
10BN23	179	Unknown	Unknown	Wedge Butte
10BN23	186	Big Southern Butte	Unknown	Big Southern Butte
10BN23	192	Unknown	Unknown	Unknown
10BN23	195	Cannonball Mountain 1	Unknown	Cannonball Mountain 1
10BN23	197	American Falls/Walcott	Unknown	American Falls/Walcott
10BN23	267a	Cannonball Mountain 1	Unknown	Cannonball Mountain 1
10BN23	279	American Falls/Walcott	Unknown	American Falls/Walcott
10BN23	325	Browns Bench	Unknown	Browns Bench
10BN23	342	American Falls/Walcott	Unknown	American Falls/Walcott
10BN23	348	Unknown	Unknown	Butte Valley A
10BN23	361	Big Southern Butte	Unknown	Big Southern Butte
10BN23	406	American Falls/Walcott	Unknown	American Falls/Walcott
10BN23	411	Big Southern Butte	Unknown	Big Southern Butte
10BN23	460	Cannonball Mountain 1	Unknown	Cannonball Mountain 1
10BN23	484	Cannonball Mountain 1	Unknown	Cannonball Mountain 1
10BN23	513	Butte Valley A	Unknown	Butte Valley A
10BN23	516	Cannonball Mountain 1	Unknown	Cannonball Mountain 1
10BN23	518	American Falls/Walcott	Unknown	American Falls/Walcott
10BN23	604	American Falls/Walcott	Unknown	American Falls/Walcott
10BN23	649	American Falls/Walcott	Unknown	American Falls/Walcott
10BN23	701	Malad	Unknown	Malad
10BN23	765	American Falls/Walcott	Unknown	American Falls/Walcott
10BN23	808	Browns Bench	Unknown	Browns Bench
10BV48	8	Unknown	Deadhorse Ridge	Pack Saddle/ Deadhorse Ridge
10BV48	13	Pack Saddle	Deadhorse Ridge	Pack Saddle/ Deadhorse Ridge
10BV48	20	Pack Saddle	Deadhorse Ridge	Pack Saddle/ Deadhorse Ridge
10BV48	29	Pack Saddle	Deadhorse Ridge	Pack Saddle/ Deadhorse Ridge
10BV48	112	Pack Saddle	Deadhorse Ridge	Pack Saddle/ Deadhorse Ridge
10BV48	127	Malad	Unknown	Malad

10BV48	201	Pack Saddle	Deadhorse Ridge	Pack Saddle/ Deadhorse Ridge
10BV48	220	Pack Saddle	Deadhorse Ridge	Pack Saddle/ Deadhorse Ridge
10BV48	225	Bear Gulch	Unknown	Bear Gulch
10BV48	235	Bear Gulch	Unknown	Bear Gulch
10BV48	284	Pack Saddle	Deadhorse Ridge	Pack Saddle/ Deadhorse Ridge
10BV48	286	Pack Saddle	Deadhorse Ridge	Pack Saddle/ Deadhorse Ridge
10BV48	297	Teton Pass 1	Unknown	Teton Pass 1
10BV48	309	Unknown	Deadhorse Ridge	Pack Saddle/ Deadhorse Ridge
10BV48	314	Bear Gulch	Unknown	Bear Gulch
10BV48	334	Pack Saddle	Deadhorse Ridge	Pack Saddle/ Deadhorse Ridge
10BV48	378	Pack Saddle	Deadhorse Ridge	Pack Saddle/ Deadhorse Ridge
10BV48	430	Pack Saddle	Deadhorse Ridge	Pack Saddle/ Deadhorse Ridge
10BV48	457	Pack Saddle	Deadhorse Ridge	Pack Saddle/ Deadhorse Ridge
10BV48	458	Pack Saddle	Deadhorse Ridge	Pack Saddle/ Deadhorse Ridge
10BV48	560	Pack Saddle	Deadhorse Ridge	Pack Saddle/ Deadhorse Ridge
10BV48	603	Unknown	Unknown	Unknown
10BV48	674	Pack Saddle	Deadhorse Ridge	Pack Saddle/ Deadhorse Ridge
10BV48	729	Pack Saddle	Deadhorse Ridge	Pack Saddle/ Deadhorse Ridge
10CN5	12	Owyhee	Owyhee	Owyhee
10CN5	13	Unknown	Jordan Creek	Jordan Creek
10CN5	35	Owyhee	Owyhee	Owyhee
10CN5	A50	Owyhee	Owyhee	Owyhee
10CN5	67	Unknown	Unknown	Owyhee
10CN5	76	Unknown	Unknown	Unknown
10CN5	161	Owyhee	Owyhee	Owyhee
10CN5	1134	Unknown	Owyhee	Owyhee
10CN6	5	Unknown	Unknown	Timber Butte
10CN6	6	Owyhee	Owyhee	Owyhee
10CN6	31	Unknown	Unknown	Unknown
10CN6	32	Unknown	Unknown	Unknown
10CN6	A48	Owyhee	Owyhee	Owyhee
10CN6	56	Owyhee	Unknown	Owyhee
10CN6	A60	Owyhee	Owyhee	Owyhee
10CN6	74	Unknown	Unknown	Unknown
10CN6	A78	Owyhee	Owyhee	Owyhee

10CN6	100	Owyhee	Owyhee	Owyhee
10CN6	A116	Owyhee	Owyhee	Owyhee
10CN6	117	Owyhee	Owyhee	Owyhee
10CN6	A121	Unknown	Unknown	Sinker Canyon
10CR52	1	Unknown	Unknown	Unknown
10CR52	17	American Falls/Walcott	Unknown	American Falls/Walcott
10CR52	21	Unknown	Unknown	Unknown
10CR52	136	Bear Gulch	Unknown	Bear Gulch
10CR52	142	Pack Saddle	Deadhorse Ridge	Pack Saddle/ Deadhorse Ridge
10CR52	143	American Falls/Walcott	Unknown	American Falls/Walcott
10CR52	149	Unknown	Unknown	Unknown
10CR52	169	Unknown	Unknown	Unknown
10CR52	170	American Falls/Walcott	Unknown	American Falls/Walcott
10CR52	189	Unknown	Unknown	Unknown
10CR52	190	Bear Gulch	Unknown	Bear Gulch
10CR52	191	American Falls/Walcott	Unknown	American Falls/Walcott
10CR52	200	American Falls/Walcott	Unknown	American Falls/Walcott
10CR52	201	Bear Gulch	Unknown	Bear Gulch
10CR52	289	Unknown	Unknown	Unknown
10CR52	290	Big Southern Butte	Unknown	Big Southern Butte
10CR52	291	Cannonball Mountain 1	Unknown	Cannonball Mountain 1
10CR52	292	Bear Gulch	Unknown	Bear Gulch
10CR52	488	Bear Gulch	Unknown	Bear Gulch
10CR52	580	American Falls/Walcott	Unknown	American Falls/Walcott
10CR52	581	American Falls/Walcott	Unknown	American Falls/Walcott
10CR52	591	Cannonball Mountain 1	Unknown	Cannonball Mountain 1
10EL110	1	Cannonball Mountain 2	Unknown	Cannonball Mountain 2
10EL110	A21	Unknown	Unknown	Murphy Hot Springs
10EL110	82	Cannonball Mountain 1	Unknown	Cannonball Mountain 1
10EL110	89	Cannonball Mountain 1	Unknown	Cannonball Mountain 1
10EL110	A93	Owyhee	Owyhee	Owyhee
10EL110	96	Cannonball Mountain 1	Unknown	Cannonball Mountain 1
10EL110	A99	Browns Bench	Browns Bench	Browns Bench
10EL110	191	Butte Valley A	Butte Valley A	Butte Valley A
10EL110	A216	American Falls/Walcott	Unknown	American Falls/Walcott
10EL110	228	Bear Gulch	Unknown	Bear Gulch
10EL110	234	Browns Bench	Unknown	Browns Bench
10EL110	247	Cannonball Mountain 1	Unknown	Cannonball Mountain 1
10EL110	259	Cannonball Mountain 1	Unknown	Cannonball Mountain 1
10EL110	261	Cannonball Mountain 1	Unknown	Cannonball Mountain 1
10EL215	4	Browns Bench	Deadhorse Ridge	Browns Bench
10EL215	7	Unknown	Unknown	Browns Bench
10EL215	8	Browns Bench	Deadhorse Ridge	Browns Bench
10EL215	9	Browns Bench	Unknown	Browns Bench

10EL215	11	Cannonball Mountain 1	Unknown	Cannonball Mountain 1
10EL215	29	Browns Bench	Unknown	Browns Bench
10EL215	37	Browns Bench	Deadhorse Ridge	Browns Bench
10EL215	42	Unknown	Unknown	Unknown
10EL215	78	Browns Bench	Unknown	Browns Bench
10EL215	88	Butte Valley A	Unknown	Butte Valley A
10EL215	95	Cannonball Mountain 1	Unknown	Cannonball Mountain 1
10EL215	117	Browns Bench	Unknown	Browns Bench
10EL215	118	Cannonball Mountain 1	Unknown	Cannonball Mountain 1
10EL215	131	Cannonball Mountain 1	Unknown	Cannonball Mountain 1
10EL215	158	Cannonball Mountain 1	Unknown	Cannonball Mountain 1
10EL215	172	Cannonball Mountain 1	Unknown	Cannonball Mountain 1
10EL215	179	Unknown	Jordan Creek	Owyhee
10EL215	180	Owyhee	Owyhee	Owyhee
10EL215	193	Cannonball Mountain 2	Unknown	Cannonball Mountain 2
10EL215	216	Browns Bench	Unknown	Browns Bench
10EL215	225	Cannonball Mountain 1	Unknown	Cannonball Mountain 1
10EL215	252	Unknown	Unknown	Browns Bench
10EL215	270	Owyhee	Owyhee	Owyhee
10EL215	280	Unknown	Owyhee	Owyhee
10EL215	289	Owyhee	Owyhee	Owyhee
10EL294	74	Browns Bench	Browns Bench	Browns Bench
10EL294	88	Browns Bench	Browns Bench	Browns Bench
10EL294	109	Unknown	Unknown	Browns Bench
10EL294	116	Owyhee	Browns Bench	Owyhee
10EL294	158	Cannonball Mountain 1	Unknown	Cannonball Mountain 1
10EL1367	9	Unknown	Butte Valley A	Butte Valley A
10EL1367	11	Browns Bench	Unknown	Browns Bench
10EL1367	19	Unknown	Butte Valley A	Butte Valley A
10EL1367	22	Browns Bench	Browns Bench	Browns Bench
10EL1367	26	Cannonball Mountain 1	Unknown	Cannonball Mountain 1
10EL1577	91	Bear Gulch	Unknown	Bear Gulch
10EL1577	173	Browns Bench	Unknown	Browns Bench
10EL1577	226	Bear Gulch	Unknown	Bear Gulch
10EL1577	246	Big Southern Butte	Unknown	Big Southern Butte
10EL1577	267	Malad	Unknown	Malad
10EL1577	274	Owyhee	Owyhee	Owyhee
10EL1577	412	Browns Bench	Browns Bench	Browns Bench
10EL1577	457	Butte Valley A	Unknown	Butte Valley A
10EL1577	476	Cannonball Mountain 1	Unknown	Cannonball Mountain 1
10EL1577	501	Cannonball Mountain 1	Unknown	Cannonball Mountain 1
10EL1577	532	Cannonball Mountain 1	Unknown	Cannonball Mountain 1
10EL1577	564	Murphy Hot Springs	Unknown	Murphy Hot Springs
10OE3686	69	Unknown	Cannonball Mountain 1	Cannonball Mountain 1

10OE3686	103	Unknown	Unknown	Unknown
10OE3686	177	Browns Bench	Browns Bench	Browns Bench
10OE3686	179	Owyhee	Owyhee	Owyhee
10OE3686	181	Owyhee	Owyhee	Owyhee
10OE3686	183	Unknown	Unknown	Unknown
10OE3686	216	Owyhee	Owyhee	Owyhee
10OE3686	255	Unknown	Unknown	Unknown
10OE3686	257	Unknown	Unknown	Unknown
10OE3686	258	Unknown	Unknown	Unknown
10OE3686	396	Unknown	Unknown	Unknown
10OE3686	442	Unknown	Unknown	Unknown
10OE3686	505	Unknown	Unknown	Unknown
10OE3686	519	Unknown	Unknown	Unknown

Table F Artifact Source Assignment Results

Site	Artifact	Pooled Assignment	NWROSL Assignment
10BN23	1	Browns Bench	--
10BN23	37	Wedge Butte	--
10BN23	48	American Falls/Walcott	--
10BN23	86	Browns Bench	--
10BN23	93	Big Southern Butte	--
10BN23	124	Cannonball Mountain 1	--
10BN23	160	Browns Bench	--
10BN23	164	Butte Valley A	--
10BN23	166	Big Southern Butte	--
10BN23	179	Wedge Butte	--
10BN23	186	Big Southern Butte	--
10BN23	192	Unknown	--
10BN23	195	Cannonball Mountain 1	--
10BN23	197	American Falls/Walcott	--
10BN23	267a	Cannonball Mountain 1	--
10BN23	279	American Falls/Walcott	--
10BN23	325	Browns Bench	--
10BN23	342	American Falls/Walcott	--
10BN23	348	Butte Valley A	--
10BN23	361	Big Southern Butte	--
10BN23	406	American Falls/Walcott	--
10BN23	411	Big Southern Butte	--
10BN23	460	Cannonball Mountain 1	--
10BN23	484	Cannonball Mountain 1	--
10BN23	513	Butte Valley A	--
10BN23	516	Cannonball Mountain 1	--
10BN23	518	American Falls/Walcott	--
10BN23	604	American Falls/Walcott	--
10BN23	649	American Falls/Walcott	--
10BN23	701	Malad	--
10BN23	765	American Falls/Walcott	--
10BN23	808	Browns Bench	--
10BV48	8	Pack Saddle/ Deadhorse Ridge	--
10BV48	13	Pack Saddle/ Deadhorse Ridge	--
10BV48	20	Pack Saddle/ Deadhorse Ridge	--
10BV48	29	Pack Saddle/ Deadhorse Ridge	--
10BV48	112	Pack Saddle/ Deadhorse Ridge	--
10BV48	127	Malad	--
10BV48	201	Pack Saddle/ Deadhorse Ridge	--
10BV48	220	Pack Saddle/ Deadhorse Ridge	--
10BV48	225	Bear Gulch	--
10BV48	235	Bear Gulch	--

10BV48	284	Pack Saddle/ Deadhorse Ridge	--
10BV48	286	Pack Saddle/ Deadhorse Ridge	--
10BV48	297	Teton Pass 1	--
10BV48	309	Pack Saddle/ Deadhorse Ridge	--
10BV48	314	Bear Gulch	--
10BV48	334	Pack Saddle/ Deadhorse Ridge	--
10BV48	378	Pack Saddle/ Deadhorse Ridge	--
10BV48	430	Pack Saddle/ Deadhorse Ridge	--
10BV48	457	Pack Saddle/ Deadhorse Ridge	--
10BV48	458	Pack Saddle/ Deadhorse Ridge	--
10BV48	560	Pack Saddle/ Deadhorse Ridge	--
10BV48	603	Unknown	--
10BV48	674	Pack Saddle/ Deadhorse Ridge	--
10BV48	729	Pack Saddle/ Deadhorse Ridge	--
10CN5	12	Owyhee	Owyhee
10CN5	13	Jordan Creek	--
10CN5	35	Owyhee	Owyhee
10CN5	A50	Owyhee	Owyhee
10CN5	67	Owyhee	Owyhee
10CN5	76	Unknown	Coyote Wells Oregon
10CN5	161	Owyhee	Owyhee
10CN5	1134	Owyhee	Owyhee
10CN6	5	Timber Butte	Timber Butte
10CN6	6	Owyhee	Owyhee
10CN6	31	Unknown	--
10CN6	32	Unknown	--
10CN6	A48	Owyhee	Owyhee
10CN6	56	Owyhee	--
10CN6	A60	Owyhee	Owyhee
10CN6	74	Unknown	--
10CN6	A78	Owyhee	Owyhee
10CN6	100	Owyhee	--
10CN6	A116	Owyhee	Owyhee
10CN6	117	Owyhee	--
10CN6	A121	Sinker Canyon	Sinker Canyon
10CR52	1	Unknown	--
10CR52	17	American Falls/Walcott	--
10CR52	21	Unknown	--
10CR52	136	Bear Gulch	--
10CR52	142	Pack Saddle/ Deadhorse Ridge	--
10CR52	143	American Falls/Walcott	--
10CR52	149	Unknown	--
10CR52	169	Unknown	--
10CR52	170	American Falls/Walcott	--

10CR52	189	Unknown	--
10CR52	190	Bear Gulch	--
10CR52	191	American Falls/Walcott	--
10CR52	200	American Falls/Walcott	--
10CR52	201	Bear Gulch	--
10CR52	289	Unknown	--
10CR52	290	Big Southern Butte	--
10CR52	291	Cannonball Mountain 1	--
10CR52	292	Bear Gulch	--
10CR52	488	Bear Gulch	--
10CR52	580	American Falls/Walcott	--
10CR52	581	American Falls/Walcott	--
10CR52	591	Cannonball Mountain 1	--
10EL110	1	Cannonball Mountain 2	--
10EL110	A21	Murphy Hot Springs	Browns Bench Area
10EL110	82	Cannonball Mountain 1	--
10EL110	89	Cannonball Mountain 1	--
10EL110	A93	Owyhee	Cannonball Mountain 1
10EL110	96	Cannonball Mountain 1	--
10EL110	A99	Browns Bench	Browns Bench
10EL110	191	Butte Valley A	--
10EL110	A216	American Falls/Walcott	--
10EL110	228	Bear Gulch	--
10EL110	234	Browns Bench	--
10EL110	247	Cannonball Mountain 1	--
10EL110	259	Cannonball Mountain 1	--
10EL110	261	Cannonball Mountain 1	--
10EL215	4	Unknown- Conflict	Browns Bench
10EL215	7	Browns Bench	Browns Bench
10EL215	8	Unknown- Conflict	Browns Bench
10EL215	9	Browns Bench	Browns Bench
10EL215	11	Cannonball Mountain 1	Cannonball Mountain 1
10EL215	29	Browns Bench	--
10EL215	37	Unknown- Conflict	--
10EL215	42	Unknown	--
10EL215	78	Browns Bench	--
10EL215	88	Butte Valley A	--
10EL215	95	Cannonball Mountain 1	--
10EL215	117	Browns Bench	--
10EL215	118	Cannonball Mountain 1	--
10EL215	131	Cannonball Mountain 1	--
10EL215	158	Cannonball Mountain 1	--
10EL215	172	Cannonball Mountain 1	--
10EL215	179	Unknown- Conflict	--

10EL215	180	Owyhee	--
10EL215	193	Cannonball Mountain 2	--
10EL215	216	Browns Bench	--
10EL215	225	Cannonball Mountain 1	--
10EL215	252	Browns Bench	--
10EL215	270	Owyhee	--
10EL215	280	Owyhee	--
10EL215	289	Owyhee	--
10EL294	74	Browns Bench	--
10EL294	88	Browns Bench	--
10EL294	109	Browns Bench	--
10EL294	116	Unknown- Conflict	--
10EL294	158	Cannonball Mountain 1	--
10EL1367	9	Butte Valley A	--
10EL1367	11	Browns Bench	--
10EL1367	19	Butte Valley A	--
10EL1367	22	Browns Bench	--
10EL1367	26	Cannonball Mountain 1	--
10EL1577	91	Bear Gulch	--
10EL1577	173	Browns Bench	--
10EL1577	226	Bear Gulch	--
10EL1577	246	Big Southern Butte	--
10EL1577	267	Malad	--
10EL1577	274	Owyhee	--
10EL1577	412	Browns Bench	--
10EL1577	457	Butte Valley A	--
10EL1577	476	Cannonball Mountain 1	--
10EL1577	501	Cannonball Mountain 1	--
10EL1577	532	Cannonball Mountain 1	--
10EL1577	564	Murphy Hot Springs	--
10OE3686	69	Cannonball Mountain 1	--
10OE3686	103	Unknown	--
10OE3686	177	Browns Bench	--
10OE3686	179	Owyhee	--
10OE3686	181	Owyhee	--
10OE3686	183	Unknown	--
10OE3686	216	Owyhee	--
10OE3686	255	Unknown	--
10OE3686	257	Unknown	--
10OE3686	258	Unknown	--
10OE3686	396	Unknown	--
10OE3686	442	Unknown	--
10OE3686	505	Unknown	--
10OE3686	519	Unknown	--